Turun yliopisto
University of Turku

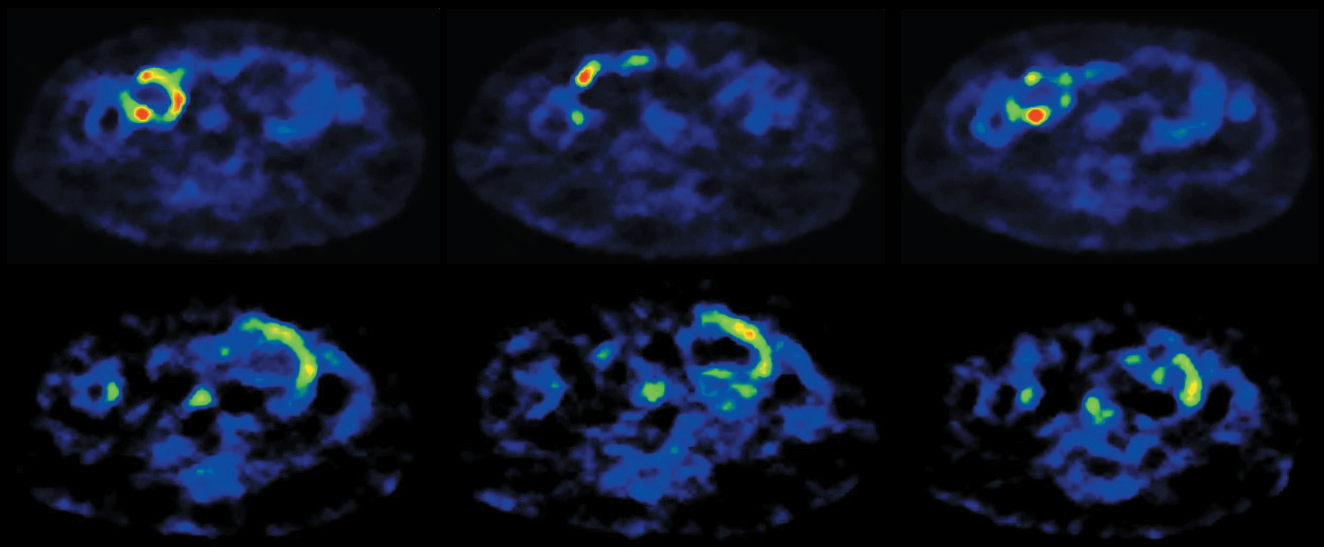

REGULATION OF INTESTINAL METABOLISM IN OBESITY AND DIABETES

Studies using positron emission tomography

Jukka Koffert

TURUN YLIOPISTON JULKAISUJA - ANNALES UNIVERSITATIS TURKUENSIS
Sarja - ser. D osa - tom. 1355 | Medica - Odontologica | Turku 2017

Turun yliopisto
University of Turku

REGULATION OF INTESTINAL METABOLISM IN OBESITY AND DIABETES

Studies using positron emission tomography

Jukka Koffert

TURUN YLIOPISTON JULKAISUJA – ANNALES UNIVERSITATIS TURKUENSIS
Sarja - ser. D osa - tom. 1355 | Medica - Odontologica | Turku 2018

University of Turku

Faculty of Medicine
Department of Internal Medicine
Doctoral Programme in Clinical Research
Turku PET Centre

Supervised by

Professor Pirjo Nuutila
Turku PET Centre
University of Turku, Finland
Department of Endocrinology
Turku University Hospital, Finland

Saila Kauhanen, MD, PhD
Division of Digestive Surgery and Urology, Turku University Hospital, Finland
Turku PET Centre
University of Turku, Finland

Reviewed by

Adjunct professor Perttu Arkkila
Department of Gastroenterology
Helsinki University Hospital, Finland

Professor André Carpentier
Department of Medicine
Division of Endocrinology
Centre de recherche du CHUS,
Université de Sherbrooke, Quebec, Canada

Opponent

Professor Kirsi Pietiläinen
Obesity Research Unit
Research Programs Unit, Diabetes and Obesity
University of Helsinki, Finland

Cover image by Jukka Koffert

ISBN 978-951-29-7247-0 (PRINT)
ISBN 978-951-29-7248-7 (PDF)
ISSN 0355-9483 (Print)
ISSN 2343-3213 (Online)
Painosalama Oy – Turku, Finland 2018

ABSTRACT

Jukka Koffert

Regulation of intestinal metabolism in obesity and diabetes

Studies using positron emission tomography

University of Turku, Faculty of Medicine, Department of Internal Medicine; Doctoral Programme in Clinical Research; Turku PET Centre, Turku, Finland

The global epidemic of obesity is a challenge to healthcare systems due to the increase in the incidence of type 2 diabetes (T2D) and its associated morbidities. Although the small intestine is the first absorptive organ to encounter the ingested and digesting nutrients, it has gained little attention in the research of T2D and obesity.

In the present study, multimodality imaging by Positron emission tomography (PET) combined with magnetic resonance imaging (MRI) or computed tomography (CT) modalities were utilized to study intestinal blood flow and metabolic substrate uptake in healthy normal-weight controls and obese patients with T2D before and after surgical or medical treatments. In the PET imaging, we focused on intestinal blood flow and volume, fatty acid, glucose uptake using ^{15}O-water, ^{15}O-labeled carbon monoxide, palmitate analogue 14(RS)-[^{18}F]fluoro-6-thia-heptadecanoic acid, ([^{18}F]FTHA) and 2-[^{18}F]fluoro-2-deoxy-D-glucose ([^{18}F]FDG), respectively.

Morbidly obese subjects (mean BMI 41±4.5kg/m^2) with T2D had similar blood flow in the intestine even after bariatric surgery when compared to healthy controls. The bariatric surgery was either Roux-en Y gastric bypass (n=13) or Sleeve gastrectomy (n=20). Post-prandially, nutrient contact with the small intestine and infusion of glucose dependent insulinotrophic polypeptide (GIP) stimulated blood flow in the small intestine of all groups. These findings suggest that despite the adaptation changes after bariatric surgery of the intestine, postprandial blood flow regulation in the small intestine remains intact in T2D and obese individuals. Intestinal fatty acid (FA) uptake was higher in obese subjects compared to healthy counterparts and unexpectedly this increased after bariatric surgery. The FA extraction rate in the small intestine also increased after bariatric surgery and this phenomenon suggests that intestinal energy expenditure relies on high FFA-to-glucose ratio in obese patients, which persists even after weight loss. Glucose uptake in the small intestines of metformin treated study subjects with T2D was increased compared to baseline and reached the level observed in healthy study subjects in previous studies.

Taken together, the data of the present study provide novel insight on the role of the small intestine in the multiorgan metabolic derangements associated with T2D. It is not known whether these changes are part of the adaptation mechanism, due to improved glycaemic control and insulin resistance breakdown or due to the fundamental pathophysiology behind T2D. The actual mechanism behind these changes should be addressed in future research.

Keywords: obesity, type 2 diabetes, intestinal glucose uptake, intestinal blood flow intestinal fatty acid uptake, bariatric surgery, incretin, metformin, positron emission tomography

TIIVISTELMÄ

Jukka Koffert

Suoliston aineenvaihdunnan säätely lihavuudessa ja diabeteksessa

Positroniemissiotomografiaa käyttäen tehtyjä tutkimuksia

Turun yliopisto, Lääketieteellinen tiedekunta, Sisätautioppi; Turun kliininen tohtoriohjelma; Valtakunnallinen PET-keskus, Turun yliopisto ja Turun yliopistollinen keskussairaala

Lihavuus on huomattavasti yleistynyt viime vuosikymmeninä ja kuormittaa terveydenhuoltoamme lisäten tyypin 2 diabeteksen ilmaantuvuutta ja yleistä sairastavuutta. Lihavuuden ja tyypin 2 diabeteksen tutkimuksessa on aiemmin keskitytty suoliston aineenvaihduntaan varsin vähän, vaikka suolisto ensimmäisenä elimenä käsittelee elimistöön tulevan ravinnon ja ruoansulatuskanavasta erittyvillä hormoneilla säätelee sokeriaineenvaihduntaa.

Tutkimuksessa verrattiin suoliston verenvirtauksen ja ravintoaineiden soluunottokyvyn muutoksia ylipainoisilla tyypin 2 diabeetikoilla ja terveillä normaalipainoisilla verrokeilla käyttäen positroniemissiotomografiaa (PET) yhdistettynä rakenteelliseen magneetti- ja tietokonetomografia kuvantamiseen. Tutkittavat osallistuivat kliinisen hoitokäytännön mukaan lihavuusleikkaukseen tai käyttivät tutkimuslääkettä protokollan mukaan. PET-kuvantamisella tutkittiin suoliston verenvirtauksen ja verimäärän muutoksia sekä rasvahappojen ja sokerin soluunottokykyä käyttäen ^{15}O-vettä, ^{15}O-leimattua hiilimonoksidia, palmitaattianalogi 14(RS)-[^{18}F]fluoro-6-thia-heptadekanoidi happoa ([^{18}F]FTHA) ja 2-[^{18}F]fluoro-2-deoxy-D-glukoosia ([^{18}F]FDG).

Sairaalloisen ylipainoisilla diabeetikoilla suoliston verenvirtaus ei poikennut terveistä kontrolleista edes lihavuusleikkauksen jälkeen. Ryhmien välisiä eroja veren virtauksessa ei todettu syömisen ja glukoosista riippuvaisen insuliinin eritystä lisäävän hormonin (GIP) annostelun jälkeen. Havainnot viittaavat siihen, että aterian jälkeinen verenvirtauksen säätely ei ole muuttunut lihavilla diabeetikoilla edes lihavuuskirurgian jälkeen, vaikka suolisto muuten sopeutuu kirurgian aiheuttamiin anatomisiin muutoksiin. Ylipainoisilla tyypin 2 diabetesta sairastavilla tutkittavilla suoliston rasvahappojen soluunottokyky todettiin lisääntyneeksi verrattuna terveisiin kontrollihenkilöihin ja odottamatta lihavuuskirurgia lisäsi kyseistä muutosta. Rasvahappojen soluunottokyvyn lisääntyminen verenkierrosta vielä lihavuuskirurgian jälkeen, osoittaa suoliston energiankäytön riippuvan korkeasta rasvahappo-sokerin käyttösuhteesta vielä laihtumisen jälkeenkin. Metformiini-lääkitys lisäsi suoliston sokerin käyttöä ja vähensi suoliston insuliiniresistenssiä, jopa normaalistaen sen terveiden tasolle.

Tämä väitöskirjatutkimus osoittaa, että suolistossa tapahtuu merkittäviä aineenvaihdunnallisia muutoksia tyypin 2 diabeteksessa, ylipainossa ja lihavuusleikkauksen jälkeen. Avoimeksi jää säätelevätkö lihavuuskirurgian ja lääkehoitojen myötä lisääntyneet suoliston rasvahappojen ja sokerin käyttö koko elimistö aineenvaihduntaa vai ovatko ne seurausta suoliston sopeutumisesta muuttuneeseen energia-aineenvaihduntaan. Koska lihavuuskirurgia johtaa usein merkittävään painonlaskuun ja tyypin 2 diabeteksen paranemiseen tulisi suoliston energia-aineenvaihdunnan tutkimusta jatkaa kyseisten tautien syntymekanismin ymmärtämiseksi.

Avainsanat: lihavuus, tyypin 2 diabetes, suoliston verenvirtaus, - rasvahappojen ottokyky, -sokerin ottokyky, positroniemissio kuvantaminen, lihavuusleikkaus, incretiinit, metformiini

TABLE OF CONTENTS

ABBREVIATIONS

2-MG	sn-2-monoacylglycero
AMP	Adenosine mono phosphate
AMPK	AMP-activated protein kinase
ANOVA	Analysis of variance
AOI	Area of interest
ATP	Adenosine triphosphate
A-V	Arterio-venous
BBDR	BioBreeding Diabetic Resistant
b.i.d.	*Bis in die,* twice a day
BF	Blood flow
BMI	Body-mass index
CA	Coeliac artery
cAMP	Cyclic adenosine mono phosphate
CCK	cholecystokinin
CD36CN	cluster of differentiation 36 transport factorControls
CO	Carbon monoxide
CT	Computed tomography
DPP-4	Dipeptidyl peptidase 4
EGP	Endogenous glucose production
EEC	Enteroendocrine cells
ER	endoplasmic reticulum
FA	Fatty acid
FABP	Fatty acid binding protein
FATP-4	Fatty acid transport protein 4
FFA	Free fatty acid
^{18}F-FDG	2-[^{18}F]fluoro-2-deoxy-D-glucose
^{18}F-FTHA	14(RS)-[^{18}F]fluoro-6-thia-heptadecanoic acid
FUR	Fraction uptake rate
FWHM	Full Width at Half Maximum
GI	Gastrointestinal
GIP	Glucose dependent insulinotrophic polypeptide
GIPR	GIP-receptor
Glc6Pase	Glucose-6-phosphatase
GLP-1	Glucagon-like peptide 1
GLP-1R	Glucagon-like peptide 1 receptor
GLUT	Glucose transporter
GU	Glucose uptake
HbA1c	Glycated haemoglobin

HDL	High-density lipoproteins
ID-IF	Image derived input function
IFG	Impaired fasting glucose
HGP	Hepatic glucose production
IGT	Impaired glucose tolerance
IQR	Interquartile range
i.v.	Intravenous
LC	Lumped constant
LPL	Lipoprotein lipase
LCFA	Long-chain fatty acids
MMS	Mixed meal solution
MRAC	MRI attenuation correction
MR	Metabolic rate
MRI	Magnetic resonance imaging
OGTT	Oral glucose tolerance test
^{15}O-CO	^{15}O-carbon monoxide
^{15}O-H_2O	^{15}O-water
pAMPK	Phosphorylated AMP-activated kinase
PET	Position emission tomography
PET-CT	Position emission tomography comuted tomography
PET-MRI	Position emission tomography magnetic resonance imaging
PS	Product permeability and surface area
PPARγ	Peroxisome proliferator-activated receptor
PSL	Photostimulated luminescence
PV	Portal vein
PVE	Partial volume effect
PYY	peptide YY
ROI	Region-of-interest
RYGB	Roux-en-Y gastric bypass
SCFA	Short-chain fatty acids
SD	Standard deviation
SGLT	Sodium glucose transporter
SMA	Superior mesenteric artery
SMV	Superior mesenteric vein
SOS	Swedish Obese Subjects Study
SU	Sulfonylurea
TAC	Time activity curve
T2D	Type 2 diabetes
TG	Triglycerides
UKPDS	UK Prospective Diabetes Study
VIP	Vasoactive intestinal polypeptide

VLDL	Very low-density lipoproteins
VOI	Volume of interest
VSG	Sleeve gastrectomy
WHO	World health organization

LIST OF ORIGINAL PUBLICATIONS

i. *__Koffert J__, *Honka H, Teuho J, Kauhanen S, Hurme S, Parkkola R, Oikonen V, Mari A, Lindqvist A, Wierup N, Groop L, Nuutila P. Effects of meal and incretins in the regulation of splanchnic blood flow. Endocr Connect. 2017 Apr;6(3):179-187.

ii. *Honka H, *__Koffert J__, Kauhanen S, Teuho J, Hurme S, Mari A, Lindqvist A, Wierup N, Groop L, Nuutila P. Bariatric Surgery Enhances Splanchnic Vascular Responses in Patients With Type 2 Diabetes. Diabetes. 2017 Apr;66(4):880-885.

iii. __Koffert J__, Ståhle M, Karlsson H, Iozzo P, Salminen P, Roivanen A, Nuutila P. Morbid obesity and type 2 diabetes alter intestinal fatty acid uptake and blood flow. Diabetes Obes Metab. 2018 Jan 20. doi: 10.1111/dom.13228. Epub ahead of print.

iv. __Koffert JP__, Mikkola K, Virtanen KA, Andersson AD, Faxius L, Hällsten K, Heglind M, Guiducci L, Pham T, Silvola JMU, Virta J, Eriksson O, Kauhanen SP, Saraste A, Enerbäck S, Iozzo P, Parkkola R, Gomez MF, Nuutila P. Metformin treatment significantly enhances intestinal glucose uptake in patients with type 2 diabetes: Results from a randomized clinical trial. Diabetes Res Clin Pract. 2017 Sep;131:208-216.

*equal contribution

1 INTRODUCTION

Evolution has resulted in a highly effective mechanism for energy absorption, which, due to changes in the composition and amounts of dietary fat and sugar consumed today, lead to the accumulation of excessive amounts of calories as fat (Cordain et al., 2005). The human body obeys the First law of Thermodynamics, which states that energy is a constant. Because obesity stems from an imbalance between energy intake and expenditure, changes in our western diet and an ever-increasing reliance on using labour-saving devices has resulted in an obesity epidemic.

The prevalence in obesity has increased since the 1980s. In Finland, the mean body mass index (BMI) has increased within each income and educational group from 1978 to 2002 according to a cross-sectional surveillance study (Prattala et al., 2012). A recent pooling analysis to evaluate the prevalence and burden of obesity found that one third of the world's adults were obese or overweight in 2005, and if the same trend continues, almost 60% of the world's adult population will be obese or overweight by 2030 (Kelly et al., 2008). More than 2.8 million people die each year because of conditions associated with being overweight and this mortality originates from harmful metabolic effects associated with increased body weight such as hypertension, type 2 diabetes (T2D) and coronary heart disease. The small intestine provides the digested nutrients for the systemic circulation and further for tissue metabolism. The aim of this thesis was to identify induced changes in intestinal metabolism that are associated with obesity and T2D. In the experimental part of the study multimodal imaging techniques including positron emission tomography combined with computer tomography (PET-CT) or magnetic resonance imaging (PET-MRI) with different drugs or mixed meal interventions were used. Study subjects comprised obese subjects with T2D treated with bariatric surgery or with oral diabetes medications and normal-weight individuals. This setting allowed the comparison of differences between obese and healthy individuals in a cross sectional longitudinal design after surgical or medical intervention.

2 REVIEW OF LITERATURE

2.1 Obesity and metabolic diseases

Obesity is defined by an excess of adipose tissue. When the energy intake of an individual exceeds that individual's needs, the extra energy is stored as fat in the adipose tissues. Obesity is a multifactorial condition, and the causes of complex pathological process that can be categorised into environmental and host-related agents (Sleisenger et al., 2010). Obesity can be defined using BMI i.e. the weight in kilograms divided by the height in meters squared. Normal-weight is defined as BMI 18.5–25 kg/m^2, BMI 25–29.9 kg/m^2 as over-weight and BMI greater than or equal to 30 kg/m^2 as obese. The BMI value does not take into account differences in non-fat and fat mass, age-related body composition and racial differences (Rahman and Berenson, 2010; Rothman, 2008) it can therefore bias the association between obesity and health outcomes.

Mortality from infectious diseases has declined since 1900 (Jones et al., 2012), which has increased the lifetime expectancy of humans by almost three decades in the United States and in Europe. At the same time, consumption of highly dense calorific foods has increased (Popkin and Hawkes, 2016) and the occupational and leisure-time physical activities has decreased, which predispose to a positive energy balance (Heymsfield and Wadden, 2017). With the global increase in obesity (Finucane et al., 2011) there is concern that the trend of the increase in life expectancy in Europe and other high-income countries may come to an end (Olshansky et al., 2005)

In addition to environmental factors, some genetic mechanisms predispose to obesity. The heritability of BMI has been consistently estimated at approximately 40–70% (Bray et al., 2016). A recent meta-analysis of 340 000 individuals identified 97 genome-wide significant loci associated with BMI variations and the authors suggested that 21% of BMI variation can be accounted for by common genetic variations (Locke et al., 2015). However, other probably associated genes remain unknown.

These environmental and genetic factors interact in a complex system that regulates the energy balance. The nucleus arcuate is located in the hypothalamus where it integrates the peripheral and central signals to control food intake, physical activity and basal energy expenditure (Badman and Flier, 2005). The small intestine and associated organs such as the pancreas, liver and visceral adipose tissue senses energy uptake and homeostasis, signalling to the hypothalamus by neural and hormonal routes. Insulin and leptin (produced in the

pancreas and adipose tissue, respectively) signal long-term energy stores to the brain, which thus reduces the appetite. Circulating leptin levels are directly in proportion to the amount of body fat, thereby reflecting the status of long-term energy stores. In common forms of obesity, leptin levels are typically elevated and subjects are resistant to leptin's effects on energy homeostasis (Bluher and Mantzoros, 2009).

The enteric nervous system influences the following mechanisms: gastric and pancreatic exocrine secretion, blood flow, motility, and secretion of gut hormones (Sleisenger et al., 2010). Afferent signals from the gut to the brain, such as luminal chemical stimuli and distension, nutrients in portal circulation and pain, are transmitted via the splanchnic and vagal nerves (Raybould et al., 2004). The gut is a source of numerous peptides that can modulate enteral nerve firing (Schwartz, 2000) but also function as messengers to alter appetite and insulin secretion. Enteroendocrine cells (EECs) in the intestine sense the nutritional milieu within the gut and secrete hormones such as cholecystokinin (CCK), glucagon-like peptide-1 (GLP-1), peptide YY (PYY), glucose-dependent insulinotrophic polypeptide (GIP), amylin, ghrelin and somatostatin to regulate food intake by activating the hindbrain via specific vagal and spinal nerves (Sleisenger et al., 2010).

These gut derived peptides have potential and well-proven beneficial actions in the treatment of obesity and currently GLP-1 agonists are available for clinical use in the treatment for T2D and obesity (Irwin and Flatt, 2013). CCK is produced in the enteroendocrine I-cells in the proximal small intestine and reduces meal size, inhibits gastric emptying, coordinate gall bladder contraction and gut motility (Otsuki, 2000; Pathak et al., 2018). Infusion of CCK has been shown to decrease food intake similarly in normal-weight and obese individuals (Drewe et al., 1992; Lieverse et al., 1995). GLP-1 excretion stimulates glucose-dependent insulin secretion, inhibits glucagon secretion and gastric emptying. GLP-1-receptors are present in the brain and intracerebroventricular infusion of GLP-1 antagonist extension in animal models increases food intake and causes obesity (Meeran et al., 1999). Previous studies suggest that central GLP-1 is necessary for normal energy balance, at least in rodents (Barrera et al., 2011). GIP has, among its insulinotrophic effects, multiple effects on adipocytes, including enhancement of insulin-stimulated glucose transport and stimulation of fatty acid synthesis and their incorporation into triglycerides. Ghrelin is synthesized throughout the gastrointestinal track but mainly in the fundus of the stomach. Plasma levels of ghrelin rise during fasting and immediately before meals and fall within an hour of food intake, suggesting a role in the initiation of eating a meal. The role of ghrelin in obesity is in part still unexplained, as ghrelin levels tend to be low in obese humans, only increasing after dietary weight loss (Cummings et al., 2002).

In patients with T2D the incretin effect is diminished (Nauck et al., 1986b) but plasma measurements of GIP (Nauck et al., 1986a) and GLP-1 (Vollmer et al., 2008) are normal compared to healthy subjects without T2D.

Excess body fat increases the risk of metabolic diseases and decreases life expectancy (Peeters et al., 2003; Stevens et al., 1998). Systemic inflammation associated with obesity is linked to the pathogenesis of hypertension, coronary artery disease, strokes, diabetes, reduced lung vital capacity, arthritis, cancers and non-alcoholic steatohepatitis (Haslam and James, 2005). Accumulation of an excess of visceral fat results in a high concentration fluxes of fatty acids, cytokines and hormones in the portal blood flow from the omentum, which changes the hepatic metabolism and thereby predisposes the individual to the aforementioned diseases (Tchkonia et al., 2013). In addition, adipose tissue surrounding the kidneys may increase blood-pressure by renal compression (Hall et al., 2010), increased pharyngeal soft tissues accompanies sleep apnoea (Ashrafian et al., 2015) and excess adipose imposes excess mechanical load to joints and osteoarthritis often ensues (Goldring and Otero, 2011).

2.1.1 Type 2 diabetes

Diabetes is defined as a group of diseases that are characterized by high blood glucose levels. Although numerous diseases and stages can lead to high blood glucose levels, T2D is the most common cause. In 2007 the prevalence of diabetes was 10% in Finland and medical treatment expenses of diabetes were 1.3 billion euros. There was a 6% growth per year over the 1998–2007 period. Six years later there were almost 290 000 patients that received medication for diabetes (types 1 and 2) according to the Finnish National Social Insurance Institution (KELA). Many of the patients with evolving T2D are symptomless and therefore are unaware of their disease and have no medical treatment.

Type 2 diabetes is linked to obesity, although a vast majority of overweight individuals do not develop diabetes. Proinflammatory cytokines, insulin resistance and raised levels of free fatty acids (FFAs) with ectopic fat accumulation and mitochondrial dysfunction are the proposed link between obesity and T2D (Bjorntorp, 1991; Bournat and Brown, 2010; Kahn et al., 2006; Larson-Meyer et al., 2011). Whether unique or shared the pathogeneses that underlie obesity and T2D require further investigation (Eckel et al., 2011).

According to WHO guidelines 2006 diagnostic criteria for T2D should be maintained. The criteria for fasting plasma glucose ≥7.0 mmol/l or 2–h plasma glucose, ≥11.1 mmol/l after 75g anhydrous glucose in the oral glucose tolerance

test (OGTT) (Deckers et al., 2006). A glycated haemoglobin (HbA1c) concentration of 48 mmol/mol (6.5%) can also be used as a cut-off point for diagnosis (WHO, 2011). This definition finds only late stage of the disease without noticing prediabetic patients with evolving insulin resistance and hyperinsulinemia.

The pathogenesis of type 2 diabetes

Normal regulation of glucose metabolism is determined by a negative feedback loop involving the islet β-cell and insulin-sensitive tissues in which tissue sensitivity to insulin determines the magnitude of the β-cell response. Stimulated β-cells release insulin, thus mediating FFA, glucose and amino acid uptake by insulin-sensitive tissues. These tissues then negatively-feedback the information regarding the need for insulin to the islet cells. The feedback mediator has not been identified but it is likely to act in between the humoral system and the brain (Kahn et al., 2014). In insulin-resistant stages, the β-cell increases its insulin secretion to maintain normal glucose concentration in the plasma. When the β-cells are incapable of reducing blood glucose, it results in the elevation of plasma glucose (Kahn et al., 2014).

Environmental drivers and genes together are crucial factors of insulin resistance and β-cell dysfunction. Genome wide association studies have found more than 50 gene loci linked to T2D (Morris et al., 2012) but do not always associate with both fasting and 2-hour glucose values (Scott et al., 2012). Since our gene pool has not changed dramatically in the last decade, environmental changes have been critical in the T2D epidemic. Increased amounts of dietary fat and especially dietary saturated fat are important factors in the development of obesity, insulin resistance and β-cell dysfunction (Hu et al., 2001). Further, environmental chemicals (Thayer et al., 2012), in utero environment (Guenard et al., 2013), vagus nerve (Miller, 1981) and dysregulation of α-cells (Dunning and Gerich, 2007) have also been studied in the pathogenesis of T2D.

When the caloric intake exceeds an individual's energy expenditure for long periods, carbohydrates undergo de novo lipogenesis under hyperinsulinaemic conditions in the peripheral tissues and in the liver (Sidossis et al., 1996). Increased levels of insulin in the portal vein (PV) increase the amounts of fatty acids synthesized from glucose, which can lead further to fatty liver and increased levels of plasma FFAs (Adiels et al., 2006). A combination of increased delivery of FFAs to other tissues such as the pancreas and a hyperglycaemia eventually inhibit the insulin secretion from the islet ß-cells, thus leading to the clinical onset of diabetes (Figure 1.).

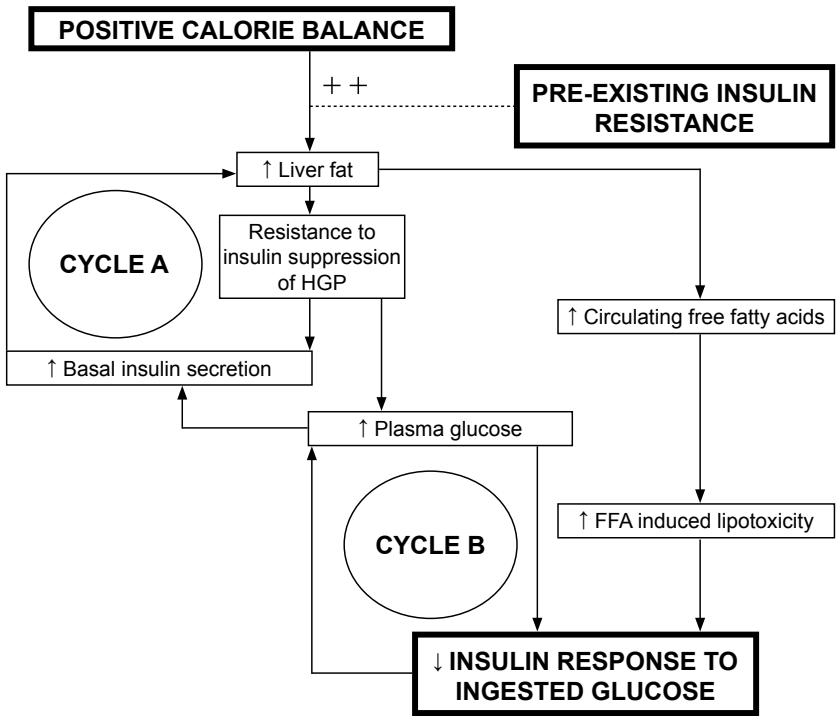

Figure 1. The two cycles represent impaired hepatic (A) and systemic (B) glucose intolerance in the pathogenesis of type 2 diabetes. Continuous positive energy balance leads to excess fat accumulation in the liver, which leads to insulin resistance in the liver. In turn, the increased liver fat will cause relative resistance to insulin suppression of hepatic glucose production. Because insulin stimulates de novo lipogenesis, individuals with a degree of insulin resistance will accumulate liver fat more readily than others because of higher plasma insulin levels. This causes systemic hyperglycaemia and increased levels of circulating free fatty acids (FFAs) due to increased hepatic glucose and FFA output and hyperinsulinemia while the ß-cells strive for normoglycaemia. Glucose mediated insulin secretion from ß-cells is decreased due to FFA induced lipotoxicity (Giacca et al., 2011). Figure adapted with permission from (Taylor, 2008).

Since intraluminal nutrients trigger a complex and integrative gut-brain feedback to prevent energy excess by suppressing food intake, the emerging evidence suggest that the gastrointestinal track plays a significant glucoregulatory role (Duca et al., 2015). The EECs are activated by a variety of nutrient-dependent machinery to stimulate gut peptide release (Psichas et al., 2015) to the circulation or locally to activate afferent nerve terminals. Intestinal nutrient sensing plays a physiological role in the maintenance of blood glucose levels by regulating hepatic glucose production (HGP) at least in rodents (Cheung et al., 2009). A blocking of the action of CCK (Cheung et al., 2009) or of GLP-1 (Vahl et al., 2007) in animal models led to disturbances in glucose metabolism. Whether these pathways are relevant in humans requires further investigations (Ramnanan et al., 2012; Titchenell et al., 2015).

Over time insulin levels decrease as a result of reduction of ß-cell function. The Whitehall II study reported that this deterioration happens three to six years before the detection of T2D (Tabak et al., 2009), which is in line with other previous studies that show the increasing trend in fasting glucose values vary from 1.5 to 3 years before diagnosis (Ferrannini et al., 2004; Laspa et al., 2007; Sattar et al., 2007). A decremental decrease in insulin secretion capacity as a consequence of ß-cell dysfunction in insulin resistant subjects finally results in frank T2D with fasting and postprandial hyperglycaemia.

Long standing T2D predispose to microvascular complications such as diabetic retinopathy, nephropathy and neuropathy (Turner and Holman, 1995). Glycation end products, polyol accumulation and oxidative stress damage the specific cell-types, which causes macrovascular complication (strokes, coronary artery disease and peripheral arterial disease) due to atheroma formation in the larger arteries.

Incretins

Incretin hormones are secreted from the EECs along the small intestine, when a mass of digesting food with bile acids comes into contact with the mucosa. Two well-known incretin hormones are GLP-1 and GIP. These hormones mediate the incretin effect, which can be defined by the amplification of insulin secretion when glucose is given via the oral route and compared to the isoglycaemic intravenous administration of glucose (Perley and Kipnis, 1967). The incretin effect primarily contributes to the postprandial regulation of glycaemia, which potentiates insulin secretion from the pancreatic islet following a meal. The insulin secretion response to oral versus intravenous (i.v.) administration is 3- to 4-fold than without the secretion of incretins and defects in incretin effects can contribute to T2D. Fasting incretin levels are low but rise shortly (within 15 minutes) after meal ingestion and return to basal levels between two to three hours (Drucker, 2006).

GLP-1 is a 30-amino acid residue polypeptide, which is secreted by L-cells that are located mainly in the distal small intestine. After its secretion into the PV, the active hormone is rapidly inactivated by dipeptidyl peptidase 4 (DDP-4) this short-cycle gives GLP-1 a half-life of only 1–2 minutes in the circulation (Heymann and Mentlein, 1978; Hopsu-Havu and Glenner, 1966). The primary function of GLP-1 is the potentiation of glucose-stimulated insulin secretion (Vilsboll et al., 2003a) but it also slows gastric emptying (Horowitz et al., 1996b), inhibits glucagon secretion, reduces appetite and increases ß-cell mass (in animals) (Xu et al., 1999).

GIP is a 42-amino acid residue polypeptide whose effects are mediated via 7 transmembrane G-protein coupled receptor, GIP-receptor (GIPR). GIP secreting K-cells are mainly located in the duodenum and the proximal part of the jejunum,

which are sites that are both bypassed in Roux-en Y gastric bypass. However, some of K-cells are also found throughout the small intestine (Mortensen et al., 2000) and are exposed earlier to nutrients after bariatric surgery. GIPs primary function is the glucose-dependent stimulation of insulin secretion (Vilsboll et al., 2003a).

Incretins in type 2 diabetes

Krarup and co-workers showed in the late 1980s that the insulinotrophic effects of GIP are lost in pigs with T2D (Krarup et al., 1987). Supra-physiological GIP doses in patients with mild T2D had only minor effects on insulin secretion, whereas GLP-1 infusion increased insulin secretion and normalized the glucose values (Nauck et al., 1993). The molecular mechanism behind the reduced secretion of incretins (Nauck et al., 1986a) and incretin facilitated insulin secretion are obscure but are strongly associated with the pathogenesis of T2D.

2.1.2 Treatment strategies

According to the World Health Organisation (WHO) 2016 report, the number of people with T2D and obesity has quadrupled in the last three decades, with estimates of around 600 million confirmed cases of obesity and 422 million cases of diabetes worldwide. This represents a huge burden in terms of societal health and associated escalating costs for the treatment and management of the diseases and related complications (Seuring et al., 2015). Our understanding of T2D pathogenesis is increasing rapidly, health care has effective medications and interventions to provide for obese individuals and patients with T2D, the food industry affluent countries offers low-calorie groceries, nourishing and healthy food and leisure-facilities are easily available to individuals. Yet despite these measures populations are still gaining weight. Without increasing the awareness of the hazards of obesity and life-style changes in risk groups, the increase in life expectancy of populations in Europe and other high-income countries may come to an end (Olshansky et al., 2005).

Diet interventions

The basis for treatment of overweight and obese individuals is the promotion of a healthy lifestyle and weight reduction over 5% of total weight by increasing the physical activity and decreasing calorie intake (WHO, 2000). Diet interventions reduce weight on average by 5 to 6% over 9 to 12 months (Dansinger et al., 2007) but the long-term outcome relies on supervision, intensity and timing of the intervention and also the motivation of the patient. In the initiation period calorie deficiency should be 500–1000 kcal/day, which usually leads to 0.5–1 kg weight

loss per week. When the target weight is achieved it should be maintained with permanent diet changes. The recommended diet for the obese subject should consist of 25–35% fat, 40–60% carbohydrates and 15–25% protein. A recent meta-analysis revealed that a low-carbohydrate diet reduced HbA1c levels, triglyceride concentration, and increased HDL in patients with T2D compared to normal or high-carbohydrate diets (Meng et al., 2017).

Exercise

In addition to diet changes, regular aerobic exercise increases the weight reduction by a few kilograms in 3–6 months (Avenell et al., 2004). To achieve a new target weight, a daily 300 kcal energy expenditure by aerobic exercise is recommended (Saris et al., 2003), which entails 45–60 minutes of moderate intensity physical exercise daily. Even though the increased activity does not always lead to weight reduction, it reduces visceral fat and the risk of T2D.

Bariatric surgery

In 1954, Kremen and co-workers devised the jejuno-ileal bypass to treat severe dyslipidemia (Kremen et al., 1954) but the procedure had major side-effects: dehydration and severe diarrhoea. In 1967, however, Drs. Mason and Ito noticed that patients lost a considerable amount of weight after having sub-total gastrectomy (Mason and Ito, 1967). Several modifications to the techniques has been suggested in recent decades but finally the first laparoscopic Roux-en-Y gastric bypass (RYGB) (Wittgrove et al., 1994) in the 1994 launched the exponential growth of metabolic surgery.

Bariatric surgery is indicated for treating morbid obesity when conservative weight lost methods are unsatisfactory and surgically induced weight loss is expected to improve obesity-related problems. The patient should have shown the ability to lose weight (at least 5–7%) and compliance for scheduled medical appointments. According to European guidelines, patients aged from 18 to 60 years with a BMI >40 kg/m^2 without co-morbidities or BMI >35 kg/m^2 with co-morbidities can be considered for surgery (Fried et al., 2013). A debate about strict BMI levels has arisen in recent years after it was shown by Cohen and his co-workers, that 88% of the T2D patients with poor glycaemic control and a BMI of between 30–35 kg/m2 went into remission after RYGB (Cohen et al., 2012). Numerous randomized controlled trials document the effect and an acceptable complication rate of bariatric surgery even for the lower BMI baseline and new DSS-II guidelines suggest a BMI cut-off point should be lowered (Parikh et al., 2014; Rubino et al., 2016). Compared to a conventional diet and pharmacological treatment with modest results bariatric surgery has been reported to be associated

with a 76% remission rate of T2D and 50% cases experienced loss of some excess weight (Buchwald et al., 2004; Dixon et al., 2008).

Standard bariatric procedures that are currently available in Finland are RYGB and sleeve gastrectomy (VSG). Currently, the RYGB is considered to be the golden standard. Both laparoscopic procedures restrict the gastric pouch and speed up the nutrient contact with small intestine mucosa. However, the mechanisms by which bariatric surgery results in the remission of T2D are unclear. In VSG, approximately 80% of the ventricle (curvature major and fundus) is excised and making the ventricle tubular, banana-shaped pouch. The RYGB by comparison entails the creation of a small ~30 ml pouch by stapling-off the top of the stomach from the rest of the stomach. The jejunum is excised at about 50 cm length from the ligamentum Treiz and then anastomosed to the created stomach pouch to construct a gastro-jejunal anastomosis. Then an enteroanastomosis is created about 150 cm distal to the gastro-jejunal anastomosis (Figure 2).

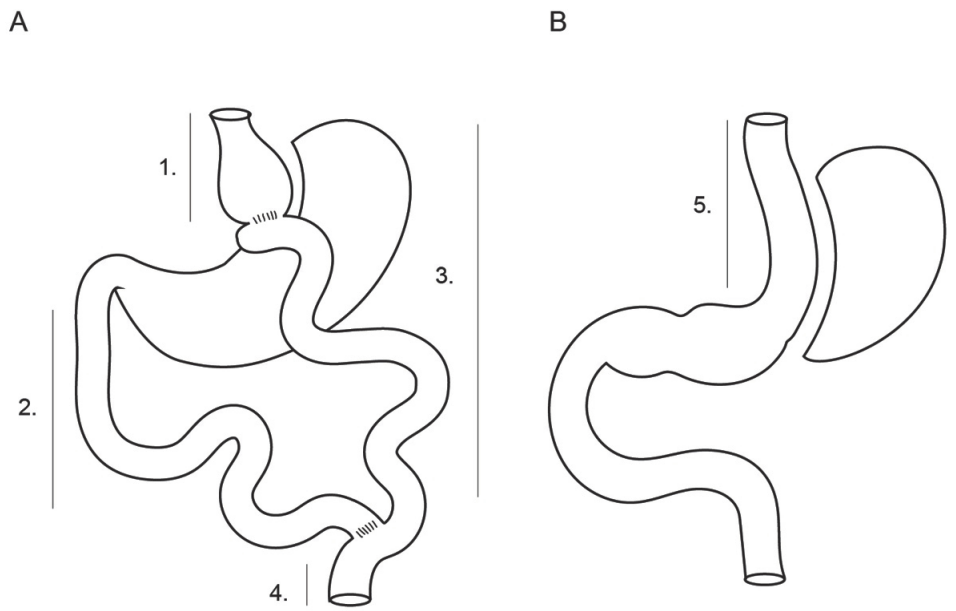

Figure 2. Bariatric procedures Roux-en-Y (RYGB, A) and sleeve gastrectomy (VSG, B). In RYGB a small 30 ml pouch (1.) is created by stapling-off and thereby dividing the top of the stomach from the rest of the stomach. An alimentary Roux-limb is constructed (3.) by transecting the jejunum about 50 cm from the ligamentum Treiz and making a gastro-jenunal anastomosis by connecting this to the created stomach pouch. Then an enteroanastomosis is created about 150 cm distal to the gastro-jejunal anastomosis (4.) The VSG procedure entails approximately 80% of the ventricle (curvature major and fundus, 5.) is excised and making the ventricle tubular, banana-shaped pouch contiguous with the Duodenum.

In studies by both the Laferrere and the Plum groups, obese patients with T2D had greater improvement in glucose tolerance and insulin sensitivity after RYGB

compared to patients who had lost the equivalent amount of weight with diet interventions (Laferrere et al., 2008; Plum et al., 2011). Although restrictive bariatric surgery reduces the size of the gastric pouch and diminishes the calorie intake by reducing appetite, changes in the gastrointestinal hormones due to altered chyme contact in the small intestine play a putative role.

Two main hypotheses are believed to influence the metabolic change after bariatric procedures and these are referred to as the foregut and the hindgut hypotheses (Patriti et al., 2007; Patriti et al., 2005; Rubino et al., 2006; Rubino and Marescaux, 2004; Wang et al., 2008) (Figure 3.). The foregut exclusion hypothesis suggests that the bypassed duodenum and proximal jejunum diminishes the effect of anti-incretin, a substance that antagonizes the action of incretins and the production of insulin (Holst et al., 2009). Many human studies have shown that GIP levels markedly decrease after RYGB, and most likely because of the lack of nutrient stimuli to the K cells in the bypassed part of the duodenum and proximal ileum (Clements et al., 2004; Rubino et al., 2004). In contrast, Hansen and his colleagues (Hansen et al., 2011) measured GIP and GLP-1-levels in venous plasma during the mixed meal solution (MMS) stimulus before and after the Roux-en-Y procedure, and found that jejunal administration of liquid meal resulted in an earlier GIP secretion peak after the surgery.

The hindgut exposure hypothesis states that early delivery of nutrients to the distal small intestine increases the production of GLP-1 (Chambers et al., 2011; Laferrere et al., 2008), which leads to the desired effects on glucose metabolism. The suggested mechanism behind this phenomenon is increased insulin secretion in response to postprandial nutrient load, which suppress endogenous glucose production and stimulate glucose clearance.

The secretion of other hormones is also altered after bariatric surgery which may interact with glucose homeostasis. Ghrelin is one of the hormones that may play a role in energy balance. It is mainly secreted from fundus and it stimulates the food intake (Druce et al., 2005; Wren et al., 2001). After diet-induced weight loss, ghrelin levels tend to rise leading to an increased appetite and increased calorie intake. Generally, gastric surgery leads to a decrease in ghrelin concentrations despite the weight loss (Cummings et al., 2002) but also opposite findings have been reported (Faraj et al., 2003). PYY is secreted from the L-cells from the distal jejunum simultaneously with GLP-1. Human studies have shown that PYY secretion decreases the food intake (Batterham et al., 2003). At least two study groups have shown that gastric surgery increase the circulating levels of PYY (Morinigo et al., 2006b; Morinigo et al., 2008) and this might explain the diminished food intake. These hormones may act on they own or potentiate the effects of incretins after metabolic surgery.

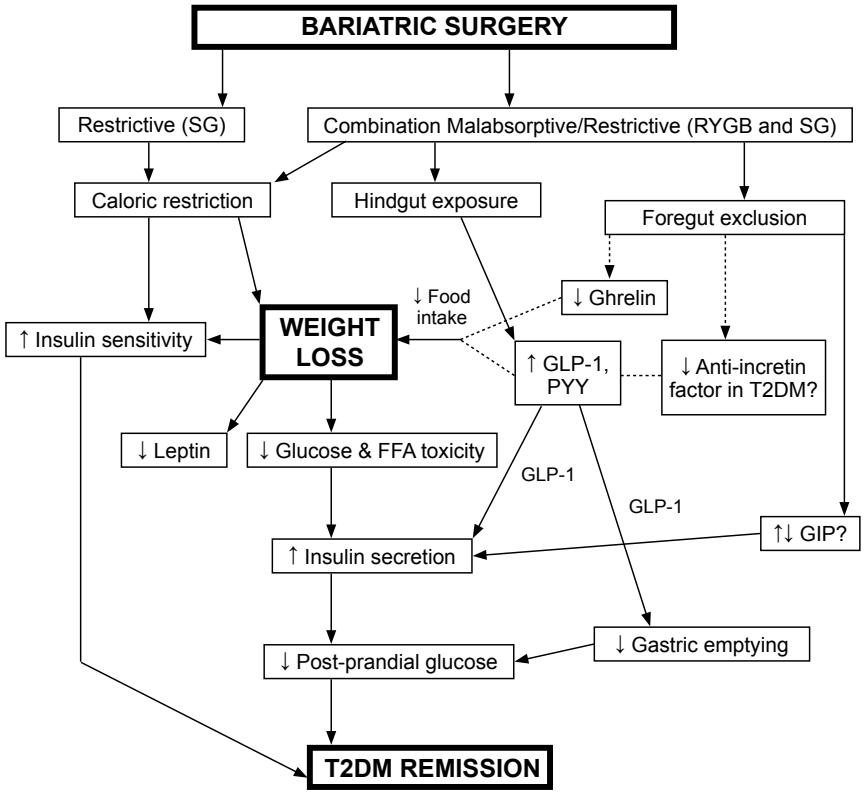

Figure 3. Potential mechanism of bariatric surgery in the type 2 diabetes remission. A courtesy of (Bose et al., 2009).

In previous studies in RYGB treated rodents, Roux limb have displayed hyperplasia and hypertrophy (le Roux et al., 2010; Taqi et al., 2010), likely to create more absorptive surfaces (Shaw et al., 2012). Shin and his colleges documented intense basolateral glucose uptake in RYBG-treated rats by Roux limb (Saeidi et al., 2013), which contributed to the better glycaemic balance. Whether bariatric surgery changes the metabolism of the entire small intestine remains unanswered.

The Swedish Obese Subjects Study (SOS) is a long-term, prospective, controlled intervention trial comprising 2010 obese patients whom had undergone bariatric surgery and whom had been matched with obese controls receiving usual care (Sjostrom, 2013). Even though only 13% of patients were guided to RYGB and majority to restricting procedures, the study provides the best evidence of long-term (10–20 years of follow up) effects of bariatric surgery. Key results from the SOS-study indicate a reduction in overall mortality (Hazard Ratio [HR] 0.76, 95% CI 0.54–0.92)(Sjostrom et al., 2007), cardiovascular events (HR 0.67, 95% CI 0.54–0.83) (Sjostrom et al., 2012) and cancer (in women only: HR 0.58, 95% CI 0.44–0.77) (Sjostrom et al., 2009).

Intestinal adaptation after bariatric surgery

After bariatric surgery, the alimentary limb and the common channel adapt to malabsorption by growth of the villi in height and width, which is already apparent on the seventh postoperative day, at least in experimental animals (Martinez Moreno et al., 2017). This hyperlplasia is shown to be associated with increased intestinal glucose uptake to support cell growth (Saeidi et al., 2013). In addition, RYGB surgery in experimental rodent study decreased SGLT1-mediated glucose uptake in the alimentary limb, which could contribute to the metabolic benefits of the surgery (Stearns et al., 2009). A recent study by Cavin and colleagues showed that glucose transport capacity of the alimentary limb was reduced and the density of cells secreting GLP-1 was increased in response to VSG. They also noted that after RYGB, the intestine became hyperplasic, the number of GLP1-secreting cells increased and thus diverted glucose for the intestine's own growing needs (Cavin et al., 2016).

Anti-obesity drugs

Currently there are two antiobesity agents in clinical use in Finland. Orlistat is long acting reversible inhibitor of gastrointestinal and pancreatic lipases, which hydrolyse dietary triglycerides. Inhibition of these lipases improved weight reduction and decreased weight regain in a placebo-controlled study of obese patients (Sjostrom et al., 1998). The most common adverse events with this drug were faecal urgency and a lack of fat-soluble vitamins (Yen and Ewald, 2012). Another available agent is extended release naltrexone/bupropion. In the animal studies this combination activates two brain areas involved in energy balance: the melanocortin system in the hypothalamus and the mesolimbic dopaminergic reward system (Ornellas and Chavez, 2011). The exact mechanism of action of naltrexone/bupropion as antiobesity treatment is poorly understood but 5–9.3% of patients have achieved clinically meaningful weight loss of >5% in placebo-controlled trials of 55 weeks (Hollander et al., 2013; Wadden et al., 2011). In addition, GLP-1 agonists have been used as anti-obesity drugs, see incretin-based therapies.

Anti-diabetic drugs

Insulins

Insulin that had been isolated from cattle pancreas was used for the first time by Banting Best and Collip to treat hyperglycaemia in a diabetic boy in Canada in 1922. Soon after these experiments, the pharmaceutical industry scaled-up the commercial production of and insulin became commercially available in the United States in 1923. The next landmark in the development of insulin was the crystallization of insulin, which 'opened the doors, for the extended-action insulin

preparations (White, 2014). Before 1983 all insulins were derived from animal sources and this changed in 1983 when the first recombinant human insulin was developed. After these achievements research has focused on short-acting and ultra-long-acting insulin development.

Insulin therapy in clinical practice is often needed to maintain glycaemic control when ß-cell failure progress. Insulin is indicated when a patient has an HbA1c >10%, hyperglycaemic symptoms or when glycaemic targets are not reached with two oral antidiabetic drugs (Inzucchi et al., 2012). Even though insulin treatment is an effective way to tackle hyperglycaemic episodes, a few concerns about its use still remain. For example, the UK Prospective Diabetes Study (UKPDS) reported that insulin therapy resulted in more hypoglycaemia events and weight gain compared to conventional treatment (1998b). Treatment intensification with insulin increased weight by 1–3 kg in 24 weeks and predisposed to hypoglycaemic events in recent trials (Control et al., 2009; Group et al., 2008).

Even today insulin adherence is low compared to oral antidiabetic treatments. This might be because of fear of hypoglycaemia and concerns about injections and adverse events (Polinski et al., 2013). New insulin preparations, monitoring technologies and delivery methods are constantly being evolved and should offer better and easier solutions for patients with T2D in the future.

Incretin-based therapies

The incretin effect in T2D is severely reduced but can be provided by supraphysiological doses of GLP-1 analogues or by the inhibition of DDP-4, which inactivates native GLP-1. The aforementioned drug classes potentiate glucose-stimulated insulin secretion from ß-cells (Nauck, 2009) and also regulate gastric emptying, appetite and weight gain.

DDP-4 inhibitors, known as gliptins, have been reported to reduce DDP-4 enzyme activity by 80% (Ahren et al., 2004) and this is associated with increased insulin and suppressed glucagon secretion. A recent systematic review found that all gliptins were equal in effect and safety in either monotherapy or in combination with other glucose lowering agents (Craddy et al., 2014). The use of DDP-4 inhibitors in patients with T2D on average reduce HbA1c by 0.5%, decrease postprandial glucose concentrations with minor risk for hypoglycaemia and weight gain (Craddy et al., 2014). Recent post-marketing reports on adverse events in DDP-4 inhibitor users reported increased cases of pancreatitis and pancreatic carcinomas, although causal association was not established.

Injection of GLP-1 receptor (GLP-1R) activators, such as exenatide, dulaglutide and liraglutide, result in a 4- to 6-fold higher GLP-1R activity compared to DDP-

4 inhibitors (Degn et al., 2004). However, it requires two injections of exenatide a day due to its short half-life (2.4 h). Development of new molecules has led to longer half-lives and prolonged duration of action. The use of GLP-1R agonists reduce HbA1c by 1%, decrease fasting and postprandial glucose values and reduces weight by 1–4 kg (Drucker et al., 2008; Shyangdan et al., 2011). The most common adverse event in the beginning of GLP-1R agonist use is nausea, which usually ameliorates in a few weeks. As in DDP-4 inhibitors, GLP-1R activators were also associated with increased risk of pancreatitis and pancreatic carcinomas, whereas the mechanism of this association in unclear (Egan et al., 2014).

Along with better glycaemic control, incretin-based therapies reduce systolic blood pressure, triglycerides and total cholesterol and improve ß-cell function. In the double-blinded randomized LEADER-study 1.8 mg of liraglutide once a week decreased death from cardiovascular and all cause death compared to placebo in patients that had a high cardiovascular risk (Marso et al., 2016). A recent critical review of five randomized placebo-controlled trials reported that liraglutide administered in a weekly dose of 3.0 mg resulted in 4 to 6 kg weight reduction of obese subjects (Mehta et al., 2017).

Sodium-glucose transporter inhibitors

Gliflozins inhibit the sodium-glucose transporter 2 (SGLT2) protein, which increases the renal glucose reabsorption threshold. The SGLT2 actively reabsorbs 90% of the glucose in the proximal nephron from the primary urine. Inhibition of these proteins leads to increased urinary excretion of glucose and finally reduce in plasma glucose. The first gliflozins were approved for clinical use in 2012 and seven molecules are currently in clinical use.

The increased urinary excretion of glucose result in a loss of calories, which might contribute to the weight loss (Neumiller et al., 2010). These agents lower the HbA1c by 0.5 to 1.0%, promote weight loss and reduce systolic and diastolic blood pressure with low risk of hypoglycaemia (Whalen et al., 2015). Glycosuria with an SGLT2 inhibitor increase the risk of genitourinary infections in both sexes which is the most common adverse event in this drug class.

Two large randomized placebo-controlled trials EMPA-REG and CANVAS documented a decreased risk for cardiovascular events in patients with T2D with high cardiovascular risk (Neal et al., 2017; Zinman et al., 2015). The gliflozins act as low-potency SGLT-1 inhibitors and at least canagliflozin seems to reduce SGLT-1 mediated glucose uptake from the small intestine after meal ingestion (Polidori et al., 2013). Further research on the action of gliflozins in the intestine is warranted in the future.

Sulfonylureas

The hypoglycaemic effects of sulfonylureas (SU) were discovered in 1937 but it took until the 1950s when the first SU was approved for marketing in Germany. The third generation SU, glimepiride, was released in 1995 and is still widely used as a first-line antidiabetic treatment (Desai et al., 2012).

The SUs stimulate exocytosis of insulin-containing granules from the ß-cells by the inhibition of ATP-sensitive potassium channels (Ashcroft and Rorsman, 1989). A recent meta-analysis of 31 trials showed that monotherapy using SU reduced HbA1c by 1.5% and SU in combination therapy reduced HbA1c by 1.6% (Hirst et al., 2013) with a 10% risk of hypoglycaemia (Schopman et al., 2014). The use of SU in recent years has decreased due to hypoglycaemic episodes, which led the way for newer treatments.

Thiazolidinediones

Thiazolinedinones are selective ligands for nuclear transcription factor peroxisome proliferator-activated receptor gamma (PPARγ) that were approved as a glucose-lowering therapy for T2D in 1997. Thiazolinediones such as pioglitazone and rosiglitazone act as insulin sensitizers that increase insulin-stimulated glucose uptake in adipose tissue (Nolan et al., 1994). The PPARγ receptors are expressed in the adipose tissue, in the pancreas and in the endothelial cells (Dubois et al., 2000; Willson et al., 2001) and the activation of these receptors results in lower fasting and postprandial plasma glucose concentrations in addition to decreased levels of insulin and FFAs (Miyazaki et al., 2001; Nolan et al., 1994). Increased insulin sensitivity in the adipose tissue steers the FFA towards the adipose tissue, which thereby might spare other insulin sensitive organs such as the liver and muscles from the potentially harmful effects of elevated FFAs. Further, it was shown in studies in rodents that PPARγ-agonists enhance adiponectin secretion from the adipocytes, which has anti-atherogenic and insulin-sensitizing effects (Maeda et al., 2002; Matsuda et al., 2002). Despite the favourable impact in glucose and fatty acid metabolism, concerns about cardiovascular problems and bladder tumours rise. In 2007, Nissen and Wolski published a meta-analysis that reported a rosiglitazone associated increase in the risk of myocardial infarction (Nissen et al., 2007). A few years later, the large multicentre RECORD study concluded that rosiglitazone increases the risk of heart failure and bone fractures (Home et al., 2009). These findings resulted in rosiglitazone's withdrawal from Europe in 2010–2011. At the same time a Canadian cohort study showed that pioglitazone had a smaller risk for heart failure and deaths compared to rosiglitazone (Juurlink et al., 2009). There are also concerns about an increased risk of blabber cancer associated with piolitazone, which has (Lewis et al., 2011) decreased its use.

Metformin

Metformin is the only biguanide in clinical use today. It has been used for its glucose lowering function since 1957 in Europe. Metformin's favourable profile in the treatment of patients with T2D was confirmed in the UKPDS in the 1998 (1998a). Metformin decreased the risk of myocardial infarction by 39%, and death of any cause by 36% when compared to diet treated study subjects. It has been shown to lower the fasting glucose and HbAlc concentrations without weight gain or risk of hypoglycaemia.

Metformin's mechanisms of action are still poorly understood. Metformin has previously been demonstrated to control hepatic glucose production through mechanisms that involve adenosine monophosphate (AMP) AMP-activated kinase (AMP-K) (Zhou et al., 2001), mitochondrial metabolism (Brunmair et al., 2004) and recently, glucagon receptor signalling and cyclic AMP (cAMP) production (Cao et al., 2014)

Wilcock and co-workers published a study in 1994 using a diabetic mouse model that showed that intravenously administered metformin selectively accumulated in the small intestine (Wilcock and Bailey, 1994). Drug concentration of metformin was 300 times higher in jejunum tissue samples than plasma concentrations after oral administration (Bailey et al., 2008). Thus, the retention of metformin by tissues of the small intestine is important and may represent a target for the drug. Metformin concentrations are higher in the intestinal mucosa than other tissues, therefore it is anticipated that the drug will have different effects in this tissue notably in terms of increasing anaerobic metabolism associated with an increase in lactate. A study that used high-fat-fed rats showed that intestinal glucose uptake (GU) is almost totally suppressed and can be restored by metformin treatment (Mithieux et al., 2006). Metformin treatment in insulin-resistant mice that had been induced by high fat low carbohydrate diet- increased the amount of GLUT2 in the apical enterocyte membrane and improved glucose homeostasis and simultaneously giving a 3-fold increase glucose release into the intestinal lumen (Ait-Omar et al., 2011). These previous findings imply that at least part of the beneficial action of the metformin on glucose haemostasis may be explained by its effect on the intestine.

2.2 Intestinal anatomy and functions in healthy and obese subjects

The small intestine is a specialized tubular structure about 300 to 700 cm of length from the pylorus of the stomach to the ileocecal valve in the proximal colon. The small intestine is nourished by the coeliac and the superior mesenteric arteries. The coeliac artery (CA) has three major divisions: the left gastric artery, the common

hepatic artery and the splenic artery. All of these division further subdivide into smaller branches (see figure 4). The CA supplies the proximal part of the duodenum and the superior mesenteric artery (SMA) the rest of the small intestine, jejunum and ileum. Venous blood drains parallel to the arteries into the superior mesenteric vein (SMV) and further to the PV, which supplies 70–80% of the liver's blood delivery. The colon is a tubular structure that starts from the ileocoecal valve and ends at the anal verge. It is about 150 cm long and nourished by the superior and inferior mesenteric arteries, the superior mesenteric artery delivers blood to the proximal part and the inferior to the distal part (Figure 4). Venous flux is delivered to the PV through the inferior mesenteric vein (Sleisenger et al., 2010).

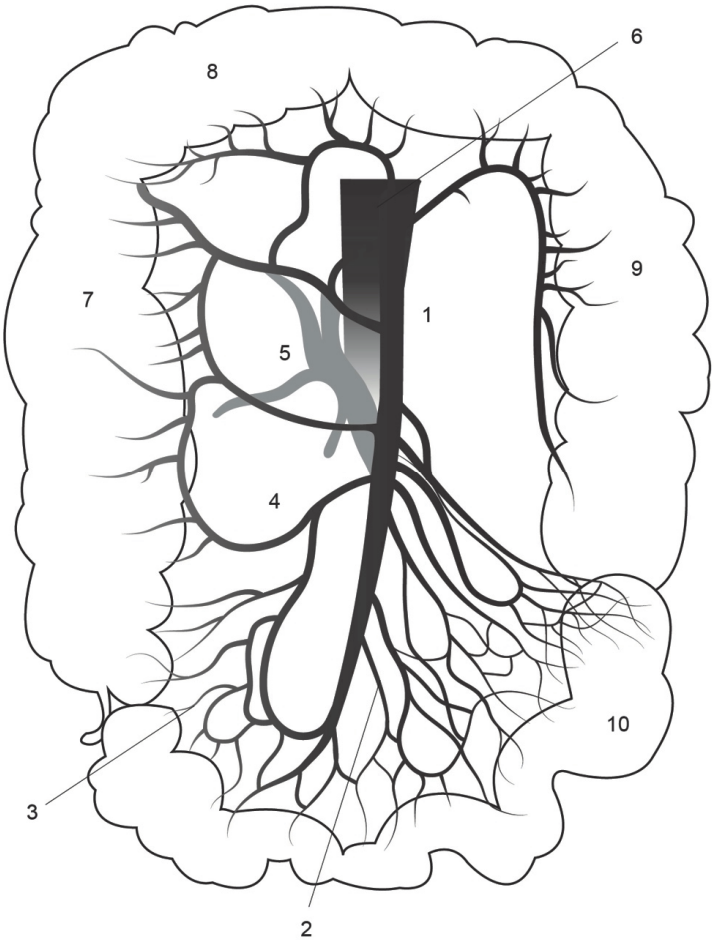

Figure 4. Representing arterial circulation to the jejunum (10) and the proximal colon (7–9). Arteria mesenterica superior (SMA) (1.) rise from abdominal aorta (6) and divides into branches that supply the small intestine (10) and the proximal colon (7–9). SMA is further divided into jejunal (2), ileal (3.) and ceolic (4) branches. Venous circulation from the intestine flow into the portal vein (5).

Although the jejunum and part of the ileum are mobile and attached to the posterior wall of the abdominal cavity by the intestinal mesentery, the proximal part of the duodenum, ascending and descending colon are retroperitoneal and fixed to their locations. The aforementioned mesentery envelopes the intraperitoneal organs, SMA and SMV, nerves, lacteals and lymph nodes.

The walls of the small intestine and colon are composed of four layers: mucosa, submucosa, muscularis and adventitia (Figure 5). The mucosa is a thick vascularized layer that consists of glandular epithelium, lamina propria and muscularis mucosae. It has folds, villus-crypt structures and microvilli, which increase the mucosal surface area 400- to 500-fold. The villi are covered with absorbing enterocytes on the capillary bed, which facilitate the rapid absorption of nutrients. The mucosal layer is composed mainly of absorptive (columnar), secretory (Paneth), mucus producing goblets, stem and neuroendocrine cells. The submucosa is fibrous connective tissue that supports the mucosal layer in its absorption function and it has a rich network of blood and lymph vessels. The muscularis propria consists of two layers of muscle fibers, which are responsible for the movement of the luminal contents. The serosa comprises connective tissue that surfaces the whole intestine.

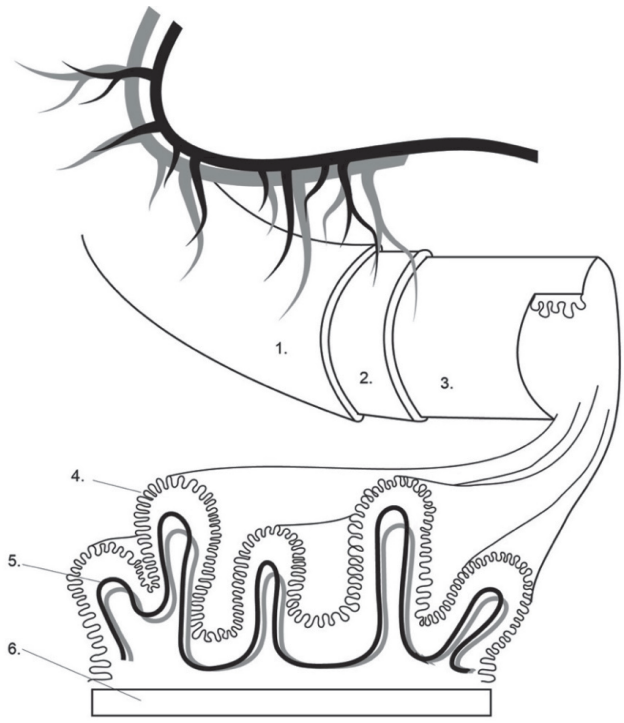

Figure 5. Representing the small intestine microarchitecture. 1. Serosa 2. Muscularis propria 3. Mucosa and submucosa 4. Epithelium 5. Lamina propria and muscularis mucosae 6. Submucosa.

The intestine participates in fluid and electrolyte absorption and in digestion and absorption of glucose, proteins and dietary fat. The whole gastrointestinal track processes about nine litres of fluids daily, and this volume of fluid is derived from the diet (1500 ml) and exocrine secretion such as salivary, gastric, biliary, pancreatic and intestinal secretions. Processed fluid is absorbed by the small intestine (seven liters) and colon (1500 ml), whereas only 100 ml is lost in the stools. This is due to a 500-fold amplification of the absorptive surface by the fold-, villus- and microvilli structure in the small intestine and spatial separation of the surface cells and crypts, which facilitates the efficient absorption of the fluids (Sleisenger et al., 2010).

Food ingestion leads to physiological responses in the regulation of appetite and plasma glucose concentration, changes in the gastrointestinal (GI) tract motility and endo- and exocrine secretion. The enteroendocrine system of the gut provides detailed signals of the ingested ingredients that are sent to the brain and the pancreas by secreting gut peptides into the blood stream (Sleisenger et al., 2010). These peptides are secreted by the enteroendocrine cells that are located in the epithelial layer of the gastrointestinal (GI) tract (Sjolund et al., 1983). Each different cell type I, K and L secrete its specific hormone CCK, GIP and GLP-1, respectively. Secretion of the aforementioned hormones is triggered by the ingestion of lipids, proteins and carbohydrates, which come in contact with the apical openings of the cells in the gut lumen and this event leads to the secretion of these peptides into the blood stream (Herrmann et al., 1995). Typically, K cells are located in the duodenum and I cells in the jejunum, ileum and colon (Sjolund et al., 1983). CCK and GIP are released into the bloodstream when the chyme enters the duodenum, whereas GLP-1 appears in blood when digesta has moved aborally further down the GI tract (Pilichiewicz et al., 2007a; Pilichiewicz et al., 2007b).

The human intestine is colonized by environmental bacteria soon after birth and in adults' the intestinal lumen contains from one to two kilograms of bacteria that comprise 9 divisions and over 1000 species of bacteria, majority belonging to Bacteroides and Firmicutes phyla (Human Microbiome Project, 2012; Sleisenger et al., 2010). The diversity of intestinal microbiota is defined by the numbers and abundance distribution of different microbial species and it is correlated to the host's energy metabolism and low-grade inflammation (Cani and Delzenne, 2009). The carriage of intestinal phyla varies over time in the same healthy subjects but the metabolic functions of the microbiome remain stable, which demonstrates the huge versatility in microbial function (Human Microbiome Project, 2012). The colon mediates the slow transit of nutrients under anaerobic conditions, wherein the microbiome ferments indigestible carbohydrates to produce short-chain fatty acids (SCFA) for the host (Cummings et al., 1987; Nicholson et al., 2012),

synthesizes vitamins (Nicholson et al., 2012) and modulates the host immune protection (Hooper et al., 2001). Although the microbiota harvest the indigestible fibers and partly convert them to SCFAs and further provides energy to host it plays a marked role in daily energy balance. The study by Shin and his co-workers show that the microbiome contribute to the antidiabetic mechanism of metformin (Shin et al., 2013). Intestinal mucosa and the microbiota on its surface provide an enormous interface for continuous complementary interaction with the host immune system and bacterial species. Further investigation on integrative pathophysiology of obesity and diabetes are warranted to understand these sophisticated interactions.

2.2.1 Intestinal blood circulation

Fasting intestinal blood flow varies from 30 to 140 ml/100 g/min. The blood is distributed unequally, thus it mainly perfuses the mucosal layer of the small intestine (Chou, 1992). The mucosal layer receives 75%, submucosa 5% and muscularis 20–25% of arterial flux to the small intestine. The mucosa villi receive 60% of blood flow, which supports the functions of absorption and active transport, whereas the rest of the blood flow perfuses the crypts. In the resting state, only one-fifth of the vascular capillaries are perfused, which demonstrates a huge adaptation capacity for supporting digestion and absorption of nutrients after ingestion. Under fasting conditions the metabolic autoregulation controls the tone of the microvasculature by changes in pCO_2, adenosine, pO_2, pH and osmolality (Sparks, 1980). The vascular tone of the larger arteries is regulated by the nervous system of the vasomotor center of the medulla (Donald and Shepherd, 1980; Hilton and Spyer, 1980).

In healthy humans, increases in the CA and SMA flow of about 50–100% have been reported following meal ingestion (Someya et al., 2008; Trahair et al., 2012), but it is not known how such increases in blood perfusion are distributed between the splanchnic organs. In the fed stage, the intestinal blood flow enhancement is localized to the intestinal segment that is exposed to chyme (Gallavan et al., 1980; Granger et al., 1980). This phenomenon has been shown to be nutrient driven mainly in the mucosal layer (Chou et al., 1976; Gallavan et al., 1980). Intestinal blood flow adapts to feeding in two phases. The cardiac output increases in the ingestion/anticipation phase, which is mainly mediated by the sympathetic nervous system, whereas the luminal contents regulate blood perfusion in the digestion phase. A multitude of interacting factors including enteroendocrine hormones, osmolality, glucose levels and chyme passing through the lumen of the GI tract regulate microcirculation by increasing or decreasing the vascular resistance by

demands of nutrient absorption and oxygen requirements. The splanchnic blood flow decreases in the first 15 minutes of the anticipation/ingestion phase whereas cardiac output and blood pressure increases. Fifteen minutes after ingestion, the splanchnic blood flow can increase by three-fold and stays upregulated for the next three to seven hours in the digestive phase (Vatner et al., 1970).

A study dating back to the early 20th century demonstrated an increase in local blood flow in isolated intestinal segments after peptone solution was injected into the lumen (Brodie et al., 1910). Two decades later, Herrick and colleagues reported an enhancement in SMA flow after the ingestion of a milk, glucose and egg meal in unconscious dogs (Herrick, 1934). A series of studies in the 1980s by Chou and Kvietys and their colleagues (Chou et al., 1972; Chou et al., 1985; Kvietys et al., 1980) described the hierarchy of nutrients for inducing intestinal hyperaemia and showed that lipids in combination with bile are the most potent flow inducers followed by glucose and proteins.

The possible regulators of the local intestinal blood flow regulation are the direct effect of the intestinal content, enteroendocrine hormones, local tissue metabolism products and prostaglandins and enteric nervous system and its reflexes (Chou et al., 1985; Nyhof and Chou, 1983).

The sympathetic nervous system regulates cardiovascular responses during ingestion (Vatner et al., 1970), but it does not influence intestinal blood perfusion in the absorptive phase (Nyhof and Chou, 1983). Infusions of ganglion blockers, Na^+-channel blockers, serotonin antagonists, extrinsic denervation of jejunal segments and infusion of atropine have all failed to show any changes in intestinal flow (Nyhof and Chou, 1983). C-fibers might have some impact in the GI track blood flow regulation (Rozsa and Jacobson, 1989), mediated by CCK, substance-P and vasoactive intestinal polypeptide (VIP).

Direct effects of bile acids in contact with the enterocyte apical layer or when infused in the intestinal blood circulation, increase the intestinal blood flow (Chou et al., 1985). Similarly, the absorption of metabolic end products, such as carbon dioxide and hydrogen ions enhance jejunal blood flow (Sparks, 1980).

Enteroendocrine hormones released after meal ingestion can be measured in the systemic circulation in concentrations, which are insufficient to induce blood flow changes (Gallavan et al., 1985; Gallavan and Chou, 1986; Gallavan et al., 1986; Premen et al., 1985). However, local concentrations of these peptides might rise to levels capable of inducing blood flow changes. GIP-infusion in anaesthetized dogs induced increases in SMA blood flow, whereas CA blood flow has been reported to be unchanged (Kogire et al., 1988). Other studies in conscious animals failed to show any vasodilatation in the gut wall arterioles in response to postprandial

incretin levels (Chou and Coatney, 1994). GLP-1 infusion prevented glucose-induced pancreatic blood flow redistribution in experimental animals (Wu et al., 2012) and GLP-1 injection in healthy Wistar rats did not regulate intestinal blood flow in the absorptive state (Svensson et al., 2007). The rate of gastric emptying in healthy individuals is highly regulated by feedback from the small intestine, wherein acute hyperglycaemia and elevated levels of GLP-1 are mutually involved (Brener et al., 1983; Ma et al., 2012; Pilichiewicz et al., 2007a; Rayner et al., 2001). Local tissue chemicals called eutanoids such as serotonin, histamine, prostaglandins are paracrine secreted but their physiological role in blood flow regulation has not been elucidated (Alemayehu and Chou, 1993; Premen et al., 1985; Rothschild et al., 1998).

Local tissue metabolism, absorption, secretion and motility are closely related to the oxygen concentrations of intestinal layers and this is suggested to be the most important of all possible mechanisms that participate in intestinal blood flow (Gallavan and Chou, 1985). Little is known about colon blood circulation in either fasting or the fed stages (Kvietys and Granger, 1981)

Tissue blood flow is increased during hyperglycaemia by vasodilatation. Early studies using microsphere technique in steptozotosin-treated rats have demonstrated increases in the small intestine blood flow by 45–55% (Lucas and Foy, 1977). The percentage of cardiac output received by the intestine in addition to absolute blood flow per tissue weight increased in the small intestine. Tissue hyperplasia was thought to be the major cause for the increased flow, which appeared to function as an adaptation mechanism to the loss of energy in the urine (Lucas and Foy, 1977). In the same study, obese Zucker rats had decreased blood flow in the small intestine, without hyperplasia. Hill and co-workers showed an increase in small intestine blood flow in steptozotosin-induced diabetic rats, whereas diet restriction normalized the tissue hyperplasia, intestinal weight gain and changes in blood flow (Hill and Larkins, 1989). Cross perfusion of the lean control rats isolated small intestine preparation with the blood from diabetic rats increased blood flow by 30% and decreased intestinal vascular resistance (Korthuis et al., 1987). In the same study, vascular resistance was decreased with infusions of sucrose, glucose and glucagon, which suggest that these blood-borne agents are involved in intestinal hyperaemia associated with diabetes mellitus.

Previously published study findings on the effect of diabetes on intestinal blood flow changes (Hill and Larkins, 1989; Korthuis et al., 1987; Lucas and Foy, 1977) were inconclusive at evaluating T2D induced intestinal blood flow changes. This is due to marked hyperglycaemia, hyperglucagonemia, glycosuria and lack of insulin in steptozotosin-treated rodent models. Human studies on this subject area are lacking, which is most likely due to a lack of the appropriate methods.

After bariatric surgery, the reduction of gastric hydrochloric acid (HCl) secretion has been noticed at least after sleeve gastrectomy due to reduced mass of parietal cells. Mucosal blood flow is adjusted by tissue acidosis whereby increasing intramucosal H^+-levels lead to an enhancement in mucosal blood flow (Starlinger et al., 1981). Changes in the blood flow of the small intestine caused by elevated incretin levels, reduced acid production or faster passage of the digesta through the intestinal lumen might modify energy absorption from the digested chyme and further lead to weight reduction.

2.2.2 Intestinal fatty acid metabolism

Pancreatic lipases hydrolyse dietary triglycerides (TGs) in the mucosal surface of the small intestine to two FFAs and one monoacylglycerol. These degradation products are directed in the endoplasmic reticulum of the enterocytes for re-synthesis into TGs. Further, TGs are packed in the chylomicron and secreted in the intestinal lymphatic circulation and canalized into the thoracic duct (Abumrad and Davidson, 2012). The TG of chylomicrons in the circulation system are hydrolysed by lipoprotein lipase (LPL), which is located at the surface of capillaries, and the released FAs are rapidly taken up by the peripheral tissues in which they are used for various cellular pathways (Su and Abumrad, 2009). The use of FAs as an energy source is proportional to the FFA levels (Trotter and Storch, 1991). The LPL-mediated hydrolysis is the main chylomicron-triglyceride clearance mechanism in humans (Carpentier et al., 2012), although some evidence for LPL-independent clearance pathways also exist (Gaudet et al., 2014).

Luminal free FAs are transported across the enterocyte membrane by diffusion or by facilitated transport by cluster differentiation 36 transport factor (CD36) or FA transporter protein 4 (FATP4) (Niot et al., 2009). CD36 is transmembrane amino acid, with broad ligand specificity for long chain FAs, lipoproteins, amyloid B, glycated proteins and also Malaria infected enterocytes (Abumrad et al., 1993; Silverstein and Febbraio, 2009). Even though CD36 participates in the absorption of FAs in the proximal small intestine, the net uptake through this transporter is known to be small (Nassir et al., 2007) and rapidly saturable and its function would be important only in the early stages of the digestion. FATP4 is expressed in villus enterocytes and it has exogenous acyl-CoA-synthase activity to metabolize transported FAs. Deletion of intestinal FATP4 had no effect on intestinal fat absorption in rodents (Moulson et al., 2007) and its role in intestinal FA uptake remains to be elucidated. Fatty acid binding proteins (FABPs) in the cytosol act as lipid sensors in the regulation of unbound FFA levels and fluxes (Gajda and Storch, 2015). Another regulatory step is the uptake of FFAs into the

mitochondrion: rapid activation to their CoA-thioesters by enzymes on the endoplasmic reticulum (ER) and outer mitochondrial membrane and carnitine-palmitoyl transferase facilitated transport in the inner mitochondrial membrane (Bieber, 1988).

The mucosa of the small intestine has a unique duality in the handling of FFAs. The FFAs and sn-2-monoacylglycerol (2-MG) that enter the mucosa from the luminal side serve the organism as energy storage, FAs are mainly esterified with glycerol to form TGs. In contrast plasma FFAs are primarily used for caloric and structural requirements of the epithelium (Gangl and Ockner, 1975; Gangl and Renner, 1978). In Caco-2 intestinal cell lines the ratio of TG to phospholipid formed from intracellularly transported free FA in the apical layer was 10-fold that of the basolateral layer (Storch et al., 2008).

There have been significant advances in our understanding of the mechanisms in luminal absorption of dietary fat (Abumrad and Davidson, 2012; Labbe et al., 2011b), although the basolateral FFA utilization has gained little attention, they are most likely due to the lack of appropriate methods.

2.2.3 Intestinal glucose metabolism

The western diet contains carbohydrates in excess of 40% of the total caloric intake. Half of the digestible carbohydrate is starch, which is made up of long chains of glucose molecules. Other major sources for dietary digestible carbohydrates are lactose, fructose, glucose and sucrose. Dietary fibers form a majority of the indigestible non-starch carbohydrates, which are resistant to digestion in the small intestine. Carbohydrate digestion begins in the mouth, where salivary amylases are secreted from the parotid and submandibular glands. Salivary amylases are subsequently inactivated by the acidic contents of the stomach, although some activation might still continue inside the food bolus. Carbohydrate digestion continues in the duodenum where it is mediated by the pancreatic amylases and the terminal products of the starch digestion are further hydrolyzed in the brush border membrane by specific hydrolases before transport into the enterocytes (Mithieux et al., 2006; Sleisenger et al., 2010). Glucose is considered to be a crucial substrate for the small intestine although it is only weakly oxidized in the intestine (Krebs, 1972; Mithieux, 2001) and it has been reported that the enterocytes use ketone bodies, glutamine and FFAs as an energy source (Sliwkowski and Windmueller, 1984; Windmueller and Spaeth, 1978). A small proportion of the carbohydrates eventually reach the colon because of incomplete digestion, lack of enzymatic activity or lack of transporters or disaccharidases (Caspary, 1992). Bacterial hydrolases degrade carbohydrates

further into smaller molecules and the remaining di- and monosaccharides are anaerobically fermented by microbiota in the colon (Cummings, 1983; Salyers, 1983). The main end products of the fermentation are SCFAs, hydrogen, carbon dioxide and methane (Salyers, 1983). Because the colon reabsorbs SCFAs (McNeil et al., 1978), fermented carbohydrates can be used for a host energy demands very effectively.

Small intestinal glucose and galactose extraction from the lumen is mediated by SGLT1 and glucose transporter type 2 (GLUT2) (Crane, 1962; Hediger et al., 1987) whereas fructose is absorbed by facilitated diffusion by GLUT5 (Burant et al., 1992). Apical GLUT2 provides a major pathway when the capacity of SGLT1 is exceeded (Gouyon et al., 2003; Kellett and Helliwell, 2000). In the basolateral membrane, GLUT2 provides an exit pathway (Cheeseman and Maenz, 1989).

Insulin stimulus in rodents internalize the GLUT2 from the apical brush border, which slows the absorption of glucose (Tobin et al., 2008). The same study by Tobin and colleagues also found that insulin resistance eliminated this transporter trafficking inside the enterocytes, which led to increased GU (Tobin et al., 2008). In experimental rodent models for diabetes, hyperinsulinemia and hyperglycaemia provoke mucosal hyperplasia and increases GLUT2 protein expression (Burant et al., 1994). In the insulin resistant stages, GLUT2 levels remain high in the apical membrane and low in the basement membrane. Despite these findings in previous animal studies, no functional GLUT2 was found in the apical brush border from the duodenal biopsies in obese human subjects with T2D (Dyer et al., 2002). However, SGLT1 and GLUT5 levels were higher compared to normal-weight controls as were glucose concentrations in the enterocytes, which suggest these transporters have a role in the pathophysiology of T2D.

The small intestine is a gluconeogenetic organ that primarily uses glutamine for glucose production (Croset et al., 2001). Rajas and co-workers showed in 1999 that glucose-6-phosphatase, the enzyme involved in liver glucose release from gluconeogenesis and glycogenolysis, is also expressed in the small intestines of rats and humans (Rajas et al., 1999). Another glyconeogenetic enzyme called PEPCK was also shown to be expressed in the small intestine (Rajas et al., 2000). The same study group demonstrated that the small intestine contributes to endogenous glucose production during fasting and in insulin deficient conditions (Croset et al., 2001). Further, Mäkinen and his co-workers documented intestinal insulin resistance in morbidly obese patients (Makinen et al., 2015). Six months after bariatric surgery insulin-driven GU was increased in obese subjects but it did not reach the level of healthy controls. It is speculated that the nutrients that control intestinal gluconeogenesis could regulate energy homeostasis and appetite through the mechanism of glucose sensing in the PV (Delaere et al., 2010).

Metformin accumulates in the mucosa in the intestine (Wilcock and Bailey, 1994), which slightly delays the absorption process from the luminal side and absorption occurs more distally in the GI-track. This delay and change in absorption site has been speculated to contribute to the blood glucose-lowering effect of the drug (Lorch, 1971; Wilcock and Bailey, 1990). Higher concentrations of metformin in the tissue inhibits the mitochondrial respiratory complex-1, thereby reducing the availability of adenosine triphosphate (ATP) (Brunmair et al., 2004) leading to AMPK phosphorylation and reduction of ATP consuming energy transport from food to blood (Ikeda et al., 2000). This mitochondrial block induces lactate production and increases pAMPK, which has been shown in recent studies (Massollo et al., 2013).

The GLUT5 found in the apical plasma membrane transports dietary fructose (Burant et al., 1992) and the high-affinity Na-coupled cotransporter SGLT1 performs glucose and galactose extraction from the lumen (Wright et al., 2007). Metformin in rodents increases intestinal sugar use (Bailey et al., 1992) and increases the expression of SGLT1 and GLUT5 but does not alter GLUT2 mRNA levels (Lenzen et al., 1996). Metformin also promotes apical GLUT2 location in rodent enterocytes via AMPK (Walker et al., 2005). In 2011 Ait-Omar and colleagues showed that morbidly obese diabetics exhibited apical GLUT2 in the fasting state, whereas GLUT2 was found only in basolateral membrane of normal-weight subjects. After metformin intervention, apical GLUT2 location was increased in normal-weight controls and remained high in obese patients, which suggest that metformin might modify trans-epithelial glucose fluxes. GLUT2 insertion into the apical membrane could thus provide compensatory mechanisms such as bidirectional glucose fluxes down concentration gradients to limit hyperglycaemia (Ait-Omar et al., 2011).

2.3 Methods to measure intestinal metabolism and blood perfusion

Intestinal mucosal metabolism and blood flow has been studied for years in animal and also in in vitro models, using highly invasive techniques such as PV cannulation and autoradiography of tissue sections. There are limitations in using these methods in the human studies due to their invasive nature.

2.3.1 The arteriovenous balance technique

The intestinal glucose uptake can be calculated by using radioactive or stable isotopes of glucose that determine the concentration difference between the arterial

and venous sides of the small intestine. The principle of the method is that study animals are infused intraluminally with [3-^{3}H] glucose for 10 minutes, thereafter the SMA is ligated in open laparotomy to exclude blood circulation from the colon and blood samples are collected simultaneously from the carotid artery and SMV in the steady state (Minassian et al., 1998). GU and release can be calculated from the concentration difference between the arterial and the venous side when the blood flow is known. Degradation products can also be measured to document tissue metabolism using tracers or labelled analogues (Croset et al., 2001; Radziuk and Pye, 2002).

2.3.2 Doppler ultrasound

Ultrasound provides a non-invasive approach to evaluate blood flow in abdominal organs, which avoids the use of ionizing radiation. Doppler ultrasound measures changes in sound wave echo frequencies from moving objects (blood cells), which is based on the Doppler effect principle that describes the change in frequency of a wave for an observer moving relative to the source of the respective wave. These differences can be processed to produce blood flow velocity and direction data. Although ultrasound with Doppler provides an inexpensive and noninvasive method for the blood flow measurements, the intersperse variation, poor visual signal to the tissue of interest and the limitation of being able measure only large caliber vasculature are challenges in the use of ultrasound in clinical trials (Qamar et al., 1986).

2.3.3 Autoradiography

The microsphere technique is one autoradiographical approach that provides detailed information on regional blood flow and it is widely used in animal studies. The technique was introduced as early as 1967 (Rudolph and Heymann, 1967, 1976) to evaluate blood flow in multiple organs simultaneously. The principle of the method is that radioactive microspheres are injected into the left ventricle and simultaneously an arterial blood sample is collected using a slow-withdrawal pump. The slow withdrawal pump is adjusted to a specific withdraw velocity setting. The radioactivity of the syringe used for microsphere injection is measured before and after injection in order to determine the total activity injected. The tissues whose blood flow is to be determined are removed and weighed and their radioactivity measured by taking the cardiac output, and the withdrawal time into account. These deposit markers measure the flow per unit volume of tissue at the level of capillaries. The results have to be evaluated with caution however, because

these particles cannot be used for measuring organs with a portal flow and the particles can also aggregate in the arteries thereby obstructing the vessels (Prinzen and Bassingthwaighte, 2000). Attention to microsphere size is needed for reliable measurement accuracy (Flameng et al., 1977). Since activity is measured in the tissue samples, this technique is limited to animal studies in static settings.

The biodistribution of the different tracers such as 2-[^{18}F]fluoro-2-deoxy-D-glucose (^{18}F-FDG) and 14(RS)-[^{18}F]fluoro-6-thia-heptadecanoic acid (^{18}F-FTHA) can be used for evaluating glucose and FFA uptake in different tissues. Tissue radioactivity is measured using a gamma counter after the scanning. The counts are corrected for radionuclide decay and reported as a percentage of the injected dose per gram of tissue (%ID/g). Tracer uptake in the tissue is then corrected for blood glucose or FFA values.

Further, ß-emitting particles can be analyzed on chromatography plates by digital autoradiography and photostimulated luminescence (PSL). The imaging plates in digital autoradiography are coated with a radiation sensitive barium fluorobromide/europium layer. The radioactive sample is pressed tightly against the radiation-sensitive medium on the imaging plates to maximize the number of radiation emissions captured and to minimize the dispersion of the radiation before entering the medium, thereby optimizing resolution (1 to 10 μm). Radiation induces latent image formation, which is registered to form a quantitative representation of the sample. PSL autoradiography is a very sensitive method, it has a high spatial resolution and a large dynamic range from mBq to kBq. These characteristics makes PSL digital autoradiography a powerful method for the determination of ß-emitting radionuclides on planar surfaces (Okuyama et al., 1994). An increasingly important application of autoradiography is the registration of autoradiograms with histological and immunohistochemical images of the same tissue section or an adjacent tissue section. The obtained autoradiograms are used to compare the small-scale distribution of the radiotracer with histological features and also to determine the expression of molecular markers in the tissues (Zanzonico, 2012).

2.3.4 Positron emission tomography

Position emission tomography (PET) utilizes the distribution of positron emitting tracers in the selected organs, thus providing quantitative information of biological processes in vivo. A wide variety of biological molecules can be labelled with short half-life positron emitting isotopes and the movements of these target tracer molecules can be measured and quantified using PET scanners.

PET imaging offers numerous advantages in clinical and preclinical research compared to the aforementioned autoradiography, ultrasound and arteriovenous balance techniques. First, the detection sensitivity of radionuclide imaging is high. The specific activity (activity per unit mass) of radiopharmaceuticals is typically in the sub-nmol range in contrast to various contrast agents used in CT and MRI imaging and therefore do not perturb the system being studied. Second, nuclear imaging is noninvasive and may be used serially in longitudinal settings. Third, nuclear imaging is quantitative. Fourth, a large number of biological molecules have been developed for the characterization of in vivo biology. In addition to all the above advantages, nuclear imaging has relatively few downsides. The most common limitations are, the spatial resolution is limited to 4–6 mm (Spanoudaki and Ziegler, 2008), the effective radiation dose given to study subjects 2–10 mSv (Stabin and Brill, 2008) and the costs of the equipment needed for the production of radioligands and for PET imaging are high. PET imaging is vulnerable to excessive motion artefacts because of peristalsis, cardiovascular pulsation, and respiration due to long acquisition times.

Radionuclides used in PET-imaging should emit sufficient amounts of penetrating radiation to escape from the body and interact with external detectors. Positron-emitting radionuclides (such as Carbon-11, Oxygen-15, Fluorine-18, Gallium-68, to name a few) are used in PET-imaging and are produced in cyclotrons or generators. The half-lives of positron emitting radionuclides used in clinical and preclinical settings must be short, and in practice they vary from 2.05 minutes to 4 days. When the radionuclide decays it emits a positron ($ß^+$) which travels generally ~1 mm in tissue (positron range) before annihilation with electron (e-). As a result of annihilation two 511-keV -rays are emitted in opposite directions. These photons are detected by a radiation detector simultaneously (true coincidence) in PET-imaging and used for creating a line of response. Finally, the raw data of one-dimensional projections are mathematically reconstructed into a set of transverse images. Before reconstructing the images scatter, attenuation, random coincidences and dead-time have to corrected by specific techniques (Turkington, 2001).

Attenuation is the loss of a true event due to scatter and absorption of the photon on its way to the detector. This leads to a loss of counts and inaccurate quantitation of the radioactivity distribution. Attenuation depends on the total thickness of the attenuation medium, therefore the CT image can be used for correction (Hitz et al., 2014; Turkington, 2001). A CT-image is a two-dimensional attenuation map with the energy of X-rays (~120 keV) and must be scaled-up to the 511-keV of the annihilation -rays. In PET-MRI, the MRI tissue intensities do not directly correspond to electron density of the tissues nor do they allow the direct transformation to tissue attenuation properties (Mehranian et al., 2016). Different

methods for MRI attenuation correction (MRAC) have been developed, but only a handful have been applied for whole-body imaging due to their pit-falls (such as inter-subject anatomical variability, movement artifacts, used flexible RF-coils, difficulty in obtaining an MR signal from the bone). None of these methods properly accounts for bone tissue attenuation, which has been shown to produce large PET image bias (Pugmire et al., 2016). However, the quality of PET images obtained in clinical diagnostics and subjected to MRAC was comparable to those of PET images obtained with the use of CT attenuation correction (Lyons et al., 2015).

The acquisition process can be divided into different parts: preparation and monitoring of the patient, injection of the tracer, and PET measurement combined with sampling of blood. Most PET-imaging studies need a relatively long time for the quantitation of the tracer kinetics (typically 20–60 minutes) and motion artifacts can be reduced by paying attention and ensuring that the study subject is in a comfortable position (Natalie Nelissen, 2012). The study subject's tissue of interest is positioned in the central part of the field of view for the optimal performance at the center of the scanner. When the study subject or patient is positioned inside the scanner gantry, the PET tracer is injected typically within a bolus of constant infusion via cannulated arm vein. A very small amount of the ligand is injected (in the range of pico- or nanograms). To know the exact amount of activity injected, the remaining dose in the syringe after injection (rest dose) should also be measured and recorded in addition to the exact time of dose measurement, injection time and rest dose measurement. Accurate timing requires the same or cross-calibrated clocks. Before PET scanning, a low dose CT or MRI scan is done for attenuation corrections. After tracer injection, tissue activity data are collected for kinetic modelling in dynamic measurements. The data collection is divided into multiple time frames, usually shorter in the beginning of the scanning. One should keep in mind that the tracer distribution should be constant during one frame, and gradually longer frames toward the end. The start and duration of the scan depend on the tracer and its kinetics and on the model that will be applied to determine the physiological parameters. In many applications, it is common practice to start the scan at the time of injection although, for simplified methods, the scan can be started at a later time point when the equilibrium is approached. Before analysis of tissue activity, it is necessary to correct for decay of the isotope. A number of kinetic models that are commonly used in PET, require the sampling of arterial blood to determine the arterial blood or plasma concentration, which indicates the quantity of tracer that is available for uptake by the tissues. This can be done by measuring radioactivity of the blood/plasma samples using a well counter and scaling this number by the volume measured or use image-derived input function (ID-IF) (Germano et al., 1992). ID-IF entails determining the time-activity curve straight from the dynamic image. Typically,

small regions of the carotid artery or the aorta have been used, which are subject to errors due to limited spatial resolution of the PET image. However, ID-IF can be used when validated with blood sampling (Zanotti-Fregonara et al., 2011).

The spatial resolution of PET imaging is limited by several factors, such as annihilation photon non-collinearity, positron range, off-axis detector penetration, detector Compton scatter, under-sampling of the signal in the linear or angular directions for the image reconstruction process, and patient motion (Natalie Nelissen, 2012). The overall spatial resolution of the systems is a convolution of these components. The finite resolution of PET scanners degrades the accuracy of quantitation and thus small objects become invisible in the scan if they are comparable or smaller than the Full Width at Half Maximum (FWHM) of the point spread function. It can also lead to a loss of contrast for larger objects due to blurring. Spatial resolution-related effects are usually referred to as 'partial volume effects' (PVEs). In general, the partial volume effect can be defined as the loss in apparent activity that occurs when an object partially occupies the sensitive volume of the imaging instrument (Hutton and Osiecki, 1998). Various PVE correction methods exist, which apply the correction either at the region level or at the voxel level, during or post reconstruction. Although the PET-scanner spatial resolution is limited to 4–6 mm in human studies (Spanoudaki and Ziegler, 2008) more exact anatomical correspondence can be confirmed from using fused MRI or CT images. The MRI provides a better soft tissue contrast in the intestine with no ionizing radiation, but due to longer scanning time predispose to pitfalls in analysis due to motion artefacts such as peristalsis, cardiovascular pulsation and respiration. CT offers some advantage compared to MRI with 1 mm slice thickness and shorter image acquisition times, which limit the motion artefacts.

After the image processing with the necessary corrections, different models are used to describe traced behaviour. When describing the pharmacokinetics of a tracer, the most commonly used method is a compartmental model where distinct pools of tracer (spatial location or chemical state) are assigned to different compartments. These accurate models describing the full behaviour of the tracers are too complex to be used in practice and are simplified for different compartmental, graphical and reference models (Natalie Nelissen, 2012). For further details regarding modelling used in this thesis, see next chapter, 5.1.5 and 5.1.6.

Glucose metabolism

^{18}F-FDG is a widely used tracer in the clinical setting for infection and tumour diagnostics. ^{18}F-FDG uses the same glucose transporter-proteins and hexokinases as glucose and after phosphorylation end-product ^{18}F-FDG-6-phosphate remains intact for an extended time and therefore assumed to be trapped inside the cells.

The retention of the ^{18}F-FDG-6-phosphate in the tissues can be quantified with PET imaging when the activity of glucose-6-phosphatase is low. The whole concept was discovered in the early 1970s by Sokoloff and colleagues when they found and reported that the regional metabolic rate of glucose utilization in the brain can be measured with an autoradiography method using 2-deoxy-D-[^{14}C]glucose (Sokoloff et al., 1977). Later on the method was modified for human studies in the late 1970s (Phelps et al., 1979) using a PET scanner for imaging the ^{18}F-FDG tracer. In 1990s the ^{18}F-FDG was introduced to metabolic research and was used in combination with an insulin clamp to mimic postabsorptive conditions (Nuutila et al., 1992). The ^{18}F-FDG kinetics in tissue can be analyzed using a three compartment model, which requires knowledge of the arterial and tissue ^{18}F-FDG concentration as function of a time. Rate constants describe tracer fluxes between the three compartments: plasma: phosphorylated tracer in tissue, unphosphorylated tracer in tissue (Sokoloff et al., 1977). Patlak and Blasberg presented graphic analysis, which simplified the three compartment method and directly estimated the combination of the rate constants (Patlak and Blasberg, 1985). In steady state conditions (i.e. the ratios of the concentration of tracer in the plasma to those in the reversible tissue compartments must remain stable), this graphic presentation represents the net transfer rate K_i that can be used for estimating the metabolic rate of a native substrate. The fractional uptake rate (FUR) is an approximation of a graphic analysis K_i and can be calculated from a single late PET scan (Ishizu et al., 1994). This FUR value (min^{-1}) can be used for metabolic rate calculations. More details of FUR analysis are presented in section 5.1.2.

Fatty acid metabolism

A palmitate analogue, ^{18}F-FTHA, can be used for evaluating FFA uptake in the tissue. ^{18}F-FTHA uses the same transportation proteins and cellular handling proteins as natural FAs. It is trapped in the mitochondria after beta-oxidation (DeGrado et al., 2000) and the tracer kinetics can be analyzed as presented for ^{18}F-FDG. ^{18}F-FTHA is rapidly metabolized in the blood circulation into label-carrying metabolites that do not participate in normal tissue trafficking and should be corrected before analyzing the tracer blood activity counts (Labbe et al., 2011a).

Blood flow

[^{15}O]water (^{15}O-H_2O) is a chemically inert and freely diffusible tracer and considered as the golden standard for tissue perfusion evaluation. The technique was first introduced for measuring cerebral blood flow (Kety and Schmidt, 1946) in 1946 and later on was used for coronary blood flow measurements (LeBlanc et al., 1974) and other tissues. The ^{15}O-H_2O has a half-life of 122 seconds which enable its use in repeated measurements in dynamic settings. For tissue blood

perfusion analysis a one-compartment method can be utilized as presented in section 5.1.5.

Blood volume

[^{15}O]carbon monoxide (^{15}O-CO) is used for blood volume measurements (Kiss et al., 2009). The tracer is mixed with the breathing air and bounded to the haemoglobin and distributed throughout the blood volume. Tissue blood volume analysis is presented in section 5.1.7.

2.3.5 Limitations of positron emission tomography in intestinal imaging

The spatial resolution of PET imaging is limited by several factors as discussed in detail in section **2.3.4**. Spatial resolutions (radial x tangential) of scanner were 5.1x5.1 mm for Philips Ingenuity, 5.9x5.9 mm for Discovery VCT and 6.7x6.5 mm for eight-ring ECAT 931/08-tomograph, for studies I-II, III and IV respectively. This is about an order of magnitude poorer compared to that of CT and MRI. The small intestine wall is 1–2 mm thick throughout its entire length and its diameter varies from 19 to 25 mm (Cronin et al., 2010). Wall thickness is within the positron range and PET imaging provides tracer activity of the whole intestinal segment in the VOI including the mucosa, the muscular layer and the serosa. In the fasting stage, the small intestine's lumen is usually collapsed and the mucosal layer are folded next to each other and the VOIs drawn on the intestinal segment represent the combination of all three layers. Although the wall thickness of the colon also varies 1–2 mm, the luminal contents and peristaltic waves largely contribute to the colon diameter. These anatomical and physiological differences between small intestine and the colon were taken into account in the VOI drawing as discussed in **5.1.4.** In addition to the anatomical consideration the luminal contents should be considered in the analysis. Digesta contents or any fluids secreted into the intestinal lumen expand the diameter of intestine and decrease the mucosa-to-VOI ratio, which leads to lower counts in TAC. If radioligands are transported or leaked into the intestinal lumen, counts from luminal content and mucosal activity cannot be separated from each other due to limited resolution of PET.

Contractions within the muscular layer of the small intestine are responsible for its motility, and this motility is controlled by a complex interaction between gastrointestinal hormones and a neural network (Wood, 2008). Muscle contractions increase the local blood flow and the glucose uptake predisposes to the overestimation of fasting stage metabolism. However, the mucosal layer receives 75% between peristaltic waves and the muscularis 20–25% of arterial flux to the small intestine as discussed in section **2.2.1.**

In addition to peristaltic waves in the GI tract, mobile intestinal segments are constantly moving as a response to intra-abdominal pressure changes and thus the position of the target in the scanning field of view change and give rise to movement artefacts. This movement applies to the jejunum and part of the ileum, which are mobile and attached to the posterior wall of the abdominal cavity only by the intestinal mesentery. This limitation can be avoided in the analysis by using the retroperitoneal and segments, which are fixed to their locations, such as the proximal duodenum, the ascending or the descending colon.

In "spillover" the apparent loss of activity in the object is distributed across adjacent voxels, which are considered outside the object, and which results in an increase in activity in these voxels (Erlandsson et al., 2012). To avoid spillover in the intestine metabolism analysis, VOIs were drawn separate from the adjacent organs.

In the PET studies two anatomical reference imaging methods were used. The MRI provides a better soft tissue contrast in the intestine with no ionizing radiation, but due to longer scanning time it predisposes to pitfalls in the analysis due to motion artefacts such as peristalsis, cardiovascular pulsation and respiration. On the other hand, CT offers some advantage compared to MRI with 1 mm slice thickness and shorter image acquisition times, which limits the motion artefacts.

2.4 Summary of the literature

Although the intestine is the first absorbing organ to encounter the ingested and digested nutrients after the stomach, it has gained little attention in the research of T2D and obesity. The body of evidence suggest that the small intestine provides crucial information via the gut-brain axis about the composition and size of the food and control of food intake. Enteroendocrine hormones secreted in the small intestine regulate the glucose metabolism in response to nutrients. Intestinal mucosal metabolism has been studied for years in animals and in, in vitro models, using highly invasive techniques that are unfeasible for human studies due to their invasive nature. Although it has limitations, PET combined with reference imaging provides non-invasive, organ-specific data on intestinal blood flow and metabolism.

Previous studies in animals suggest that GIP-hormone and digesta regulate intestinal blood flow but studies on human subjects are missing. Diabetes and obesity regulate intestinal blood flow in animal models but the impact of bariatric surgery in blood flow changes is unclear. The small intestine is an important site for metformin action but its significance on intestinal glucose uptake is not fully understood.

3 AIMS OF THE STUDY

The hypotheses formulated for the studies reported in this thesis were the following: 1) GIP regulate blood flow of the small intestine in normal-weight subjects but not in study subjects with T2D whom have incretin resistance; 2) T2D increases intestinal blood flow which is "normalized" after bariatric surgery; 3) increased FA uptake in the small intestine is subsequently decreased after bariatric surgery; and 4) metformin treatment increases intestinal GU in humans.

The aims of the study were addressed in one or more published study, which are hereafter referred to by their Roman numerals:

1) To compare the vasoactive effects of incretins and food ingestion in the human intestine (I).

2) To characterize the obesity related changes in the intestinal perfusion in humans and determine the effects of bariatric surgery (II–III).

3) To study GIP induced blood flow changes in the intestine before and after bariatric surgery (I–II).

4) To establish a decrease in intestinal FFA uptake after bariatric surgery (III).

5) To study effects of metformin and rosiglitazone on intestinal glucose uptake in T2D patients (IV).

4 SUBJECTS AND STUDY DESIGNS

4.1 Study subject characteristics and animal models

The study population comprised 41patients with T2D, 30 healthy controls and 27 obese patients with (n=11) and without (n=16) diabetes. Characteristics of study subjects are given in Table 1. Validation for human PET studies were done in experimental animals.

4.1.1 Humans (I-IV)

For study I (GIP-PET, NCT01880827) 10 healthy subjects were recruited through personal contacts, electronic and traditional bulletin boards, and newspaper advertisements. The subjects had BMI 20-27 kg/m^2, fasting plasma glucose below 6.1 mmol/l, and were aged between 18–60 years. Subjects were in good health, as determined by physical examination, screening laboratory measurements and medical history. Exclusion criteria were any chronic disease, smoking, previous or present abnormal renal, thyroid or hepatic function, hypertension (>140/90 mmHg) to avoid any disease related splanchnic blood flow changes.

Study II (GIP-PET, NCT01880827) consisted of 10 morbidly obese, non-smoking patients with T2D who were scheduled to undergo RYGB and VSG in a specialized referral centre for the treatment of diabetes and obesity. In addition, 10 normal-weight non-diabetic subjects from study I served as controls. The exclusion criteria for the study subjects were BMI over 60 kg/m^2, weight over 170 kg, waist circumference >150cm, insulin dependence for diabetes, eating or mental disorder, active ulcus disease, eating disorder, smoking, known cardiovascular disease and previous or present abnormal renal or hepatic function, pregnancy and the presence of any ferromagnetic object that would render MR imaging contraindicated. Inclusion criteria were selected to enable the measurements of obesity and T2D induced blood flow changes in the splanchnic area without exogenous insulin. The size of the gantry and table carrying capacity of MRI was a limiting factor for study subjects with excessive BMI, weight and waist circumference.

Study III (SleevePET2, NCT01373892) included 27 morbidly obese patients who were evaluated for bariatric surgery according to standard bariatric surgery criteria and 15 normal-weight controls were recruited from a larger data collection SleevePET2. Obese patients were recruited from a specialized referral centre for

the treatment of diabetes and obesity and healthy subjects recruited through personal contact, electronic and traditional bulletin boards, and newspaper advertisements. Before surgery, 10 obese patients had been diagnosed with T2D, 11 individuals had normal glucose tolerance and 6 had impaired glucose tolerance (American Diabetes Association criteria). Exclusion criteria were eating disorder, known cardiovascular disease, hypertension, insulin-dependent diabetes, and previous or present abnormal renal or hepatic function.

Study IV (RosiPET, NCT02526615) comprised 41 patients with newly diagnosed T2D as defined by WHO criteria (Alberti and Zimmet, 1998). Patients were recruited in primary health care facilities by general practitioners and excluded when they had a fasting plasma glucose value <6.1 mmol/l or >11.0 mmol/l after the run-in period. Furthermore, patients with cardiovascular disease, blood pressure 160/100 mmHg, previous or present abnormal hepatic or renal function, antidiabetic medication, anaemia, or oral corticosteroid treatment were excluded.

Table 1. Baseline clinical characteristics

Study	I, II		III			IV
Group	C	T2D	C	T2D	ND	T2D
N	10	10	15	11	16	41
M/F	2/8	2/8	0/15	0/11	0/16	28/13
Age	46 ± 10	52 ± 7	45 ± 12	41 ± 11	45 ± 7	58 ± 2
BMI (kg/m^2)	23 ± 2	41 ± 6	22 ± 3	50 ± 3	51 ± 4	30 ± 1
GHbA$_{1C}$	5.2 ± 0.3	5.8 ± 0.4	5.6 ± 0.3	6.3 ± 0.7	5.6 ± 0.3	6.6 ± 0.8

Data are shown as mean ± SD. C = healthy control group, T2D = type 2 diabetes study patients, ND = non-diabetic obese subjects, M = male, F = female.

4.2 Study designs

4.2.1 Clinical study designs

All human studies (I–IV) were performed after an overnight fast. The study subjects lay in the supine position on the PET scanner bed, and the area of interest (AOI) was positioned in the gantry and in the field of view. Catheters were placed in both antecubital veins, one for tracer and gastric hormone administration and the other for blood sampling. A CT/MRI scan was performed for the correction of attenuation and as an anatomical reference of the abdomen. During the entire imaging session, arterialized blood was frequently drawn to measure plasma glucose, insulin, free fatty acids (FFAs), and total radioactivity concentration and radio-metabolites. Moreover, blood pressure and the clinical condition of the subjects and patients were constantly monitored. Prior to PET-studies a routine 75-gram 2-hour OGTT was

performed on all subjects. The imaging studies were repeated after the bariatric surgery procedure or medical intervention for study subjects.

4.2.2 Intestinal blood flow and volume in healthy controls (I, GIP-PET)

Principle: Intestinal blood perfusion and volume after mixed meal and incretin infusions were assessed by fused ^{15}O-H_2O PET-MRI imaging on 10 healthy subjects.

Study design: Subjects of the control group underwent three different imaging experiments in randomized order on different days. The subjects were imaged when lying in the supine position with a combined PET/MRI scanner to investigate the changes in intestinal blood flow and volume after a mixed-meal test, GIP infusion, and GLP-1 infusion (Figure 2). ^{15}O-H_2O and ^{15}O-CO PET scans were repeated at 20- and 50-minutes and at 30- and 60-minutes post-ingestion to quantitate the splanchnic blood flow and volume responses, respectively (Figure 6). During the experiments plasma levels of glucose, insulin, GIP and GLP-1 were measured at time points 0, 15, 30, 45, 60 and 90 minutes post-administration.

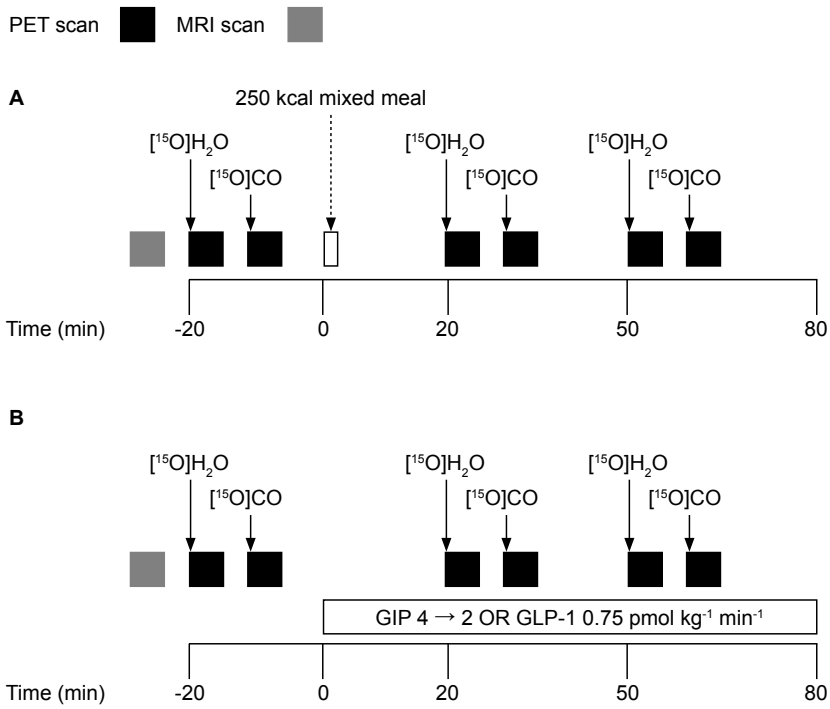

Figure 6. Diagram of the experimental protocol of study I, GIP-PET. The grey boxes denote MRI imaging and the black boxes PET-imaging of the abdominal region. After baseline scanning, either mixed meal solution ingested (A) or incretin infusions (B) were initiated. Black arrows with ^{15}O-H_2O and ^{15}O-CO stand for radiotracer bolus injection or inhalation, respectively.

4.2.3 Intestinal blood flow and volume responses in morbidly obese patients after bariatric surgery (II, GIP-PET)

Principle: The effect of bariatric surgery on intestinal blood perfusion and volume after mixed meal and incretin infusions were assessed by fused ^{15}O-H_2O PET-MRI imaging on 10 healthy subjects and 10 morbidly obese patients with T2D.

Study design: 10 morbidly obese, non-smoking patients with T2D who were scheduled to undergo RYGB and VSG underwent four abdominal PET scanning on separate days (Figure 7) as explained in detail in the previous section. Baseline ^{15}O-H_2O and ^{15}O-CO PET-acquisition of the abdomen was done. Experiments were performed prior to a very-low calorie diet before surgery and then repeated at a median of 76 (51–96) days after the surgery. The morbidly obese patients participated only in the mixed-meal and GIP-infusion interventions before and after bariatric surgery.

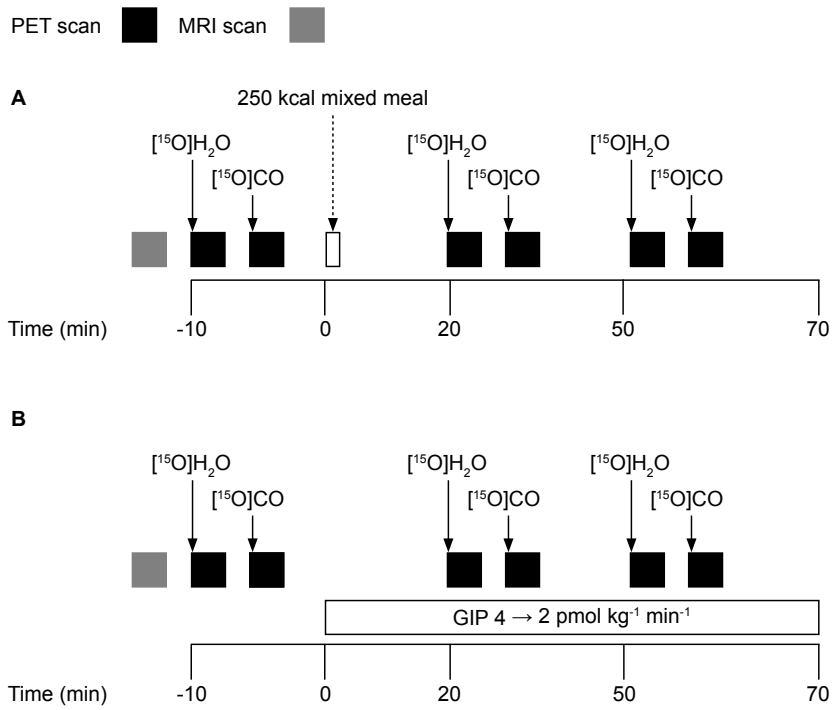

Figure 7. Diagram of the experimental protocol of study II, GIP-PET. The grey boxes denote MRI imaging and the black boxes PET-imaging of the abdominal region. After baseline scanning either a mixed meal solution was ingested (A) or incretin infusion was initiated (B). The black arrows with ^{15}O-H_2O and ^{15}O-CO indicate radiotracer bolus injection or inhalation, respectively.

4.2.4 The effects of bariatric surgery on intestinal fatty acid uptake (III, SleevePET2)

Principle: The effect of bariatric surgery on intestinal FA uptake and blood perfusion were assessed by fused ^{15}O-H_2O and ^{18}F-FTHA in PET-CT imaging on 15 healthy subjects and 27 morbidly obese patients.

Study design: Intestinal FA uptake and blood flow were measured in 27 obese patients before and at six months after bariatric surgery and in 15 healthy age-matched controls (Figures 8 and 9). The experiments were conducted on the obese group four weeks before the planned bariatric surgery and the initiation of the standard very-low calorie diet. During the entire imaging session, arterialized blood was frequently drawn to measure plasma glucose, insulin, FFA, and total radioactivity concentration and radiometabolites.

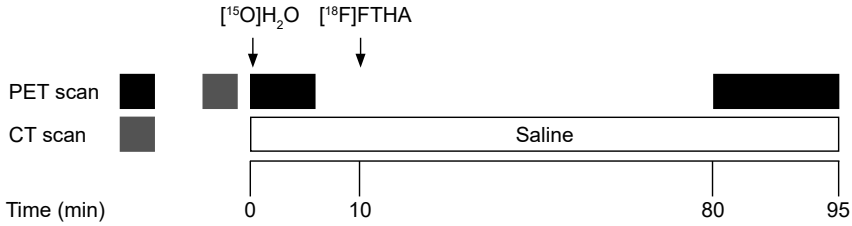

Figure 8. Diagram of the experimental protocol of study III, SleevePET2. Grey boxes denote CT imaging and the black boxes indicate PET-imaging of the abdominal region. The black arrows with ^{15}O-H_2O and ^{18}F-FTHA depict radiotracer bolus injection.

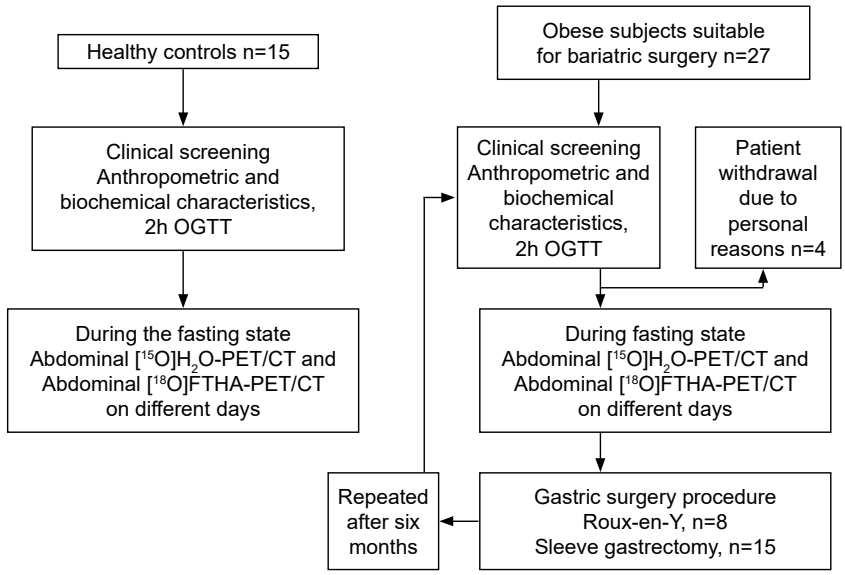

Figure 9. Study III flow chart, sleevePET2.

4.2.5 The effects of metformin and rosiglitazone on insulin mediated intestinal glucose uptake (IV, RosiPET)

Principle: The effects of metformin and rosiglitazone interventions on intestinal GU were assessed by fused ^{18}F-FDG PET-CT imaging during euglycaemic hyperinsulinaemic clamp on 45 patients with T2D in a placebo-controlled trial.

Study design: A total of 45 patients with newly diagnosed uncomplicated T2D (Alberti and Zimmet, 1998), were assigned to the protocol and randomized for treatment order. The study consisted of a 4-week run-in period after which patients were randomly assigned for treatment with rosiglitazone (2 mg b.i.d. for 2 weeks, thereafter 4 mg b.i.d.), metformin (500 mg b.i.d. for 2 weeks, thereafter 1 g b.i.d.), or placebo for a 26-week double-blinded trial (Figure 11). PET studies were performed using the same protocol before treatment and in the 26th week of the trial (Hallsten et al., 2002). The rates of whole-body, skeletal (quadriceps) muscle and intestinal GU were determined (Figure 10) after an overnight fast by combining the euglycaemic-hyperinsulinemic clamp for 140 minutes (with an insulin infusion rate of 1 mU *kg^{-1} *min^{-1}) and ^{18}F-FDG PET scanning (Hallsten et al., 2002).

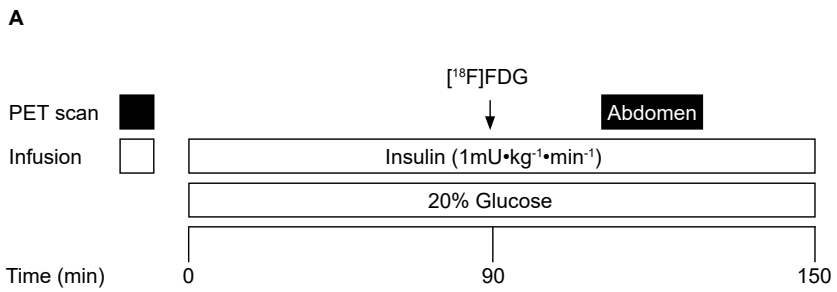

Figure 10. Diagram of the experimental protocol in study IV, RosiPET. The grey box denotes MRI imaging and black box PET-imaging of the abdominal region and white boxes euglycemic-hyperinsulinemic clamp. The black arrow with ^{18}F-FDG denotes radiotracer bolus injection.

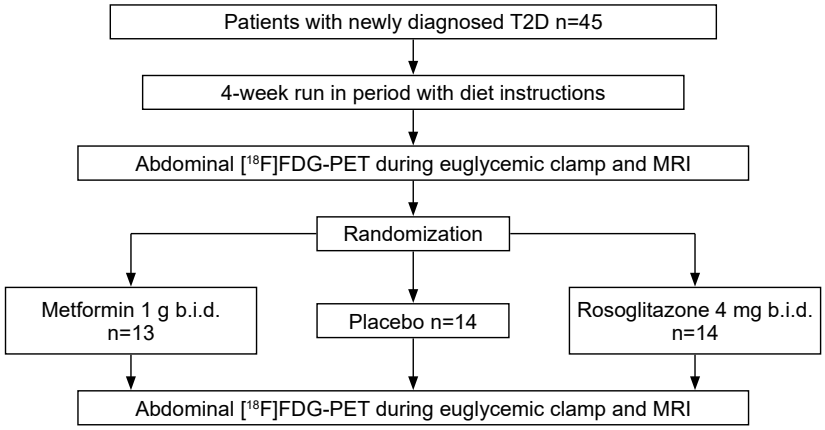

Figure 11. Study IV flow chart. b.i.d = twice daily.

4.2.6 Animal models (III-IV)

Animal models were used to confirm tracer uptake in the mucosal layer of the small intestine. The preclinical studies consisted of eight experimental mice (study III) and nine experimental rats (study IV). For intestinal ^{18}F-FTHA validation, four IGF-II/LDLR$^{-/-}$ApoB$^{100/100}$ mice were used and four age-matched healthy C57BL/6N mice fed with normal chow diet served as controls. Nine adult male BioBreeding Diabetic Resistant (BBDR) normoglycaemic rats were used for intestinal ^{18}F-FDG validation. All of the experiments were performed after a 4–6 hour fast and the studies were conducted for the validation of intestinal mucosal FUR evaluations in humans.

The intestinal ^{18}F-FTHA validation (study III) required four IGF-II/LDLR$^{-/-}$ ApoB$^{100/100}$ (hypercholesterolaemic and insulin resistant) mice (Heinonen et al., 2007) were studied for ^{18}F-FTHA uptake in the mucosa of the small intestine, and four age-matched healthy C57BL/6N mice fed a normal chow diet served as controls.

After ^{18}F-FTHA injection tissue samples of multiple splanchnic organs (duodenum, jejunum, ileum, liver, pancreas) in addition to the myocardium and muscle were obtained. Intestinal contents were carefully removed and measured.

The small intestinal ^{18}F-FDG uptake measurements (study IV) were conducted in nine adult male BBDR normoglycaemic rats were treated with metformin and vehicle treated animals served as controls. ^{18}F-FDG was injected as a bolus and thereafter blood, faecal contents and selected tissues were dissected, weighed and radioactivity measured. Cryosections were analyzed using autoradiography.

5 MATERIALS AND METHODS

5.1 PET imaging

In the PET imaging, we focused on intestinal blood flow and volume, FFA and glucose uptake using ^{15}O-H_2O, ^{15}O-CO, palmitate analogue ^{18}F-FTHA and ^{18}F-FDG tracers.

^{15}O-H_2O and ^{15}O-CO tracers were produced by using a low-energy accelerator Cyclone 3 and diffusion-membrane technique. The synthesis of the ^{18}F-FDG and ^{18}F-FTHA took place in the radiochemistry Laboratory of Turku PET Centre. The radiochemical purity for all tracers exceeded 95%.

PET scans were performed using a combined PET/MRI–scanner Philips Ingenuity (Philips Healthcare, Cleveland, OH), PET/CT scanner (Discovery VCT, General Electric Medical Systems, Milwaukee, WI, USA) and eight-ring ECAT 931/08-tomograph (Siemens/CTI, Knoxville, TN) for studies I, II, III and IV.

5.1.1 Intestinal blood flow and volume

To investigate changes in intestinal blood flow and volume (GIP-PET) after a mixed-meal ingestion, GIP- and GLP-1 infusions subjects were imaged using a combined PET/MRI –scanner Philips Ingenuity (Philips Healthcare, Cleveland, OH) with 38x38 cm axial field of view (Zaidi et al., 2011).

Baseline ^{15}O-H_2O and ^{15}O-CO PET-acquisition and whole-body MRI preceded the experiments. The intestinal blood flow was assessed by using a dynamic PET scanning of 310 seconds was performed following an intravenous bolus injection of ^{15}O-H_2O. Effective radiation dose per ^{15}O-H_2O injection was 0.47 mSv. To study the changes in intestinal blood volume, subjects inhaled room air mixed with 0.14% ^{15}O-CO through a three-way inhalation flap-valve. The inhalation-period lasted for two minutes, the total radioactivity dose being 0.57 mSv. After the administration, another two minutes was allowed for the CO to combine with haemoglobin before the 4-minute static PET scan.

Subjects ingested a 250-kcal liquid meal (Nutridrink, Nutricia Advanced Medical Nutrition, Amsterdam, Netherlands) consisting of 40 grams of carbohydrates, 6 grams of fat, and 9 grams protein in 10 minutes. The dose was selected to enable the ingestion of the meal in a 10-minute timeframe during scanning episodes by patients who have had bariatric surgery. ^{15}O-H_2O and ^{15}O-CO PET scans were repeated at 20- and 50-minutes and at 30- and 60-minutes post-ingestion to

quantitate the splanchnic blood flow and volume responses, respectively. A previous study showed that plasma incretin levels peak within 20 minutes after the ingestion of a meal and the group's hypothesis was that incretin hormones regulate intestinal blood flow (Hansen et al., 2011).

The incretins were dissolved in sterilized water with 2% human serum albumin solution in the hospital pharmacy and administered into the peripheral forearm vein via a cannula with syringe pumps after baseline PET-scans. GIP infusions commenced after baseline scans of a constant 75-minute GIP_{1-42} (Bachem Holding AG, Bubendorf, Switzerland). The GIP infusion was delivered at a rate 4.0 pmol kg^{-1} min^{-1} and that rate was halved at the 15-minute time point (Christensen et al., 2011). GLP-1 infusions were started after baseline scans of a constant 75-minute GLP-1 (Bachem Holding AG, Bubendorf, Switzerland). The starting infusion was delivered at the rate of 0.75 pmol kg^{-1} min^{-1} and the rate was maintained throughout the experiment (Plamboeck et al., 2005).

5.1.2 Intestinal fatty acid uptake

The small intestinal FFA uptake was (SleevePET2) assessed thus; a ^{18}F-FTHA bolus was administered intravenously. The effective radiation dose per ^{18}F-FTHA injection was 7.4 mSv. After 86 (3.3) minutes, dynamic PET imaging on abdominal area was initiated (Figure 8.). In study III four obese subjects did not proceed to bariatric surgery for personal reasons. The remaining subjects underwent laparoscopic Roux-en-Y gastric bypass (n=8) or laparoscopic sleeve gastrectomy (n=15).

5.1.3 Intestinal glucose uptake

In study IV (RosiPET), patients with newly diagnosed T2D and no prior antidiabetic medicine were assigned to the protocol and randomized according to sex and smoking. Follow-up data were not obtained from two patients: one patient of the rosiglitazone group and one patient from the metformin group due to technical problems during the second PET imaging. Two patients of the metformin group withdrew from the study during treatment period: one patient for personal reasons and other due to ischaemic heart disease. MRIs were performed immediately after PET studies on the same day to avoid inconvenience for the study subjects.

The ^{18}F-FDG tracer was injected intravenously at 90 min after starting the clamp and a dynamic scan lasting 20 minutes was performed for skeletal muscle and a 18-

minutes dynamic scan of the abdominal area was obtained with arterial blood sampling as described in previous studies (Hallsten et al., 2002; Iozzo et al., 2003) (Figure 10.). Endogenous glucose production (EGP) calculations were based on the plasma clearance of ^{18}F-FDG used to estimate the rate of appearance of glucose, which was validated against deuterated glucose (Iozzo et al., 2006). The ^{18}F-FDG is partly lost in the urine, which gives an overestimation of the metabolic clearance of glucose, therefore we estimated the urinary loss based on our previous data (Iozzo et al., 2006) and subtracted the obtained factor in the calculation of EGP.

5.1.4 Regions of interest

We obtained organ specific time-activity curves (TACs) and static data by manually drawing the volumes of interest (VOIs) on fused images of the small intestine and the colon. Images obtained from CT of MRI scans were fused with PET scans to identify the anatomically correct location of the VOIs. Cylinder-shaped VOIs were used in the small intestine analysis (Figure 12). The Hollow tube-shaped VOIs were used for the colon analysis. To avoid a spillover from the nearby organs, renal organs, aorta and caput of the pancreas were avoided. The TACs are expressed as the mean radioactivity per volume of tissue as a function of time. Intestinal TACs were corrected with a delay of 4.2 seconds, which was calculated in and obtained from study III data by comparing rise of radioactivity in the aorta and in the intestine from the moment of ^{15}O-water injection.

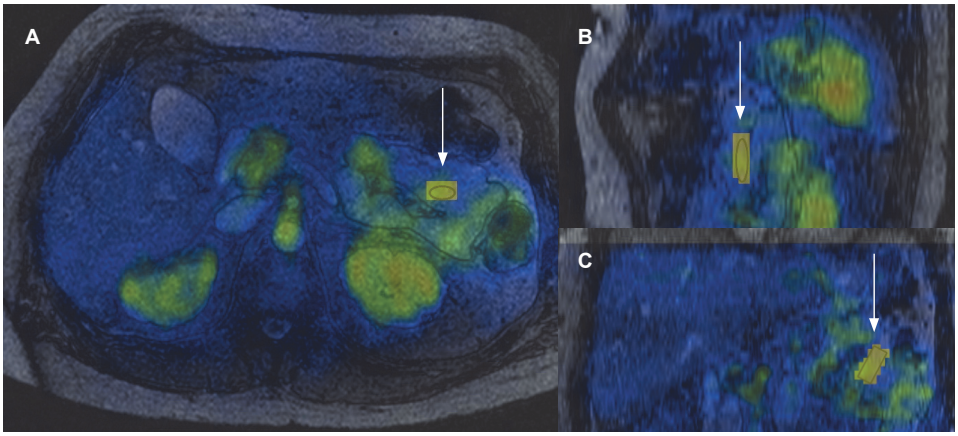

Figure 12. Fused ^{15}O-H_2O positron emission tomography and magnetic resonance images. Cylinder-shaped volume of interest (marked with a yellow arrow) drawn in transaxial (A), coronal (B) and sagittal (C) projections of the small intestine.

Blood flow and volume analyses were achieved by deriving the input function from the images (Germano et al., 1992). Small regions of interest (ROIs) were manually

drawn in seven on 10 horizontal image plains in the thoracic and abdominal aorta. The ^{18}F-FTHA and ^{18}F-FDG analyses was carried out by using arterialized blood as an input function and correcting the obtained function for the time delay.

All data were corrected for dead time, decay, and measured photon attenuation and reconstructed in a 256×256 matrix. Regional TACs were obtained from the 3-dimentional ROIs that had been drawn in the duodenum and jejunum images using Carimas 2.9 software (Turku PET Centre, downloadable at http://turkupetcentre.fi). For intestinal blood flow and volume analysis an image-derived input function was obtained from the abdominal aorta, as described previously (Germano et al., 1992). MRI scans were used as an anatomical reference to ensure reliable analysis (Grubb et al., 1978)

5.1.5 One tissue compartmental analysis (I-III)

The methods to measure blood perfusion with ^{15}O-H_2O tracer are based on the principle of exchange of inert gas between blood and tissues (Kety and Schmidt, 1946) and on Fick's principle. Blood flow (volume of blood passing per unit of time) refers to nonnutritive vessel blood flow, whereas blood perfusion refers to nutritive capillary blood flow. Fick's principle states that tissue uptake of a tracer equals blood perfusion multiplied by the difference between arterial and venous concentrations of the tracer in steady state. According to the one tissue compartment model, tracer concentration in the tissue as a function of time can be expressed as

$$\frac{dC_1(t)}{dt} = K_1 C_0(t) - K_2 C_1(t)$$

Where C_0 is the first compartment ^{15}O-H_2O concentration in blood or plasma curve and C_1 is the second compartment ^{15}O-H_2O concentration in tissue. K_1 and K_2 are the constants between these two compartments. The K_1 represent unidirectional transport of the tracer from the plasma or blood compartment to first tissue compartment and it depends on perfusion (f) and the product permeability and surface area (PS). This can be expressed as

$$K_1 = f(1 - e^{\frac{-PS}{f}})$$

The rate constant K_2 represents the unidirectional transport back from tissue to the blood and it is defined as

$$K_2 = \frac{K_1}{V_1}$$

where V_1 denotes the distribution volume of the tracer.

5.1.6 Patlak graphical analysis and fractional uptake rate (III-IV)

In the present work we used a three-compartment model (Sokoloff et al., 1977) to quantitate ^{18}F-FDG and ^{18}F-FTHA tissue uptake. Plasma and tissue time-activity curves were analyzed graphically (Patlak and Blasberg, 1985) to quantitate the fractional rate of tracer uptake (Ki) (Nuutila et al., 1992). The concentration ratio between the interstitial space and the cellular space is nearly in equilibrium at all times. Therefore, the interstitial and the cellular space can be approximated as a single compartment and model simplified to a two-compartment model. The analysis is based on the assumption that phosphorylated i.e. ^{18}F-FDG-6P and oxidized ^{18}F-FTHA are trapped in the tissue of interest and the dephosphorylation rate is small enough to be ignored and the equation can be further simplified to:

$$FUR = \frac{C_T(t)}{\int_0^T C_P(t)dt}$$

$$K_i = \frac{K_1 x K_3}{K_2 + K_3}$$

$$MR_{glucose} = \frac{C_{glucose}}{LC} x K_1$$

Where FUR denote the fractional uptake ratio, LC the lumped constant and MR metabolic rate. ^{18}F-FDG and glucose behave differently because ^{18}F-FDG uptake becomes trapped after phosphorylation. The influx/uptake of ^{18}F-FDG is only proportional to the influx/uptake of glucose and this constant of proportionality is called the lumped constant (LC).

5.1.7 Tissue blood volume

Intestinal blood volume was measured using inhaled room air mixed with 0.14% ^{15}O-CO. Blood radioactivity counts were measured at 4-, 6- and 8-minute time-points after the inhalation. Intestinal blood volume was calculated according to the equation:

$$V_{Blood} = \frac{100 x C_{Blood}}{C_{Tissue} x \rho_{Tissue} x \frac{HCT_{Sv}}{HCT_{Lv}}}$$

Where C_{Tissue} and C_{Blood} denote radioactivity during static imaging, ρ_{Tissue} tissue is the tissue density (1.047 and 1.042 g ml^{-1} for duodenum and jejunum,

respectively) and $\frac{HCT_{Sv}}{HCT_{Lv}}$ represents the tissue-to-large vessel haematocrit ratio (Snyder WS, 1975).

5.1.8 Animal model

For intestinal ^{18}F-FTHA validation (study III), four hypercholesterolaemic low density lipoprotein receptor deficient mice that express only apolipoprotein B100 with T2D caused by pancreatic overexpression of insulin-like growth factor II IGF-II/LDLR$^{-/-}$ApoB$^{100/100}$, A. I. Virtanen Institute for Molecular Sciences, University of Eastern Finland, Kuopio, Finland) (Heinonen et al., 2007) were used. The mice were fed a high-fat diet (0.2% total cholesterol, TD 88137, Harlan Teklad, Harlan Laboratories, Madison, WI, USA) for 5 months, starting at the age of 2 months. The mice were fasted for 4 hours and blood samples were drawn from the femoral vein for the measurement of plasma FFAs, glycerol and glucose. Then they were anaesthetized with isoflurane (4% for induction and 2.5% for maintenance), a tail vein cannula was inserted, and body temperature was maintained by using a heating pad. A ^{18}F-FTHA 14 ± 2.1 MBq bolus was injected intravenously and after 30 minutes, blood was collected by cardiac puncture and mice were sacrificed by cervical dislocation. After sacrifice, the abdominal cavity was rapidly accessed, and tissue samples were obtained from multiple splanchnic organs (duodenum, jejunum, ileum, liver, pancreas) in addition to the myocardium and muscle. Intestinal contents were carefully removed and measured. Ex vivo tissue radioactivity was measured using a gamma counter (Triathler 3", Hidex, Turku, Finland). Values were normalized for injected radioactivity dose (ID) and the weight of the respective tissue sample resulting in tissue-specific %ID/g-values.

Nine adult male BBDR normoglycaemic rats weighing 415 (51) grams were used. Metformin Hydrochloride (Spectrum Chemical MFG Corp., Gardena, CA 90248, New Brunswick) was administered via osmotic pumps (50 mg/kg/24h; Alzet Osmotic Pump model 2ML2, DURECT Corporation, Cupertino, CA 95014) placed subcutaneously between the scapulae of the five rats and four rats were used as controls. Pumps were replaced every two weeks and the total exposure to metformin or saline was for three months. Animals were sedated by 3% isoflurane and moved to the gantry bed of an Inveon preclinical PET/CT scanner (Siemens). Anaesthesia was maintained by 2.5% isoflurane in 400 ml air/min via a face-mask. Body temperature was supported by a heated bed. B-glucose levels were monitored before and after the scan. The animals were positioned by CT, with the abdomen in the center 127 mm axial field of view (FOV). ^{18}F-FDG (39.5±1.3 MBq) was injected as a bolus into the tail vein, and the animals were then examined by PET

in list mode for 60 minutes from injection of ^{18}F-FDG. Tissue samples were collected as described above.

Autoradiography

The relative intestinal distribution of ^{18}F-FTHA and ^{18}F-FDG were determined by digital autoradiography, whereby duodenal, jejunal and ileal tissue samples were frozen in cooled isopentane and cut into sequential transverse cryosections of 20–40 µm. Cryosections were placed on an imaging plate (Fuji Imaging Plate BAS-TR2025, Fuji Photo Film Co., Ltd., Tokyo, Japan) for 4 hours and then scanned using a Fuji Analyser BAS-5000 (internal resolution of 25 µm, Fuji, Tokyo, Japan). Tracer accumulation was measured as photostimulated luminescence per square millimeter (PSL mm^{-2}) in the ROIs as defined on the mucosa using Tina 2.1 software (Raytest Isotopemessgeräte, GmbH, Straubenhardt, Germany). Background radiation was subtracted from the image data and the results were decay corrected for injection-time and exposure-time, and normalized for the injected radioactivity per animal weight. Parallel tissue sections stained by haematoxylin-eosin served as the histological reference. The results are expressed as normalized photostimulated luminescence PSL/mm^2 values in addition to the mucosa: non-mucosa PSL-ratios.

5.2 Calculations of whole-body glucose uptake, insulin sensitivity and insulin clearance

The hyperinsulinaemic clamp is the reference measure of insulin resistance. In the euglycaemic variant of the test, insulin is infused into a peripheral vein to increase the plasma insulin concentration to a target range. Without further intervention, the hyperinsulinaemia would induce hypoglycaemia. However, in the clamp procedure, the plasma glucose concentration is measured every 3–5 min and the glucose is infused peripherally to maintain glucose concentrations within the desired normal range. When a steady state has been reached (usually 90–120 min), the rate of exogenous glucose infusion needed to maintain the glucose concentration is expressed as an index of the glucose clearance rate and of the subject's insulin sensitivity (DeFronzo et al., 1979). The homeostatic model assessment for insulin resistance ($HOMA_{IR}$) was determined from the steady glucose and insulin concentrations measured under basal conditions (Matthews et al., 1985). Insulin clearance ml min^{-1} was calculated from the equation weight-based infusion rate 1mU weight in kg^{-1} for P-insulin (mU min^{-1}) in steady state (60 minutes).

5.3 Statistical methods

Results are expressed as median (interquartile range, IQR) in studies I and II. Changes over time and between groups were tested with repeated measures analyses using linear mixed models, and Tukey-Kramer's method was used to adjust the P-values of the pairwise comparisons. The normality of the residuals was checked for justification of the analyses and transformations were used for variables, which were not normally distributed. Differences between different surgery groups were tested using the Student's t test or the Wilcoxon rank-sum test. Data in study III are presented as means and ± standard deviation (SD). Normality was examined by a Shapiro-Wilk test, and equality of variances was tested with Levene's test. The Student's t-test for unpaired and the paired t-test for paired data were used for comparisons between- and within-group differences, respectively. For study IV the data are expressed as means and SD for variables with normal distributions. Differences between groups were compared using repeated measurements analysis of variance (ANOVA) and if a significant interaction was found, by one-way ANOVA and Tukey's honestly significant difference post hoc test were performed to test changes between the groups. Differences between two groups of uneven size were evaluated using the unpaired Student's t-test for single repeated measurements. Spearman's correlation (ρ) coefficient was calculated to explore the correlations between variables. $P<0.050$ values were considered to be statistically significant. Statistical analyses were performed using SAS System for Windows, version 9.4 (SAS Institute, Cary, NC, USA).

6 RESULTS

6.1 GIP is the major regulator of the intestinal blood flow (I)

Baseline median, intestinal blood flow in normal-weight study subjects was 0.79 (IQR 0.70–0.92), and 0.54 (IQR 0.43–0.66) ml/ml/min for duodenum and in jejunum respectively. Mixed meal ingestion increased jejunal blood flow 1.68-fold ($P=0.023$ for time factor) at 20 minutes and blood flow remained elevated during the whole test (Figure 13 A), whereas duodenal blood flow was unchanged ($P=0.307$ for time factor).

Mixed meal ingestion led to simultaneous rise in plasma GIP levels at the 30-minute time point ($P<0.050$ for time factor) whereas GLP-1 levels remained unchanged (Figure 13 B).

Neither GLP-infusion nor GIP-infusion had influence on duodenal blood flow ($P=0.756$ for time factor and $P=0.906$ for time x intervention interaction). During the GIP-infusion jejunal blood flow was increased 2.4-fold ($P<0.001$ for time factor) but unchanged during the GLP-1-infusion (Figure 13 A).

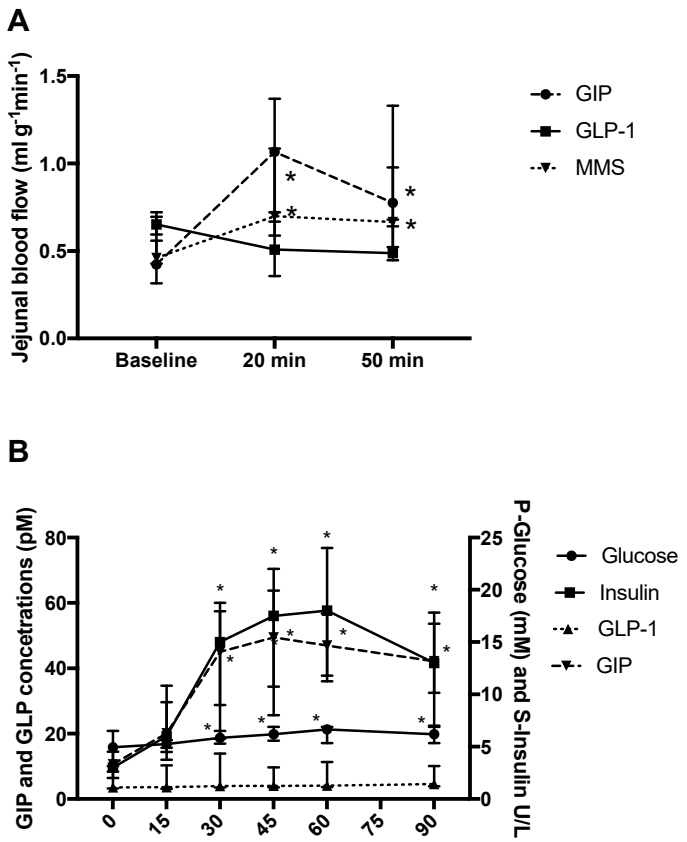

Figure 13. Graph A demonstrates blood flow changes small intestine (jejunum) as a function of time after incretin infusions and mixed meal ingestion. Graph B show changes in plasma and serum incretin, insulin and glucose concentrations after mixed meal ingestion. Data are median (interquartile range, IQR), n=10, *P<0.050 vs. baseline in repeated measurements ANOVA with Tukey–Kramer correction for individual interventions. MMS denotes mixed meal solution, GIP glucose depending insulinogenic polypeptide and GLP-1 glucagon like polypeptide-1.

Blood volumes at baseline were 16.9 (10.3–19.7) and 13.4 (9.53–17.4) ml $100g^{-1}$ in the duodenum and in the jejunum, respectively. The blood volumes remained unchanged throughout the mixed-meal test and incretin infusions.

After the ingestion of the mixed meal solution plasma glucose, serum insulin and C-peptides were increased (P<0.05 for time factor) for all parameters. Infusion of incretins reached supraphysiological levels of plasma GIP and GLP-1 concentrations within 15 minutes after the start, and this was accompanied by a sharp and transient increase in serum insulin (P<0.05 for time factor) and C-peptide concentrations (P<0.050 for time factor). Decrease in plasma glucose was evident only during the GLP-1 infusion, but not during the GIP infusion (P<0.050 for time factor).

6.2 Bariatric surgery upregulates blood perfusion in the small intestine after meal ingestion (II-III)

Prior to having bariatric surgery, obese subjects were insulin resistant and hyperglycaemic compared to controls. Weight at two months after surgery was decreased by a median of 14.7 (IQR 12.2–20.4) kg, which was accompanied by significant improvements in insulin sensitivity and glycaemic control (Table 2). Postoperatively, five subjects were normally-glucose tolerant and only two subjects still received oral antidiabetic medication.

Basal blood perfusion of the duodenum and jejunum was unchanged at two months after the bariatric surgery (P=0.983 and P=1.00, study II). However, six months after bariatric surgery (study III) the jejunal blood flow had decreased (0.41 ± 0.33 vs. 0.25 ± 0.14 ml $100g^{-1}$ min^{-1}, P< 0.05). The glucose tolerance did not impact the fasting blood flow when study subjects were divided in subgroups according to their OGTT results.

No statistical differences in intestinal perfusion after liquid meal were seen between the patients in preoperative situation and controls. Two months after the bariatric procedure a mixed meal solution induced a 2.15-fold increase in jejunum blood flow (P<0.001 for time interaction) compared to the baseline measurements (Figure 14 A). In the postoperative situation, mixed meal ingestion induced an increase in plasma GLP-1 levels (P< 0.050 for time factor) and GIP reached its peak concentration earlier compared to controls and patients before surgery (Figure 14 C and D).

The mixed meal test did not induce blood flow changes in the duodenum in any group. Consistent with the surgical manipulation, duodenal BF response after meal ingestion was markedly increased in the VSG group but not in the RYGB group, whereas jejunal blood flow response did not differ between the two surgical groups. The type of bariatric surgery did not influence basal small intestine blood flow in two or six months timepoints (study II and III, respectively).

GIP-infusion increased jejunal BF approximately 100–130% (both P<0.001) in all of the studied groups, whereas no changes between groups were seen (P=0.655 for time and group interaction) (Figure 14 B).

Table 2. Glycaemic control after interventions

Study	II		III				IV					
Group	T2D	2 months	T2D	6 months	ND	6 months	Metformin	26 weeks	Rosiglitazone	26 weeks	Placebo	26 weeks
N	10		11		16		13		14		14	
Age	52 (7)		41 (11)		45 (7)		58 (2)		59 (2)		58 (2)	
FPG (mmol/l)	7.1 ± 1.1	5.7 ± 0.7**	7.0 ± 0.8	5.7 ± 0.9#	5.4 ± 0.4	5.2 ± 0.5*	8.0 ± 0.5	6.8 ± 1.2**	7.2 ± 0.3	7.2 ± 1.0	7.2 ± 0.3	6.8 ± 1.1
Fasting insulin (U/ml)	19.4 ± 9.3	12.2 ± 7.1*	17.8 ± 14.5	7.6 ± 7.6*	9.5 ± 6.3	7.3 ± 11.8	11.7 ± 7.7	8.8 ± 4.1	8.6 ± 5.6	6.6 ± 1.6	10.1 ± 4.9	9.6 ± 3.4
BMI (kg/m^2)	38.9 ± 4.3	34.4 ± 2.3**	49 ± 3.4	43 ± 5.6#	51 ± 4.5	42 ± 3.8#	29.9 ± 1.1	29.2 ± 1.1*	29.1 ± 1.0	29.5 ± 1.1	30.3 ± 1.2	30.3 ± 1.2
$GHbA_{1c}$ (%)	5.8 ± 0.4	5.4 ± 0.2*	6.3 ± 0.7	5.6 ± 0.4	5.6 ± 0.3	5.3 ± 0.3	6.9 ± 0.2	6.2 ± 1.2#	6.8 ± 0.9	6.5 ± 0.9	6.2 ± 0.6	6.1 ± 0.5
$HOMA_{IR}$ (fraction)	5.8 ± 0.4	3.1 ± 1.9**	5.9 ± 3.2	2.2 ± 2.2**	3.8 ± 2.6	1.9 ± 1.0*	4.2 ± 3.3	2.7 ± 1.4	2.8 ± 2.2	2.0 ± 0.5	3.3 ± 1.8	3.1 ± 1.1

*Data are shown as means (SD). T2D = type 2 diabetes study subjects, ND = subjects with normal or impaired glucose intolerance. *P<0.030, **P<0.001, #P<0.0005 vs. baseline in student t-test. FPG=fasting plasma glucose, BMI=Body mass index.*

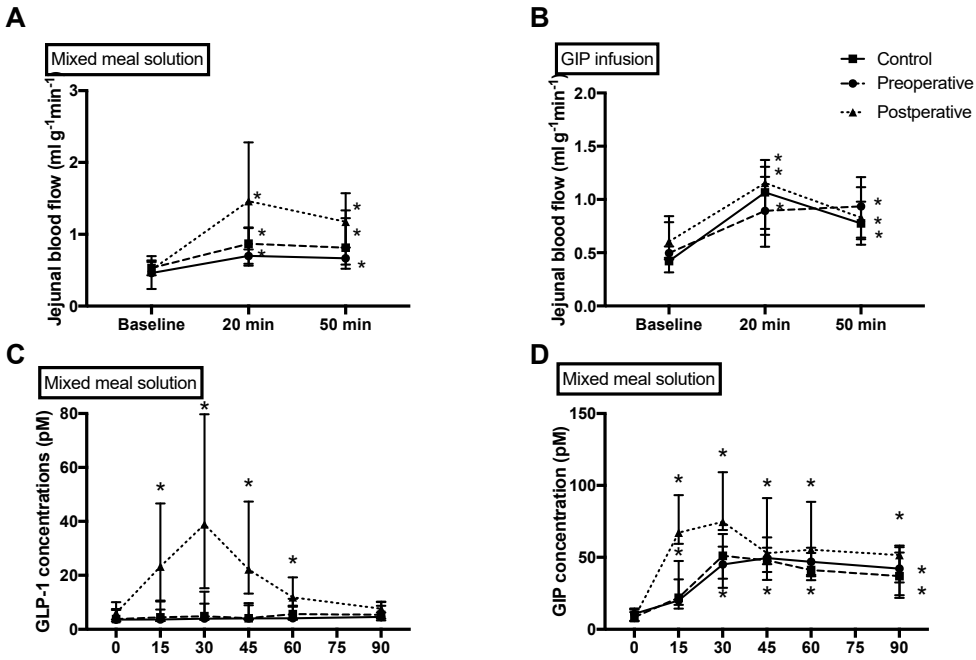

Figure 14. Graph A demonstrates blood flow changes in the small intestine (jejunum) as the function of time mixed meal ingestion and panel B changes after GIP-infusion. Panel C and D graphs represent incretin concentrations as the function of time after a mixed meal. Data are expressed as median (IQR). *P<0.050 vs. baseline in the linear mixed model with Tukey-Kramer correction for individual group. MMS denotes mixed meal solution, GIP glucose depending insulinogenic polypeptide and GLP-1 glucagon like polypeptide-1.

6.3 Obesity and T2D induced small intestine FA uptake of the mucosa cannot be normalized by bariatric surgery (III)

Six months after bariatric surgery, the mean weight loss was 26 ± 8.3 kg, and although study subjects were still classified as obese (BMI of 32 ± 4.3 kg/m^2), fasting and 2-hour plasma glucose and HbA1c returned to normal levels. In the follow-up, weight loss continued for the next 12 months. Insulin sensitivity was significantly increased (P<0.030) whereas serum FFA levels remained elevated (0.86 ± 0.18 mM vs. 0.76 ± 0.17) mM, post vs. pre) and higher than in normal-weight subjects (0.56 ± 0.17 mM, P < 0.03).

Before surgery, morbidly obese patients had higher duodenal (3.1 ± 1.2 vs. 1.8 ± 1.0 µmol 100ml^{-1} min^{-1}, P<0.01) and jejunal (3.1 ± 1.2 vs. 1.6 ± 1.0, P<0.001) FA uptakes compared to normal-weight subjects (Figure 15 B). The jejunum fractional tracer uptake rates K_i was higher in obese subjects compared to their normal-weight study counterparts. However, in duodenum this elevated K_i was not caused by higher K_i in the enterocyte layer but due to the availability of FAs in the

circulation because it was found that FFA levels in obese patients were higher compared to controls. Unexpectedly, the intestinal blood flow was not altered in the morbidly obese when compared to their controls. Intestinal blood flow and FA uptake were not associated with each other (15 A).

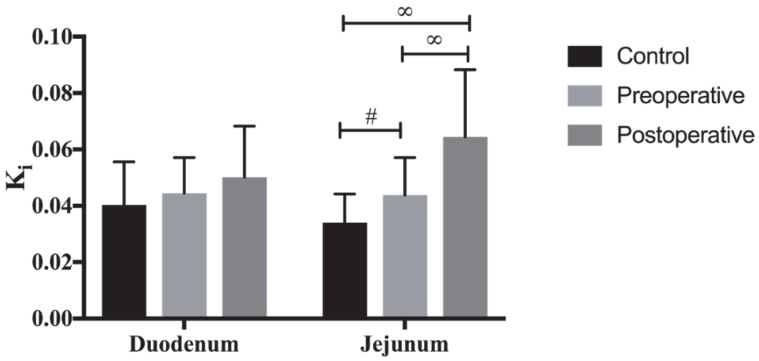

Figure 15. Fractional tracer uptake rates (Ki) in the duodenum and jejunum. Data are expressed as mean (SD). * P<0.05 vs. baseline, # P<0.03 vs. baseline, ∞ P<0.005 vs. control in Student's t-test.

Six months after surgery, the FA uptake from the circulation in the jejunum was further increased to 4.3 ± 2.0) mmol $100g^{-1}$ min^{-1} (P<0.03 vs. baseline) (Figure 16 B), whereas FA uptake decreased in other organs, namely: the heart, the adipose tissue and the pancreas.

Bariatric surgery led to a decrease in jejunal blood flow (0.41 ± 0.33 vs. 0.25 ± 0.14 ml $100g^{-1}$ min^{-1}, P<0.050) (Figure 16 A). Consequently, the ratio of FA uptake to FFA delivery rate (FFA*blood flow) was doubled in the jejunum from 1.1 ± 0.5% to 2.0 ± 1.1% (P=0.011) but not in in the duodenum (from 0.8 ± 0.5% to 0.9 ± 0.5%; P = 0.98). The type of surgical manipulation had no difference for intestinal blood flow nor for FA uptake.

The ^{18}F-FTHA tracer in experimental mice was taken at different parts of the small intestine and similarly in IGF-II/LDLR-/-ApoB100/100 and normal-weight mice. IGF-II/LDLR-/-ApoB100/100 mice had higher FFA and glycerol plasma concentrations compared to their leaner counterparts (0.50 ± 0.11) mmol/l vs. 0.22 ± 0.03); P=0.003 and 0.35 ± 0.10) mmol/l vs. 0.12 ± 0.03; P=0.001 respectively) whereas no differences were seen at baseline. ^{18}F-FTHA uptake in the mucosal layer of the small intestine was enhanced compared to lean controls as determined by PSL. Mucosa: non-mucosa PSL–ratios varied from 1.8 to 3.8 in the small intestine.

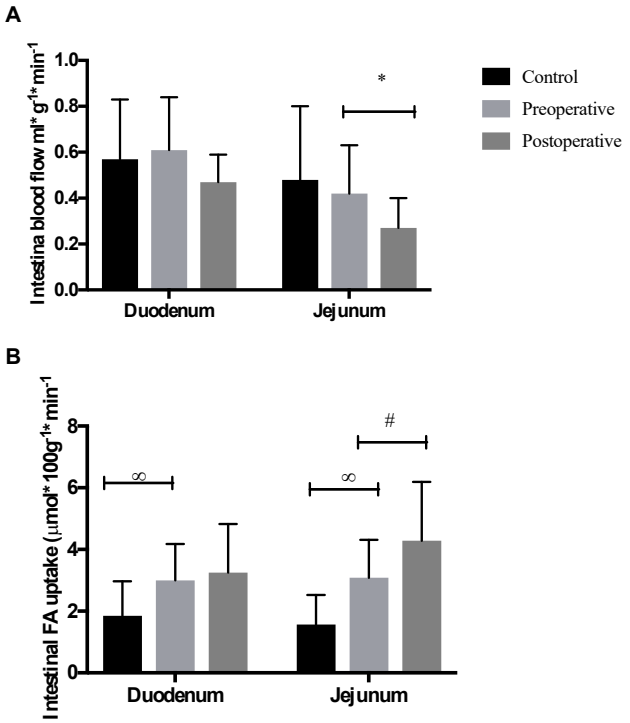

Figure 16. Panel A shows blood flow in the duodenum and jejunum pre- and postoperatively. Panel B shows FA uptake in the duodenum and jejunum pre-and postoperatively. Data are presented as mean (SD). Bariatric surgery decreased blood blow at the jejunum (A) and increased FA uptake at the jejunum (B) * $P<0.05$ vs. baseline, # $P<0.03$ vs. baseline, ∞ $P<0.005$ vs. control in the Student's t-test.

Radioactivity measurements of faecal samples showed a movement of ^{18}F-FTHA from the blood circulation into the intestinal lumen but no significant differences were seen in faecal activity between groups (16.2 ± 1.2%ID/g vs. 12.5 ± 2.9%ID/g; P=0.057, 6.7 ± 6.7 vs. 8.1 ± 4.8; P=0.75 and 4.9 ± 0.7 vs. 8.3 ± 3.5; P=0.11, for the duodenum, jejunum and ileum, respectively). The faecal to intestine wall biodistribution ratio varied from 1.8:1 to 2.5:1 in different small intestinal segments.

6.4 Metformin increases glucose uptake from the small intestine enterocyte layer (IV)

Metformin and rosiglitazone treatments improved HbA1c but only rosiglitazone improved whole body insulin sensitivity (M-value) ($P<0.001$) and skeletal muscle insulin sensitivity (P=0.047) in patients with T2D (study IV).

Intestinal glucose uptake in the small intestine and in the colon were similar between the groups before the intervention. After 26 weeks of treatment with metformin, GU in the small bowel increased 2-fold, (P<0.001) and in the colon 3-fold, (P<0.001) compared to baseline. The GU in the small intestine increased only slightly for the rosiglitazone group but the GU increased significantly compared to baseline (P=0.029) (Figure 17).

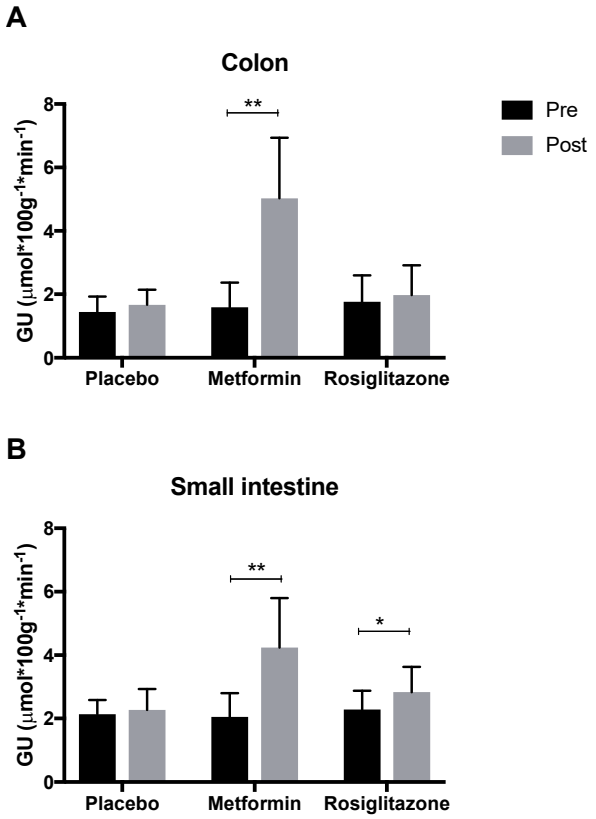

Figure 17. Bar-chart A represents glucose uptake (GU) in the colon and B the GU in small intestine after different interventions. Data are expressed as mean ± SD, *P<0.030 and **P<0.001 vs. baseline.

Changes in HbA1c in the pooled dataset were associated with changes in the GU in the small intestine (r = -0.40, P=0.016 and) and in the colon (P=0.005, r=-0.46). In addition, enhanced intestinal GU in colon correlated with changes in M-values and with fasting plasma glucose. Changes in $HOMA_{IR}$ and M-values were associated with differences in the small intestine GU in the rosiglitazone group (r=0.56, P=0.056 and r=0.67, P=0.017; respectively). Insulin clearance increased after metformin and rosiglitazone interventions (from 1.02 ± 0.27 ml/min to 1.23 ± 0.25 and from 0.96 ± 0.32 to 1.19 ± 0.29; P=0.010 and P=0.001; respectively). EGP/kg increased only in the rosiglitazone group from 20.7 ± 11.9 $\mu mol*kg^{-1}min^{-1}$

to 27.6 ± 9.9; P=0.012. Baseline vs. intervention lactate levels elevated in the metformin group from 1.0 ± 0.2 to 1.18 ± 0.3 mmol/l (P=0.01) but no correlations between EGP were found.

In the animal model, the metformin treated group had significantly higher ^{18}F-FDG tracer uptake in the duodenum (1.8 ± 0.5%ID/g vs. 1.1 ± 0.3%ID/g, P=0.026) and ileum (1.8 ± 0.4%ID/g vs. 0.8 ± 0.2%ID/g, P=0.002) compared to the controls, but no difference in the colon. Metformin treatment increased the ^{18}F-FDG uptake in the mucosal layer of the small intestine as determined by photostimulated luminescence (P=0.002 between metformin and control). In concert with this, imaging derived ^{18}F-FDG uptake was higher in the small intestine of rats given the metformin intervention compared to controls (10.0%ID/g vs. 4.4, P=0.002). There was also an increase in ^{18}F-FDG uptake by the colon albeit from a lower baseline level (P<0.026).

Radioactivity measurements of faecal samples showed a movement of ^{18}F-FDG from the blood circulation to the intestinal lumen but no significant differences were seen in faecal activity between the metformin group and the control group (5.6 vs. 7.8 1%ID/g *Mm, P=0.096).

7 DISCUSSION

7.1 Meal ingestion and elevated plasma GIP concentrations are the most potent blood flow inducers in the healthy human small intestine (I)

The present study in humans demonstrated that ingesting a mixture of carbohydrates, lipids and proteins led to a 1.68-fold increase in jejunal blood flow but no changes in the duodenum. According to previous early studies in rodents and dogs, exposing the small intestinal mucosa to a peptone solution, lipids, glucose or proteins increases blood flow (Brodie et al., 1910; Chou et al., 1976; Chou et al., 1985; Kvietys et al., 1980). Nutrients that come into contact with the apical surface of the mucosa stimulate incretin release from enteroendocrine cells and mediate local changes in the vascular milieu most likely by vasodilatation to increase perfusion to meet metabolic demands. Degradation and oxidation of nutrients in the mucosa decrease pO_2, pH and increase pCO_2, which are the most potent blood flow inducers (Gallavan and Chou, 1985). Intestinal blood volume was unchanged, which indicates that increased perfusion flushes absorbed nutrients from the small intestine mucosa further to portal blood flow.

The rate of gastric emptying is tightly regulated by small intestinal feedback, wherein acute hyperglycaemia and elevated levels of GLP-1 are involved. In healthy subjects, glucose is constantly emptied from the stomach 2–3 kcal/min (Horowitz et al., 1996a) and when the threshold of glucose load of 1.8 kcal/min i.e. maximal absorption capacity in duodenum is exceeded (Schirra et al., 1996) the feedback mechanism of GLP-1 modulates gastric emptying, which delays the absorption and subsequent flux of glucose into the splanchnic circulation. Exogenous GLP-1 work similarly by slowing down the gastric emptying (Nauck et al., 1997), which decreases the glucose excursion into the proximal duodenum. In the present study, duodenal blood flow remained at the baseline level during the whole study protocol after the mixed meal ingestion. The reason for this difference between the duodenum and the jejunum is unknown but could have several contributory factors. First, after the ingestion of a low-calorie meal, 10–20% of the stomach contents are expelled through the pylorus into the descending duodenum over 30 minutes and this proportion rises to 40–50% after 60 minutes (Tougas et al., 2000). Unfortunately, we did not measure gastric emptying velocity with the paracetamol absorption technique (Willems et al., 2001) to verify nutrient contact velocity of the mucosa of the duodenum over a period of imaging time points. Second, gastric acids are diluted by the ingested nutrients and the contents in the proximal part of the duodenum might be alkalotic due to exocrine alkali secretion

from the pancreas and such an increase pH of digesta might interact with the mucosal blood perfusion (Starlinger et al., 1981). The different blood flow regulation between the duodenum and jejunum raises the question as to whether the primary role for the proximal duodenum is that of nutrient sensing (Gribble, 2012) in addition to the roles of iron absorption and absorption of digested nutrients.

Infusion of GLP-1 had no effect on intestinal blood flow, which is in line with earlier studies (Bremholm et al., 2017; Svensson et al., 2007). However, GLP-1 may regulate intestinal blood flow in conditions of hyperglycaemia, which was shown in 2007 by Svensson and co-workers (Svensson et al., 2007). A study by Hansen and Holst, showed that GLP-1 decreased the vascular resistance in the perfused ileum segment in pigs (Hansen and Holst, 2002). Trahair and co-workers reported that GLP-1 infusion in increased blood flow in the SMA of healthy study subjects in combination with the intraduodenal administration of glucose, whereas GLP-1 infusion alone, led to a decrease of flow in the same arteria (Trahair et al., 2014). In addition to the small intestine, the SMA supplies blood for other abdominal organs such as the pancreas and the colon. Our results thus suggest that GLP-1 participate in splanchnic blood flow redistribution by decreasing pancreatic perfusion (Koffert et al., 2017), whereas regulation of the small intestine seems to be relatively unaffected in humans.

This study on the other hand demonstrates the pivotal role of GIP in the blood flow regulation of the small intestine. After GIP infusion, jejunal blood flow was increased 2.4-fold whereas no changes were seen in the duodenum. The rise of GIP-concentrations in plasma 30 minutes after meal ingestion is in line with previous findings (Lund et al., 2013). Although GIP secreted from the proximal small intestine has not been shown to increase plasma levels in systemic circulation that are sufficient to induce blood flow changes (Gallavan and Chou, 1985), the local tissue GIP concentration may plausibly rise to levels capable of increasing blood perfusion. Previous studies in animal models showed that the SMA blood flow (measured using a Doppler ultrasound technique) during GIP-infusion is dose related (Kogire et al., 1988). When the blood flow in the SMA was increased, the CA flow remained unchanged. Our study suggests that GIP is a potent blood flow regulator in the small intestine that prepares the mucosa for nutrient absorption from the luminal side and /secretion from the basolateral border into the systemic circulation

7.2 Mild hyperglycaemia does not regulate basal intestinal blood flow in humans (II, III)

Unexpectedly, obese study patients with T2D and impaired glucose tolerance (IGT) had similar basal stage blood perfusion in the small intestine compared to normal-weight healthy controls. Previous studies on intestinal blood flow changes in diabetes have been done using diabetic animal models with marked hyperglycaemia, hyperglucagonemia, glycosuria and lack of insulin, however, our T2D patients were in good glycaemic control as their mean HbA1c ranged from 5.8 to 6.3 and fP-glucose from 7.0 to 7.1 mmol/l, in studies II and III, respectively. This suggests that the main regulators of intestinal blood flow in diabetes seems to be hyperglycaemia (Lucas and Foy, 1977) plasma osmolarity and glucagon concentration (Korthuis et al., 1987), all of which decreased vascular resistance in experimental animals and thereby enhanced the intestinal circulation. Whether the blood circulation in the small intestine increases as the type II diabetes progress over time, still remains unanswered.

7.3 Intestinal blood flow after bariatric surgery and incretin infusions (II-III)

Despite the anatomical changes that occur in the proximal small intestine after bariatric surgery, the fasting stage blood flow changes were minor. Interestingly no changes were seen two months after the surgery (II), but at six months postoperatively jejunal blood flow was decreased (III). The glycaemic control was not different but the decrease in BMI postoperatively was greater with the longer follow-up. Existing literature going back to the late 1970s suggest that obesity decreases intestinal blood flow (Lucas and Foy, 1977) but it is unclear, whether results of early animal studies can be generalized to humans. Although fasting blood perfusion in the intestine is largely regulated by oxygen, hydrogen ions, carbon dioxide, adenosine and lactate; the mechanism by which obesity might influence blood circulation requires further investigation.

Surgical manipulation of the antrum in VSG and small gastric pouch size after RYGB accelerate nutrient delivery to the proximal small intestine after bariatric surgery (Quercia et al., 2014). After the ingestion of a mixed meal solution blood flow changes were similar in the control, pre- and postoperative groups despite the increased gastric emptying velocity found in the postoperative group. In postoperative settings, jejunal blood flow increased 2.14-fold compared to baseline at the 20-minute time-point and this increase was accompanied by left-shifted plasma glucose excursion when nutrients were absorbed more rapidly from the

small intestine. A recent elegant study showed that RYGB led to hypertrophy of the alimentary Roux-limb in experimental animals compared to sham operated controls (Cavin et al., 2016). In addition, villus weight and crypt depth were increased thereby thickening the mucosa. This hyperplasia in animal models was associated with reprogramming of the intestinal glucose metabolism towards increased glucose uptake for tissue growth (Mumphrey et al., 2015; Saeidi et al., 2013). Findings from these recent studies show that the mass of the Roux-limb increases after RYGB. The blood flow per 100g of tissue reported in this thesis was unchanged, however, which suggests that the total blood supply to the Roux limb was increased. Cavin and co-workers studied a small patient cohort and showed that the GU is increased in the Roux-limb after RYGB compared to normal-weight subjects in fasting conditions (Cavin et al., 2016). Whether increased GU following the Roux-limb procedure is associated with blood flow, warrants further investigation.

The GIP-infusion increased jejunal blood flow at the 20-minutes time-point in all studied groups, whereas no changes were seen in the duodenum. A comparison of the mixed meal induced systemic GIP peak concentrations of 70 ± 40 pM to pharmacological induced concentration of 261 ± 85.6 pM, raises questions about the physiological regulation of GIP. The infusion rate of GIP was 4.0 pmol/kg/min, which has been used in previous studies in normal-weight study subjects, and which was shown to lead to physiological concentrations under 100 pM (Christensen et al., 2011). The GIP infusion rate should probably have been adjusted to lean body mass in obese subjects to achieve physiological concentration. However, the saturation level of GIP-receptors reported in, in vitro studies has varied been between 50 to 75 pM (Gourni et al., 2014), which suggests caution in interpreting our slightly higher result as being a physiological response. Early studies in experimental animal models suggest that enteroendocrine hormones released after ingesting a meal and measured in the systemic circulation lead to concentrations that were insufficient to induce blood flow changes (Gallavan et al., 1985; Gallavan and Chou, 1986; Gallavan et al., 1986; Premen et al., 1985) but local concentrations of these peptides might rise to levels capable of mediating blood flow changes.

The existing literature offers contradictory findings about GLP-1 secretion in T2D. Toft-Nielsen and co-workers documented decreased postprandial GLP-1 response 60 minutes after meal ingestion in patients with T2D (Toft-Nielsen et al., 2001), but their finding was not confirmed in more recent studies (Ryskjaer et al., 2006; Vollmer et al., 2008). A further analysis of these former studies found that long duration and severity of T2D and BMI were associated with poor GLP-1 secretion (Holst et al., 2011; Muscelli et al., 2008). Study subjects in our cohort were in relatively good glycaemic balance, which explains the lack of GLP-1

concentration changes after ingesting the mixed meal in the preoperative studies. The GLP-1 levels increased only in the postoperative group due to a faster delivery of nutrients to the hindgut, which is in line with findings in the literature (Hansen and Holst, 2002; Laferrere et al., 2007; Laferrere et al., 2008; Morinigo et al., 2006a). The numbers of GLP-1 and GIP secreting enteroendocrine cells are increased in the Roux-limb after RYGB in experimental animals and humans (Cavin et al., 2016), which might explain part of the dramatic rise in postprandial incretin levels after bariatric surgery. Interestingly, VSG did not induce mucosal hypertrophy in the jejunum but the number of GLP-1 secreting cells were increased and the glucose absorption from the lumen was delayed in experimental animals (Cavin et al., 2016), which leads to an increased glucose delivery to the distal jejunum. Taken together, the re-modelling of the GI tract manifested as soon as two weeks after bariatric surgery, and this plays a crucial role in incretin secretion.

In the present study, the response to mixed meal ingestion manifested as the enhancement of GIP levels in all groups at the 15-minute time-point and concentrations remained elevated for the whole intervention. Previous studies have documented decreased postprandial concentrations of GIP in patients with T2D (Toft-Nielsen et al., 2001). The difference in these concentrations in previous studies were found to be small in matched comparisons and might therefore have been missed in our study due to the smaller study population. However, obesity is linked to increased GIP secretion (Vilsboll et al., 2003b; Yip and Wolfe, 2000) and therefore a comparison of the effects of obesity and T2D to GIP secretion would need further investigation using subjects with T2D matched with normoglycaemic obese counterparts. The GIP reached its peak concentration earlier in the postoperative group due to a more rapid delivery of nutrients to the jejunum, which is line with the study by Hansen and co-workers (Hansen et al., 2011). On the other hand, this early peak of GIP might be due to hyperplasia of the Roux-limb after the RYGB procedure and also due to earlier nutrient contact with the mucosa of the distal small intestine which increases the GIP secretion after meal ingestion. In contrast to this finding, Jorgensen and colleagues (Jorgensen et al., 2012) documented identical GIP secretions in mixed meal tests before and after bariatric surgery. The differences between the study protocols were primarily the time-points for mixed meal testing 1 and 6 weeks (Hansen et al., 2011) vs. 1 week, 3 months, 12 months (Jorgensen et al., 2012) vs. 77 days postoperatively (II), all of which had almost identical plasma incretin findings for bariatric procedures and mixed meal solution responses. Whether increased GIP-secretion is part of the adaptation phase after bariatric surgery amelioration during the first months requires further investigation.

The RYGB procedure increases the rate of glucose delivery to the small intestine and further to the caecum (Nguyen et al., 2014) and caecal arrival time of ingested

glucose has been shown to inversely-correlate with GLP-1 peak levels. In addition, RYGB patients who had more rapid pouch emptying also had a greater weight loss than those with slower emptying (Akkary et al., 2009), which provides indirect evidence to support the contribution of a rapid transit of nutrients to the distal small intestine as a consequence of the exaggerated release of distal gut hormones. VSG accelerates small bowel transit but delays the initiation of caecal filling and prolongs the contact time of nutrients in the distal small intestine (Melissas et al., 2013). These findings suggest that motility of the small intestine is increased after bariatric surgery. Coordinated motility patterns in longitudinal and circular muscle layers induce peristaltic waves, which impels the luminal contents in the aboral direction. The limited spatial resolution of PET scanning prevents the imaging of the increased tracer accumulation in the mucosa or the separation the muscle layer in the scans. Moreover, the muscle contractions in the small intestinal walls increase the local blood flow temporarily, which predisposes to an overestimation of the fasting stage blood flow.

Taken together, the rapid gastric emptying after a meal ingestion following VSB or RYGB (Chambers et al., 2014; Marathe et al., 2013) expose the intestinal mucosa to nutrient contact, to increasing blood flow, to increased GIP-secretion and in a later phase to GLP-1 secretion. The differences between blood flow dynamics in the duodenum and jejunum can only be speculated. The role of the duodenum in the strategic crossroads as a nutrient sensing and hostile intruders sensing organ has been suggested in a recent review (Ronnestad et al., 2014).

7.4 Bariatric surgery enhances intestinal fatty acid uptake

Intestinal insulin resistance in obese leads to changes in the glucose-to-FFA energy ratio. In the catabolic state, fat tissue releases FFAs into the circulation to meet nutritional demands. Intestinal FA uptake was higher in obese subjects with T2D compared to healthy controls, which is in line with previous publications that investigated other abdominal organs such as the pancreas (Honka et al., 2015), the liver (Immonen et al., 2017) and subcutaneous and visceral fat (Dadson et al., 2017). Interestingly, this increase in uptake was due to higher availability of FFA in the blood circulation of the duodenum where K_i (and fractional extraction of fatty acid tracer) was unchanged but K_i was higher in the jejunum compared to those of normal-weight study subjects. This suggests that the small intestine has different metabolic regulation properties in different segments/sites/ of the organ. The small intestine oxidizes glucose and FFA for metabolic demands. When FA uptake is increased the probable counteraction in the intestine is GU downregulation at least in the postprandial state as reported by Mäkinen and co-

workers (Makinen et al., 2015). In that same study, they demonstrated that obese patients with T2D had lower insulin stimulated GU in the intestine compared tonormal-weight controls even at 6 months after bariatric surgery. Oxygen consumption and nutrient metabolism in the tissue rely on blood supply and intestinal blood flow was similar between normal-weight and obese individuals, which suggests that the energy need for mucosa was unchanged and only the FFA-to-glucose ratio was altered. Whether the increased intestinal FA uptake in obese patients continues in the postprandial situation despite the decreasing FFA plasma concentration, warrants further investigation.

After bariatric surgery, the intestinal FA uptake increased in the jejunum whereas blood flow was decreased in the same site. Such a finding is paradoxical compared to other abdominal organs such as the liver, visceral fat and the pancreas (Dadson et al., 2017; Honka et al., 2015; Immonen et al., 2017). The recent study by Mäkinen (2015) and colleagues demonstrated that GU in the jejunum is increased after bariatric surgery but remained unchanged in the duodenum. Although RYGB leads to hypertrophy of the alimentary limb, it is tempting to speculate that the increased cell mass in the mucosa enhances FA uptake and GU after surgical manipulation of the GI tract. On the other hand, VSG does not induce mucosal hypertrophy in the jejunum (Cavin et al., 2016) and no significant differences in the operation-induced changes in intestinal GU (Makinen et al., 2015) or FA uptake were observed between the two surgical procedures. This increment in FA uptake rate suggest that in obese subjects with T2D, intestinal energy expenditure relies on high FFA-to-glucose ratio and this also persists after bariatric surgery.

The aforementioned finding was confirmed in the animal model, in which ^{18}F-FTHA accumulation in the intestinal mucosa of insulin resistant mice was increased compared to healthy controls. In addition, the ^{18}F-FTHA tracer was found in the luminal contents at even higher counts than those measured in the intestinal wall: a finding that raises the question about whether the mucosa allows FA flux from the blood into the intestinal lumen. It was hypothesized that reduced FFA loss in the faeces could contribute to weight gain in mice, but this was not confirmed. We were unable to measure luminal ^{18}F-FTHA activity in humans, therefore further studies to investigate FFA fluxes in the intestinal mucosa after bariatric surgery are warranted.

After RYGB, malabsorption accounts for approximately 10–12 g of faecal fat loss daily (Mahawar and Sharples, 2017). The enterocytes use FFAs for metabolism and structural components, increased basolateral FFA uptake might be a compensation mechanism for decreased absorption from the luminal side. Further investigation regarding simultaneously apical and basolateral FA is warranted to understand the changes after bariatric surgery.

7.5 Metformin and rosiglitazone enhanced intestinal GU during insulin stimulation

Insulin stimulated intestinal GU was lower in patients with T2D when compared to recent data from our laboratory on healthy subjects but the current data are in line with findings reported for obese T2D patients (Honka et al., 2013; Makinen et al., 2015). The molecular mechanism behind this phenomenon is tentative. Insulin resistance and metformin treatment has been shown to increase apical GLUT2 (Ait-Omar et al., 2011; Tobin et al., 2008), whereas basolateral GLUT2 presence in the epithelium in insulin resistant stages has gained little attention.

Case reports on intestinal ^{18}F-FDG retention "hot spots" has been published (Bahler et al., 2016; Gontier et al., 2008) but quantitative analysis on metformin induced GU is still lacking. Metformin treatment in the present study enhanced intestinal GU in humans by 2–3-fold. GU of the patients with T2D equalled and even exceeded the level of healthy controls in the study conducted by Mäkinen and colleagues (Makinen et al., 2015). An animal model was used to localize the increased GU to the intestinal epithelium. Rosiglitazone enhanced intestinal GU by 20% in the small intestine in addition to improving the peripheral insulin sensitivity, which was not seen after metformin intervention. These findings suggest that a component of metformin action is intestine specific.

In this study (IV) the change in the total intestinal GU per organ was 21 µmol min^{1} after metformin treatment. The small intestine GU was increased by 13.4 µmol kg^{1} min^{-1} and the colon GU was increased by 12.2 µmol kg^{-1} min^{-1}, for calculations weights of 640g and 1000g were used for small intestine and colon, respectively (Snyder WS CM, 1975). Total intestinal GU increased 13.4 µmol kg^{-1} min^{-1}*0.640 + 12.2 µmol kg^{-1} min^{-1}*1.0kg = 20.8 µmol min^{-1}) and skeletal muscle GU after rosiglitazone intervention 230 µmol min^{-1} (skeletal mucle GU was increased 7.6 µmol kg^{-1} min^{-1}and skeletal muscle weight 30 kg (Snyder WS CM, 1975), 7.6 µmol kg^{-1} min^{-1}*weight 30kg = 228 µmol min^{-1}). Due to their being an order of magnitude difference in GU between these organs, GU of intestine play only a minor part in the glucose clearance from the blood circulation.

An interesting result in the animal study was the finding of radioactivity in the faecal samples. This activity was significant as it amounted to 10–30% of the total activity of intestinal segment depending on the selected section, individual and the location in the bowel. This increase in faecal activity suggest that metformin might permit glucose fluxes down the concentration gradient into the intestinal lumen. If glucose is actively transported into the enterocytes from the circulation, then the intestine can be assumed to act as a sink for the cleared glucose and thus play a role in preventing hyperglycaemia. The most common side-effects of metformin

treatment are abdominal discomfort, diarrhoea and bloating, and it is plausible that increased luminal glucose concentrations might be related to these symptoms and signs. Whether the alterations in microbiota that occur after metformin treatment (Shin et al., 2013) are induced by luminal glucose or metformin per se, requires further investigation. It is not currently technically possible to quantify intestinal wall and luminal activity in humans in vivo due to limitations of PET imaging resolution. Oral ^{18}F-FDG tracer offers a new insight for the action of metformin. However, it also has limitations due to the retention of tracer in the lumen, radiation exposure and modelling. In addition, Higashi and co-workers have shown that the glucose absorption rate is faster than the ^{18}F-FDG absorption as 19–26% of the administered ^{18}F-FDG dose still remained in the gastrointestinal lumen at 2 hours after administration under the same conditions (Higashi et al., 2002). It is obvious that the metformin treatment regulates the intestinal glucose fluxes that adapt the intestine to the metabolic pathology. However, further studies are needed to uncover the exact molecular mechanism for this regulation.

7.6 Limitations and future directions

It must be acknowledged that in addition to its advantages, the multimodal imaging has a few limitations compared to more traditional methods. The associated high costs, a demanding technical requirement for operating the imaging equipment, and the need for radiotracer production facilities, limited the possibility for having a larger cohort size in this study. In addition, a radiation burden and the inconvenience of the imaging sessions restrict the opportunities for longitudinal studies with multiple PET-scanning's. This could have affected the capability of our studies to have the statistical power to determine minor changes between different groups. The study population consisted of obese study patients with T2D in good treatment balance whom were age matched with healthy controls. The obese age-matched controls would have offered us new insight into comparing obesity induced changes. Therefore, caution must be used in generalizing the current findings to a larger population and to patients with T2D whom are in a worse treatment balance than the participants of the present study.

The spatial resolution in current human PET-scanning is a limiting factor. PET imaging allows us to analyze extraction rates in a specific intestinal segment but not in different layers. The thickness of the colon mucosa varies from 1 to 2 mm, but luminal contents and peristaltic waves largely contribute to the colon diameter. The luminal contents such as faeces or the fluids secreted into the intestinal lumen expand the diameter of the intestine and decrease the mucosa-to-VOI ratio, which lead to lower counts/volume in TAC. Radiotracers transported or leaked into the

intestinal lumen as demonstrated in this thesis, can distort the results of mucosal tracer extraction rates and must therefore be interpreted with caution. It is unlikely that we can achieve our goals of understanding the changes in the epithelial layer of the colon without using an animal model to verify the tracer location. Analyses of the radiotracer uptake from the small intestine have fewer pitfalls compared to the measurement of the uptake of the same tracer in the colon. Therefore, when considering that the small intestine is the first absorption organ to process the partly digested nutrients, the studies in this thesis have only "scratched the surface" of the possibilities that intestinal PET studies have to offer.

Using simplified equations for GU modelling has some limitations for its use in intestinal GU analysis, which must be discussed. The small intestine is shown to be a gluconeogenic organ expressing glucose-6-phosphatase (Glc6Pase) (Croset et al., 2001), the enzyme catalyzing the hydrolysis of glucose-6-phosphate and ^{18}F-FDG-6P into glucose and ^{18}F-FDG, respectively. The study by Rajas and co-workers found the activity of glucose-6-phospatase (Glc6Pase) was 300% higher in streptozotocin diabetic rats compared to healthy controls and the Glc6Pase messenger RNA abundance was increased 8-fold and 6-fold in the duodenum and jejunum of diabetic rats respectively (Rajas et al., 1999). These levels were subsequently normalized after insulin treatment. The changes in Glc6Pase activity in different interventions and study subjects must be acknowledged in intestinal GU analysis and further investigations for more accurate models is urgently needed. A two-tissue compartment model with a measured input function is considered to be the best model for GU estimations. In practice, this model is sensitive to all kinds of errors such as movement of the patient, errors in timing, errors in determining the input function, etc. More complex models are developed to describe tracer kinetics, but models with too many parameters are not suitable for use in PET imaging.

Recent studies have shown that RYGB surgery is associated with hypertrophy of the alimentary Roux-limb, an increase in its diameter and a thickening of the mucosa. The hyperplasia of the Roux-limb is associated with a reprogramming of intestinal glucose metabolism towards increased glucose uptake for tissue growth in animal models. The extent of the hyperplasia in the small intestine after surgery, and the association of intestinal blood flow and GU with these anatomical and histological changes should be addressed in future research.

Quantitative PET studies can provide new and accurate information on tissue metabolism, which could be used more in integrative analysis of the splanchnic tissues for metabolic research and drug discovery. Although the methodologies used in this study focused on the basolateral uptake of tracers, there is an urgent need for understanding the luminal absorption and the pathways of nutrients in target organs.

8 SUMMARY AND CONCLUSION

This study aimed at clarifying the role of the small intestine metabolism in T2D and obesity in the human. Multimodal imaging provides novel noninvasive methods to measure quantitative metabolism in the small intestine and revealed that obesity and metabolic syndromes and their treatments interact with the intestinal blood flow and metabolic substrate uptake.

In this thesis, I demonstrated that 1) an ingestion of meal and GIP secretion are the most potent inducers of the intestinal blood flow in normal-weight and obese subjects with T2D, 2) morbid obesity and T2D do not alter the blood flow regulation of the intestine, 3) intestinal FA uptake is increased in morbidly obese individuals compared to healthy subjects even after bariatric surgery, 4) intestinal energy expenditure relies on a high FFA-to-glucose ratio in obese patients and this relationship also persists after weight loss, 5) metformin treatment doubles the GU in the intestine.

Major limitations to be addressed in future studies are as follows: 1) PET resolution in colon imaging, 2) estimating radiotracer fluxes from the blood circulation into the lumen, 3) estimations of the small intestine mass after RYBG induced hyperplasia in the Roux-limb.

The implications of my findings are 1) GIP has an important role in the blood flow regulation of the small intestine in humans, 2) T2D does not alter blood flow in the small intestine, 3) intestinal energy expenditure relies on high FFA-to-glucose ratios in obese individuals, 4) the small intestine is an important site for metformin action.

The findings presented in this thesis narrow the gap between previous studies on the metabolism of the small intestine in animal models and humans. However, it is not known whether these changes in the intestinal metabolism and blood flow are part of an adaptation mechanism, or are due to improved glycaemic control and insulin resistance breakdown, or are due to the fundamental pathophysiology behind the T2D. The actual mechanism behind these changes should be elucidated in future research.

ACKNOWLEDGEMENTS

This study was conducted as part of the Finnish Centre of Excellence in Molecular Imaging in Cardiovascular and Metabolic Research programme, and was carried out in the Turku PET Centre, University of Turku, Turku, Finland, during the years 2012–2018.

I owe my sincere gratitude for my supervisor's professor Pirjo Nuutila and Saila Kauhanen for all the guidance throughout this project. Without you I wouldn't be writing these remarks today. I want to thank Pirjo for introducing me to the world of metabolic research with her passion to explore this field. I have enjoyed our meetings from the beginning, strict and honest feedback from the work, challenging my thoughts and still showing faith on my own ideas. You let me grow as a researcher and were encouraging when it was needed. I want to thank Saila for guiding me to the scientific world, from the start helping with practical issues, showing the right direction. I admire your ability to find time for everything along with the pursuit of your clinical career.

Professor Markku Voutilainen and Docent Perttu Arkkila, the members of my supervisory committee, are thanked for their valuable comments and advice during this project. I am grateful to professor emeritus Jorma Viikari and professor Markus Juonala for granting me permission to conduct this work at the Institute of Clinical Medicine, University of Turku. I warmly thank Professor Juhani Knuuti, a director of Turku PET Centre, for providing facilities and resources for this research.

Professor André Carpentier and Docent Perttu Arkkila are sincerely thanked for reviewing this thesis and providing constructive criticism and valuable comments.

I am grateful to all my co-authors for their contributions to the original publications. I want to thank Henri Honka for all the good moments and discussions in science. I owe my sincere thanks to Patricia Iozzo, who has provided her expertize, time and effort to revise our manuscripts and guided me to deeply understand our findings. Kirsi Mikkola and Mia Ståhle are acknowledged for their expertise and valuable help with the preclinical studies. I also want to express my gratitude to professor Leif Groop for collaboration between researchers of the Universities of Lund and Turku. Professor Nils Wierup and Andreas Lindqvist are acknowledged for their collaboration. Physicists Virva Saunavaara, Mika Teräs, Jarmo Teuho and Tuula Tolvanen offered invaluable help in technical issues. Nobu Kudomi, Vesa Oikonen and Hannu Sipilä are acknowledged for helping in the modelling of the data and Saija Hurme for the statistical help.

Moreover, co-authors of the original communications: Henry Karlsson, Riitta Parkkola, Anne Roivainen, Paulina Salminen, Antti Saraste, Kirsi Virtanen, Andrea Mari, Anna-Maria Andersson, Linda Faxius, Kirsti Hällsten, Mikael Heglind, Letizia Guiducci, Tam Pham, Johanna Silvola, Jenni Virta, Olof Eriksson, Sven Enerbäck and Maria Gomez are acknowledged.

I want to thank my fellow researchers of Turku PET Centre, especially Jarna Hannukainen, Robert Badeau, Marco Bucci, Prince Dadson, Miikka Honka, Ville Huovinen, Aino Hyypiä, Heidi Immonen, Jaakko Mäkinen and Mueez Y Din for building a scientific atmosphere.

This work would have not been possible without the help of the personnel of Turku PET Centre and University of Turku; especially: research nurses Mia Koutu, Niina Gröndahl, Anni Storrank, secretary Mirja Jyrkinen, radiographers Minna Aatsinki, Anne-Mari Jokinen, Hannele Lehtinen, Johanna Pasanen and Tiina Santakivi, and laboratory nurses Hanna Liukko-Sipi, Heidi Partanen, Emilia Puhakka, Eija Salo, Sanna Suominen and Tiina Tuominen are thanked for the data collection. Marita Kailajärvi is thanked for her administrative contribution. Hanna Kivikoski and Lauri Laitinen are acknowledged for their expertise in pharmacy.

I am grateful to my colleagues Kimmo Salminen, Teppo Stenholm, Heikki Nuutinen, Satu Haikio, Juha Liikala, Juho Lindberg, Juhani Koskinen for their support in my research work and enjoyable working atmosphere in the clinic.

Markus Ingström, Petri Karvinen, Mikko Helin are thanked for their unconditional friendship, even though the busy years have kept us apart. My friends from the medical school Jani Söderström, Jarkko Mäkelä, Teemu Juntunen and Jussi Jalkanen are thanked for all the unforgettable and fun experiences during the years.

I am fortunate for having the family I do. Ulla and Eero, you have always encouraged me in all my personal choices and helped throughout life. There are no words to express my gratitude. I want to thank my sister Marja and brothers Mikko and Jaakko, you have brought a lot of joy into my life.

Finally, I want to thank my wife Anna for all her support, patience and unconditioned love during all these years. Otto and Anton, you bring joy and meaning to my life.

This work was financially supported by the Academy of Finland and the Sigrid Jusélius Foundation, and grants from the Diabetes Research Foundation, the Emil Aaltonen Foundation, the Finnish Cultural Foundation, the Finnish Medical Foundation, the Jalmari and Rauha Ahokas Foundation, the Kyllikki and Uolevi Lehikoinen Foundation and the Maud Kuistila Foundation

REFERENCES

Diabeteksen ehkäisyn ja hoidon kehittämisohjelma Dehko 2000-2010 loppuraportti.

(1998a). Effect of intensive blood-glucose control with metformin on complications in overweight patients with type 2 diabetes (UKPDS 34). UK Prospective Diabetes Study (UKPDS) Group. Lancet *352*, 854-865.

(1998b). Intensive blood-glucose control with sulphonylureas or insulin compared with conventional treatment and risk of complications in patients with type 2 diabetes (UKPDS 33). UK Prospective Diabetes Study (UKPDS) Group. Lancet *352*, 837-853.

(2000). Obesity: preventing and managing the global epidemic. Report of a WHO consultation. World Health Organ Tech Rep Ser *894*, i-xii, 1-253.

(2011). In Use of Glycated Haemoglobin (HbA1c) in the Diagnosis of Diabetes Mellitus: Abbreviated Report of a WHO Consultation (Geneva).

Abumrad, N.A., and Davidson, N.O. (2012). Role of the gut in lipid homeostasis. Physiol Rev *92*, 1061-1085.

Abumrad, N.A., el-Maghrabi, M.R., Amri, E.Z., Lopez, E., and Grimaldi, P.A. (1993). Cloning of a rat adipocyte membrane protein implicated in binding or transport of long-chain fatty acids that is induced during preadipocyte differentiation. Homology with human CD36. J Biol Chem *268*, 17665-17668.

Adiels, M., Taskinen, M.R., Packard, C., Caslake, M.J., Soro-Paavonen, A., Westerbacka, J., Vehkavaara, S., Hakkinen, A., Olofsson, S.O., Yki-Jarvinen, H., et al. (2006). Overproduction of large VLDL particles is driven by increased liver fat content in man. Diabetologia *49*, 755-765.

Ahren, B., Landin-Olsson, M., Jansson, P.A., Svensson, M., Holmes, D., and Schweizer, A. (2004). Inhibition of dipeptidyl peptidase-4 reduces glycemia, sustains insulin levels, and reduces glucagon levels in type 2 diabetes. J Clin Endocrinol Metab *89*, 2078-2084.

Ait-Omar, A., Monteiro-Sepulveda, M., Poitou, C., Le Gall, M., Cotillard, A., Gilet, J., Garbin, K., Houllier, A., Chateau, D., Lacombe, A., et al. (2011). GLUT2 accumulation in enterocyte apical and intracellular membranes: a study in morbidly obese human subjects and ob/ob and high fat-fed mice. Diabetes *60*, 2598-2607.

Akkary, E., Sidani, S., Boonsiri, J., Yu, S., Dziura, J., Duffy, A.J., and Bell, R.L. (2009). The paradox of the pouch: prompt emptying predicts improved weight loss after laparoscopic Roux-Y gastric bypass. Surg Endosc *23*, 790-794.

Alberti, K.G., and Zimmet, P.Z. (1998). Definition, diagnosis and classification of diabetes mellitus and its complications. Part 1: diagnosis and classification of diabetes mellitus provisional report of a WHO consultation. Diabetic medicine : a journal of the British Diabetic Association *15*, 539-553.

Alemayehu, A., and Chou, C.C. (1993). Differences in vascular response to thromboxane between intestinal mucosa and muscularis. Prostaglandins *45*, 447-457.

Ashcroft, F.M., and Rorsman, P. (1989). Electrophysiology of the pancreatic beta-cell. Prog Biophys Mol Biol *54*, 87-143.

Ashrafian, H., Toma, T., Rowland, S.P., Harling, L., Tan, A., Efthimiou, E., Darzi, A., and Athanasiou, T. (2015). Bariatric Surgery or Non-Surgical Weight Loss for Obstructive Sleep Apnoea? A Systematic Review and Comparison of Meta-analyses. Obesity surgery *25*, 1239-1250.

Avenell, A., Broom, J., Brown, T.J., Poobalan, A., Aucott, L., Stearns, S.C., Smith, W.C., Jung, R.T., Campbell, M.K., and Grant, A.M. (2004). Systematic review of the long-term effects and economic consequences of treatments for obesity and implications for health improvement. Health Technol Assess *8*, iii-iv, 1-182.

Badman, M.K., and Flier, J.S. (2005). The gut and energy balance: visceral allies in the obesity wars. Science *307*, 1909-1914.

Bahler, L., Stroek, K., Hoekstra, J.B., Verberne, H.J., and Holleman, F. (2016). Metformin-related colonic glucose uptake; potential role for increasing glucose disposal?--A retrospective analysis of (18)F-FDG uptake in the colon on PET-CT. Diabetes Res Clin Pract *114*, 55-63.

Bailey, C.J., Wilcock, C., and Day, C. (1992). Effect of metformin on glucose metabolism in the splanchnic bed. British journal of pharmacology *105*, 1009-1013.

Bailey, C.J., Wilcock, C., and Scarpello, J.H. (2008). Metformin and the intestine. Diabetologia *51*, 1552-1553.

Barrera, J.G., Sandoval, D.A., D'Alessio, D.A., and Seeley, R.J. (2011). GLP-1 and energy balance: an integrated model of short-term and long-term control. Nature reviews. Endocrinology *7*, 507-516.

Batterham, R.L., Cohen, M.A., Ellis, S.M., Le Roux, C.W., Withers, D.J., Frost, G.S., Ghatei, M.A., and Bloom, S.R. (2003). Inhibition of food intake in obese subjects by peptide YY3-36. The New England journal of medicine *349*, 941-948.

Bieber, L.L. (1988). Carnitine. Annu Rev Biochem *57*, 261-283.

Bjorntorp, P. (1991). Metabolic implications of body fat distribution. Diabetes care *14*, 1132-1143.

Bluher, S., and Mantzoros, C.S. (2009). Leptin in humans: lessons from translational research. Am J Clin Nutr *89*, 991S-997S.

Bose, M., Olivan, B., Teixeira, J., Pi-Sunyer, F.X., and Laferrere, B. (2009). Do Incretins play a role in the remission of type 2 diabetes after gastric bypass surgery: What are the evidence? Obesity surgery *19*, 217-229.

Bournat, J.C., and Brown, C.W. (2010). Mitochondrial dysfunction in obesity. Current opinion in endocrinology, diabetes, and obesity *17*, 446-452.

Bray, M.S., Loos, R.J., McCaffery, J.M., Ling, C., Franks, P.W., Weinstock, G.M., Snyder, M.P., Vassy, J.L., Agurs-Collins, T., and Conference Working, G. (2016). NIH working group report-using genomic information to guide weight management: From universal to precision treatment. Obesity (Silver Spring) *24*, 14-22.

Bremholm, L., Andersen, U.B., Hornum, M., Hilsted, L., Veedfald, S., Hartmann, B., and Holst, J.J. (2017). Acute effects of glucagon-like peptide-1, GLP-19-36 amide, and exenatide on mesenteric blood flow, cardiovascular parameters, and biomarkers in healthy volunteers. Physiol Rep *5*.

Brener, W., Hendrix, T.R., and McHugh, P.R. (1983). Regulation of the gastric emptying of glucose. Gastroenterology *85*, 76-82.

Brodie, T.G., Cullis, W.C., and Halliburton, W.D. (1910). The gaseous metabolism of the small intestine: Part II. The gaseous exchanges during the absorption of Witte's peptone. J Physiol *40*, 173-189.

Brunmair, B., Staniek, K., Gras, F., Scharf, N., Althaym, A., Clara, R., Roden, M., Gnaiger, E., Nohl, H., Waldhausl, W., et al. (2004). Thiazolidinediones, like metformin, inhibit respiratory complex I: a common mechanism contributing to their antidiabetic actions? Diabetes *53*, 1052-1059.

Buchwald, H., Avidor, Y., Braunwald, E., Jensen, M.D., Pories, W., Fahrbach, K., and Schoelles, K. (2004). Bariatric surgery: a systematic review and meta-analysis. JAMA *292*, 1724-1737.

Burant, C.F., Flink, S., DePaoli, A.M., Chen, J., Lee, W.S., Hediger, M.A., Buse, J.B., and Chang, E.B. (1994). Small intestine hexose transport in experimental diabetes. Increased transporter mRNA and protein expression in enterocytes. The Journal of clinical investigation *93*, 578-585.

Burant, C.F., Takeda, J., Brot-Laroche, E., Bell, G.I., and Davidson, N.O. (1992). Fructose transporter in human spermatozoa and small intestine is GLUT5. J Biol Chem *267*, 14523-14526.

Cani, P.D., and Delzenne, N.M. (2009). Interplay between obesity and associated metabolic disorders: new insights into the gut microbiota. Current opinion in pharmacology *9*, 737-743.

Cao, J., Meng, S., Chang, E., Beckwith-Fickas, K., Xiong, L., Cole, R.N., Radovick, S., Wondisford, F.E., and He, L. (2014). Low concentrations of metformin suppress glucose production in hepatocytes through AMP-activated protein kinase (AMPK). J Biol Chem *289*, 20435-20446.

Carpentier, A.C., Frisch, F., Labbe, S.M., Gagnon, R., de Wal, J., Greentree, S., Petry, H., Twisk, J., Brisson, D., and Gaudet, D. (2012). Effect of alipogene tiparvovec (AAV1-LPL(S447X)) on postprandial chylomicron metabolism in lipoprotein lipase-deficient patients. J Clin Endocrinol Metab *97*, 1635-1644.

Caspary, W.F. (1992). Physiology and pathophysiology of intestinal absorption. Am J Clin Nutr *55*, 299S-308S.

Cavin, J.B., Couvelard, A., Lebtahi, R., Ducroc, R., Arapis, K., Voitellier, E., Cluzeaud, F., Gillard, L., Hourseau, M., Mikail, N., et al. (2016). Differences in Alimentary Glucose Absorption and Intestinal Disposal of Blood Glucose After Roux-en-Y Gastric Bypass vs Sleeve Gastrectomy. Gastroenterology *150*, 454-464 e459.

Chambers, A.P., Jessen, L., Ryan, K.K., Sisley, S., Wilson-Perez, H.E., Stefater, M.A., Gaitonde, S.G., Sorrell, J.E., Toure, M., Berger, J., et al. (2011). Weight-independent changes in blood glucose homeostasis after gastric bypass or vertical sleeve gastrectomy in rats. Gastroenterology *141*, 950-958.

Chambers, A.P., Smith, E.P., Begg, D.P., Grayson, B.E., Sisley, S., Greer, T., Sorrell, J., Lemmen, L., LaSance, K., Woods, S.C., et al. (2014). Regulation of gastric emptying rate and its role in nutrient-induced GLP-1 secretion in rats after vertical sleeve gastrectomy. American journal of physiology. Endocrinology and metabolism *306*, E424-432.

Cheeseman, C.I., and Maenz, D.D. (1989). Rapid regulation of D-glucose transport in basolateral membrane of rat jejunum. The American journal of physiology *256*, G878-883.

Cheung, G.W., Kokorovic, A., Lam, C.K., Chari, M., and Lam, T.K. (2009). Intestinal cholecystokinin controls glucose production through a neuronal network. Cell metabolism *10*, 99-109.

Chou, C.C. (1992). Intestinal blood flow regulation. (San Diego, Academic Press).

Chou, C.C., Burns, T.D., Hsieh, C.P., and Dabney, J.M. (1972). Mechanisms of local vasodilation with hypertonic glucose in the jejunum. Surgery *71*, 380-387.

Chou, C.C., and Coatney, R.W. (1994). Nutrient-induced changes in intestinal blood flow in the dog. The British veterinary journal *150*, 423-437.

Chou, C.C., Hsieh, C.P., Yu, Y.M., Kvietys, P., Yu, L.C., Pittman, R., and Dabney, J.M. (1976). Localization of mesenteric hyperemia during digestion in dogs. The American journal of physiology *230*, 583-589.

Chou, C.C., Nyhof, R.A., Kvietys, P.R., Sit, S.P., and Gallavan, R.H., Jr. (1985). Regulation of jejunal blood flow and oxygenation during glucose and oleic acid absorption. The American journal of physiology *249*, G691-701.

Christensen, M., Vedtofte, L., Holst, J.J., Vilsboll, T., and Knop, F.K. (2011). Glucose-dependent insulinotropic polypeptide: a bifunctional glucose-dependent regulator of glucagon and insulin secretion in humans. Diabetes *60*, 3103-3109.

Clements, R.H., Gonzalez, Q.H., Long, C.I., Wittert, G., and Laws, H.L. (2004). Hormonal changes after Roux-en Y gastric bypass for morbid obesity and the control of type-II diabetes mellitus. Am Surg *70*, 1-4; discussion 4-5.

Cohen, R.V., Pinheiro, J.C., Schiavon, C.A., Salles, J.E., Wajchenberg, B.L., and Cummings, D.E. (2012). Effects of gastric bypass surgery in patients with type 2 diabetes and only mild obesity. Diabetes care *35*, 1420-1428.

Control, G., Turnbull, F.M., Abraira, C., Anderson, R.J., Byington, R.P., Chalmers, J.P., Duckworth, W.C., Evans, G.W., Gerstein, H.C., Holman, R.R., et al. (2009). Intensive glucose control and macrovascular outcomes in type 2 diabetes. Diabetologia *52*, 2288-2298.

Cordain, L., Eaton, S.B., Sebastian, A., Mann, N., Lindeberg, S., Watkins, B.A., O'Keefe, J.H., and Brand-Miller, J. (2005). Origins and evolution of the Western diet: health implications for the 21st century. Am J Clin Nutr *81*, 341-354.

Craddy, P., Palin, H.J., and Johnson, K.I. (2014). Comparative effectiveness of dipeptidylpeptidase-4 inhibitors in type 2 diabetes: a systematic review and mixed treatment comparison. Diabetes Ther *5*, 1-41.

Crane, R.K. (1962). Hypothesis for mechanism of intestinal active transport of sugars. Federation proceedings *21*, 891-895.

Cronin, C.G., Delappe, E., Lohan, D.G., Roche, C., and Murphy, J.M. (2010). Normal small bowel wall characteristics on MR enterography. European journal of radiology *75*, 207-211.

Croset, M., Rajas, F., Zitoun, C., Hurot, J.M., Montano, S., and Mithieux, G. (2001). Rat small intestine is an insulin-sensitive gluconeogenic organ. Diabetes *50*, 740-746.

Cummings, D.E., Weigle, D.S., Frayo, R.S., Breen, P.A., Ma, M.K., Dellinger, E.P., and Purnell, J.Q. (2002). Plasma ghrelin levels after diet-induced weight loss or gastric bypass surgery. The New England journal of medicine *346*, 1623-1630.

Cummings, J.H. (1983). Fermentation in the human large intestine: evidence and implications for health. Lancet *1*, 1206-1209.

Cummings, J.H., Pomare, E.W., Branch, W.J., Naylor, C.P., and Macfarlane, G.T. (1987). Short chain fatty acids in human large intestine, portal, hepatic and venous blood. Gut *28*, 1221-1227.

Dadson, P., Ferrannini, E., Landini, L., Hannukainen, J.C., Kalliokoski, K.K., Vaittinen, M., Honka, H., Karlsson, H.K., Tuulari, J.J., Soinio, M., et al. (2017). Fatty acid uptake and blood flow in adipose tissue compartments of morbidly obese subjects with or without type 2 diabetes: effects of bariatric surgery. American journal of physiology. Endocrinology and metabolism *313*, E175-E182.

Dansinger, M.L., Tatsioni, A., Wong, J.B., Chung, M., and Balk, E.M. (2007). Meta-analysis: the effect of dietary counseling for weight loss. Ann Intern Med *147*, 41-50.

Deckers, J.G., Schellevis, F.G., and Fleming, D.M. (2006). WHO diagnostic criteria as a validation tool for the diagnosis of diabetes mellitus: a study in five European countries. Eur J Gen Pract *12*, 108-113.

DeFronzo, R.A., Tobin, J.D., and Andres, R. (1979). Glucose clamp technique: a method for quantifying insulin secretion and resistance. The American journal of physiology *237*, E214-223.

Degn, K.B., Juhl, C.B., Sturis, J., Jakobsen, G., Brock, B., Chandramouli, V., Rungby, J., Landau, B.R., and Schmitz, O. (2004). One week's treatment with the long-acting glucagon-like peptide 1 derivative liraglutide (NN2211) markedly improves 24-h glycemia and alpha- and beta-cell function and reduces endogenous glucose release in patients with type 2 diabetes. Diabetes *53*, 1187-1194.

DeGrado, T.R., Wang, S., Holden, J.E., Nickles, R.J., Taylor, M., and Stone, C.K. (2000). Synthesis and preliminary evaluation of (18)F-labeled 4-thia palmitate as a PET tracer of myocardial fatty acid oxidation. Nuclear medicine and biology *27*, 221-231.

Delaere, F., Magnan, C., and Mithieux, G. (2010). Hypothalamic integration of portal glucose signals and control of food intake and insulin sensitivity. Diabetes Metab *36*, 257-262.

Desai, N.R., Shrank, W.H., Fischer, M.A., Avorn, J., Liberman, J.N., Schneeweiss, S., Pakes, J., Brennan, T.A., and Choudhry, N.K. (2012). Patterns of medication initiation in newly diagnosed diabetes mellitus: quality and cost implications. The American journal of medicine *125*, 302 e301-307.

Dixon, J.B., O'Brien, P.E., Playfair, J., Chapman, L., Schachter, L.M., Skinner, S., Proietto, J., Bailey,

M., and Anderson, M. (2008). Adjustable gastric banding and conventional therapy for type 2 diabetes: a randomized controlled trial. JAMA *299*, 316-323.

Donald, D.E., and Shepherd, J.T. (1980). Autonomic regulation of the peripheral circulation. Annual review of physiology *42*, 429-439.

Drewe, J., Gadient, A., Rovati, L.C., and Beglinger, C. (1992). Role of circulating cholecystokinin in control of fat-induced inhibition of food intake in humans. Gastroenterology *102*, 1654-1659.

Druce, M.R., Wren, A.M., Park, A.J., Milton, J.E., Patterson, M., Frost, G., Ghatei, M.A., Small, C., and Bloom, S.R. (2005). Ghrelin increases food intake in obese as well as lean subjects. Int J Obes (Lond) *29*, 1130-1136.

Drucker, D.J. (2006). The biology of incretin hormones. Cell metabolism *3*, 153-165.

Drucker, D.J., Buse, J.B., Taylor, K., Kendall, D.M., Trautmann, M., Zhuang, D., Porter, L., and Group, D.-S. (2008). Exenatide once weekly versus twice daily for the treatment of type 2 diabetes: a randomised, open-label, non-inferiority study. Lancet *372*, 1240-1250.

Dubois, M., Pattou, F., Kerr-Conte, J., Gmyr, V., Vandewalle, B., Desreumaux, P., Auwerx, J., Schoonjans, K., and Lefebvre, J. (2000). Expression of peroxisome proliferator-activated receptor gamma (PPARgamma) in normal human pancreatic islet cells. Diabetologia *43*, 1165-1169.

Duca, F.A., Bauer, P.V., Hamr, S.C., and Lam, T.K. (2015). Glucoregulatory Relevance of Small Intestinal Nutrient Sensing in Physiology, Bariatric Surgery, and Pharmacology. Cell metabolism *22*, 367-380.

Dunning, B.E., and Gerich, J.E. (2007). The role of alpha-cell dysregulation in fasting and postprandial hyperglycemia in type 2 diabetes and therapeutic implications. Endocr Rev *28*, 253-283.

Dyer, J., Wood, I.S., Palejwala, A., Ellis, A., and Shirazi-Beechey, S.P. (2002). Expression of monosaccharide transporters in intestine of diabetic humans. Am J Physiol Gastrointest Liver Physiol *282*, G241-248.

Eckel, R.H., Kahn, S.E., Ferrannini, E., Goldfine, A.B., Nathan, D.M., Schwartz, M.W., Smith, R.J., and Smith, S.R. (2011). Obesity and type 2 diabetes: what can be unified and what needs to be individualized? J Clin Endocrinol Metab *96*, 1654-1663.

Egan, A.G., Blind, E., Dunder, K., de Graeff, P.A., Hummer, B.T., Bourcier, T., and Rosebraugh, C. (2014). Pancreatic safety of incretin-based drugs--FDA and EMA assessment. The New England journal of medicine *370*, 794-797.

Erlandsson, K., Buvat, I., Pretorius, P.H., Thomas, B.A., and Hutton, B.F. (2012). A review of partial volume correction techniques for emission tomography and their applications in neurology, cardiology and oncology. Phys Med Biol *57*, R119-159.

Faraj, M., Havel, P.J., Phelis, S., Blank, D., Sniderman, A.D., and Cianflone, K. (2003). Plasma acylation-stimulating protein, adiponectin, leptin, and ghrelin before and after weight loss induced by gastric bypass surgery in morbidly obese subjects. J Clin Endocrinol Metab *88*, 1594-1602.

Ferrannini, E., Nannipieri, M., Williams, K., Gonzales, C., Haffner, S.M., and Stern, M.P. (2004). Mode of onset of type 2 diabetes from normal or impaired glucose tolerance. Diabetes *53*, 160-165.

Finucane, M.M., Stevens, G.A., Cowan, M.J., Danaei, G., Lin, J.K., Paciorek, C.J., Singh, G.M., Gutierrez, H.R., Lu, Y., Bahalim, A.N., et al. (2011). National, regional, and global trends in body-mass index since 1980: systematic analysis of health examination surveys and epidemiological studies with 960 country-years and 9.1 million participants. Lancet *377*, 557-567.

Flameng, W., Winkler, B., Wusten, B., and Schaper, W. (1977). Minimum requirements for the measurement of regional myocardial flow using tracer microspheres. Bibl Anat, 24-29.

Fried, M., Yumuk, V., Oppert, J.M., Scopinaro, N., Torres, A.J., Weiner, R., Yashkov, Y., Fruhbeck, G., European Association for the Study of, O., and International Federation for the Surgery of Obesity - European, C. (2013). Interdisciplinary European Guidelines on metabolic and bariatric surgery. Obes Facts *6*, 449-468.

Gajda, A.M., and Storch, J. (2015). Enterocyte fatty acid-binding proteins (FABPs): different functions of liver and intestinal FABPs in the intestine. Prostaglandins Leukot Essent Fatty Acids *93*, 9-16.

Gallavan, R.H., Jr., Chen, M.H., Joffe, S.N., and Jacobson, E.D. (1985). Vasoactive intestinal polypeptide, cholecystokinin, glucagon, and bile-oleate-induced jejunal hyperemia. The American journal of physiology *248*, G208-215.

Gallavan, R.H., Jr., and Chou, C.C. (1985). Possible mechanisms for the initiation and maintenance of postprandial intestinal hyperemia. The American journal of physiology *249*, G301-308.

Gallavan, R.H., Jr., and Chou, C.C. (1986). The effects of mefenamic acid on postprandial intestinal carbohydrate metabolism. Prostaglandins *31*, 1069-1076.

Gallavan, R.H., Jr., Chou, C.C., Kvietys, P.R., and Sit, S.P. (1980). Regional blood flow during digestion in the conscious dog. The American journal of physiology *238*, H220-225.

Gallavan, R.H., Jr., Shaw, C., Murphy, R.F., Buchanan, K.D., Joffe, S.N., and Jacobson, E.D.

(1986). Effects of micellar oleic acid on canine jejunal blood flow and neurotensin release. The American journal of physiology *251*, G649-655.

Gangl, A., and Ockner, R.K. (1975). Intestinal metabolism of plasma free fatty acids. Intracellular compartmentation and mechanisms of control. The Journal of clinical investigation *55*, 803-813.

Gangl, A., and Renner, F. (1978). In vivo metabolism of plasma free fatty acids by intestinal mucosa of man. Gastroenterology *74*, 847-850.

Gaudet, D., Brisson, D., Tremblay, K., Alexander, V.J., Singleton, W., Hughes, S.G., Geary, R.S., Baker, B.F., Graham, M.J., Crooke, R.M., et al. (2014). Targeting APOC3 in the familial chylomicronemia syndrome. The New England journal of medicine *371*, 2200-2206.

Germano, G., Chen, B.C., Huang, S.C., Gambhir, S.S., Hoffman, E.J., and Phelps, M.E. (1992). Use of the abdominal aorta for arterial input function determination in hepatic and renal PET studies. J Nucl Med *33*, 613-620.

Giacca, A., Xiao, C., Oprescu, A.I., Carpentier, A.C., and Lewis, G.F. (2011). Lipid-induced pancreatic beta-cell dysfunction: focus on in vivo studies. American journal of physiology. Endocrinology and metabolism *300*, E255-262.

Goldring, M.B., and Otero, M. (2011). Inflammation in osteoarthritis. Curr Opin Rheumatol *23*, 471-478.

Gontier, E., Fourme, E., Wartski, M., Blondet, C., Bonardel, G., Le Stanc, E., Mantzarides, M., Foehrenbach, H., Pecking, A.P., and Alberini, J.L. (2008). High and typical 18F-FDG bowel uptake in patients treated with metformin. European journal of nuclear medicine and molecular imaging *35*, 95-99.

Gourni, E., Waser, B., Clerc, P., Fourmy, D., Reubi, J.C., and Maecke, H.R. (2014). The glucose-dependent insulinotropic polypeptide receptor: a novel target for neuroendocrine tumor imaging-first preclinical studies. J Nucl Med *55*, 976-982.

Gouyon, F., Caillaud, L., Carriere, V., Klein, C., Dalet, V., Citadelle, D., Kellett, G.L., Thorens, B., Leturque, A., and Brot-Laroche, E. (2003). Simple-sugar meals target GLUT2 at enterocyte apical membranes to improve sugar absorption: a study in GLUT2-null mice. J Physiol *552*, 823-832.

Granger, D.N., Richardson, P.D., Kvietys, P.R., and Mortillaro, N.A. (1980). Intestinal blood flow. Gastroenterology *78*, 837-863.

Gribble, F.M. (2012). The gut endocrine system as a coordinator of postprandial nutrient homoeostasis. Proc Nutr Soc *71*, 456-462.

Group, A.C., Patel, A., MacMahon, S., Chalmers, J., Neal, B., Billot, L., Woodward, M., Marre, M., Cooper, M., Glasziou, P., et al. (2008). Intensive blood glucose control and vascular outcomes in patients with type 2 diabetes. The New England journal of medicine *358*, 2560-2572.

Grubb, R.L., Jr., Raichle, M.E., Higgins, C.S., and Eichling, J.O. (1978). Measurement of regional cerebral blood volume by emission tomography. Ann Neurol *4*, 322-328.

Guenard, F., Deshaies, Y., Cianflone, K., Kral, J.G., Marceau, P., and Vohl, M.C. (2013). Differential methylation in glucoregulatory genes of offspring born before vs. after maternal gastrointestinal bypass surgery. Proceedings of the National Academy of Sciences of the United States of America *110*, 11439-11444.

Hall, J.E., da Silva, A.A., do Carmo, J.M., Dubinion, J., Hamza, S., Munusamy, S., Smith, G., and Stec, D.E. (2010). Obesity-induced hypertension: role of sympathetic nervous system, leptin, and melanocortins. J Biol Chem *285*, 17271-17276.

Hallsten, K., Virtanen, K.A., Lonnqvist, F., Sipila, H., Oksanen, A., Viljanen, T., Ronnemaa, T., Viikari, J., Knuuti, J., and Nuutila, P. (2002). Rosiglitazone but not metformin enhances insulin- and exercise-stimulated skeletal muscle glucose uptake in patients with newly diagnosed type 2 diabetes. Diabetes *51*, 3479-3485.

Hansen, E.N., Tamboli, R.A., Isbell, J.M., Saliba, J., Dunn, J.P., Marks-Shulman, P.A., and Abumrad, N.N. (2011). Role of the foregut in the early improvement in glucose tolerance and insulin sensitivity following Roux-en-Y gastric bypass surgery. Am J Physiol Gastrointest Liver Physiol *300*, G795-802.

Hansen, L., and Holst, J.J. (2002). The effects of duodenal peptides on glucagon-like peptide-1 secretion from the ileum. A duodeno--ileal loop? Regulatory peptides *110*, 39-45.

Haslam, D.W., and James, W.P. (2005). Obesity. Lancet *366*, 1197-1209.

Hediger, M.A., Coady, M.J., Ikeda, T.S., and Wright, E.M. (1987). Expression cloning and cDNA sequencing of the Na+/glucose co-transporter. Nature *330*, 379-381.

Heinonen, S.E., Leppanen, P., Kholova, I., Lumivuori, H., Hakkinen, S.K., Bosch, F., Laakso, M., and Yla-Herttuala, S. (2007). Increased atherosclerotic lesion calcification in a novel mouse model combining insulin resistance, hyperglycemia, and hypercholesterolemia. Circ Res *101*, 1058-1067.

Herrick, J.F.E.H.E.M.F.C.B.E.J. (1934). The Effect of digestion on the blood flow in certain blood vessels of the dog. American Journal of Physiology *108*, 621-628.

Herrmann, C., Goke, R., Richter, G., Fehmann, H.C., Arnold, R., and Goke, B. (1995). Glucagon-like peptide-1 and glucose-dependent insulin-releasing polypeptide plasma levels in response to nutrients. Digestion *56*, 117-126.

Heymann, E., and Mentlein, R. (1978). Liver dipeptidyl aminopeptidase IV hydrolyzes substance P. FEBS Lett *91*, 360-364.

Heymsfield, S.B., and Wadden, T.A. (2017). Mechanisms, Pathophysiology, and Management of Obesity. The New England journal of medicine *376*, 1492.

Higashi, T., Fisher, S.J., Nakada, K., Romain, D.J., and Wahl, R.L. (2002). Is enteral administration of fluorine-18-fluorodeoxyglucose (F-18 FDG) a palatable alternative to IV injection? Pre-clinical evaluation in normal rodents. Nuclear medicine and biology *29*, 363-373.

Hill, M.A., and Larkins, R.G. (1989). Alterations in distribution of cardiac output in experimental diabetes in rats. The American journal of physiology *257*, H571-580.

Hilton, S.M., and Spyer, K.M. (1980). Central nervous regulation of vascular resistance. Annual review of physiology *42*, 399-441.

Hirst, J.A., Farmer, A.J., Dyar, A., Lung, T.W., and Stevens, R.J. (2013). Estimating the effect of sulfonylurea on HbA1c in diabetes: a systematic review and meta-analysis. Diabetologia *56*, 973-984.

Hitz, S., Habekost, C., Furst, S., Delso, G., Forster, S., Ziegler, S., Nekolla, S.G., Souvatzoglou, M., Beer, A.J., Grimmer, T., et al. (2014). Systematic Comparison of the Performance of Integrated Whole-Body PET/MR Imaging to Conventional PET/CT for (1)(8)F-FDG Brain Imaging in Patients Examined for Suspected Dementia. J Nucl Med *55*, 923-931.

Hollander, P., Gupta, A.K., Plodkowski, R., Greenway, F., Bays, H., Burns, C., Klassen, P., Fujioka, K., and Group, C.O.-D.S. (2013). Effects of naltrexone sustained-release/bupropion sustained-release combination therapy on body weight and glycemic parameters in overweight and obese patients with type 2 diabetes. Diabetes care *36*, 4022-4029.

Holst, J.J., Knop, F.K., Vilsboll, T., Krarup, T., and Madsbad, S. (2011). Loss of incretin effect is a specific, important, and early characteristic of type 2 diabetes. Diabetes care *34 Suppl 2*, S251-257.

Holst, J.J., Vilsboll, T., and Deacon, C.F. (2009). The incretin system and its role in type 2 diabetes mellitus. Mol Cell Endocrinol *297*, 127-136.

Home, P.D., Pocock, S.J., Beck-Nielsen, H., Curtis, P.S., Gomis, R., Hanefeld, M., Jones, N.P., Komajda, M., McMurray, J.J., and Team, R.S. (2009). Rosiglitazone evaluated for cardiovascular outcomes in oral agent combination therapy for type 2 diabetes (RECORD): a multicentre, randomised, open-label trial. Lancet *373*, 2125-2135.

Honka, H., Koffert, J., Hannukainen, J.C., Tuulari, J.J., Karlsson, H.K., Immonen, H., Oikonen, V., Tolvanen, T., Soinio, M., Salminen, P., et al. (2015). The effects of bariatric surgery on pancreatic lipid metabolism and blood flow. J Clin Endocrinol Metab *100*, 2015-2023.

Honka, H., Makinen, J., Hannukainen, J.C., Tarkia, M., Oikonen, V., Teras, M., Fagerholm, V., Ishizu, T., Saraste, A., Stark, C., et al. (2013). Validation of [18F]fluorodeoxyglucose and positron emission tomography (PET) for the measurement of intestinal metabolism in pigs, and evidence of intestinal insulin resistance in patients with morbid obesity. Diabetologia *56*, 893-900.

Hooper, L.V., Wong, M.H., Thelin, A., Hansson, L., Falk, P.G., and Gordon, J.I. (2001). Molecular analysis of commensal host-microbial relationships in the intestine. Science *291*, 881-884.

Hopsu-Havu, V.K., and Glenner, G.G. (1966). A new dipeptide naphthylamidase hydrolyzing glycyl-prolyl-beta-naphthylamide. Histochemie *7*, 197-201.

Horowitz, M., Cunningham, K.M., Wishart, J.M., Jones, K.L., and Read, N.W. (1996a). The effect of short-term dietary supplementation with glucose on gastric emptying of glucose and fructose and oral glucose tolerance in normal subjects. Diabetologia *39*, 481-486.

Horowitz, M., Wishart, J.M., Jones, K.L., and Hebbard, G.S. (1996b). Gastric emptying in diabetes: an overview. Diabetic medicine : a journal of the British Diabetic Association *13*, S16-22.

Hu, F.B., van Dam, R.M., and Liu, S. (2001). Diet and risk of Type II diabetes: the role of types of fat and carbohydrate. Diabetologia *44*, 805-817.

Human Microbiome Project, C. (2012). Structure, function and diversity of the healthy human microbiome. Nature *486*, 207-214.

Hutton, B.F., and Osiecki, A. (1998). Correction of partial volume effects in myocardial SPECT. J Nucl Cardiol *5*, 402-413.

Ikeda, T., Iwata, K., and Murakami, H. (2000). Inhibitory effect of metformin on intestinal glucose absorption in the perfused rat intestine. Biochemical pharmacology *59*, 887-890.

Immonen, H., Hannukainen, J.C., Kudomi, N., Pihlajamaki, J., Saunavaara, V., Laine, J., Salminen, P., Lehtimaki, T., Pham, T., Iozzo, P., et al. (2017). Increased Liver Fatty Acid Uptake Is Partly Reversed and Liver Fat Content Normalized After Bariatric Surgery. Diabetes care.

Inzucchi, S.E., Bergenstal, R.M., Buse, J.B., Diamant, M., Ferrannini, E., Nauck, M., Peters, A.L., Tsapas, A., Wender, R., Matthews, D.R., et al. (2012). Management of hyperglycemia in type 2 diabetes: a patient-centered approach: position statement of the American Diabetes Association

(ADA) and the European Association for the Study of Diabetes (EASD). Diabetes care *35*, 1364-1379.

Iozzo, P., Gastaldelli, A., Jarvisalo, M.J., Kiss, J., Borra, R., Buzzigoli, E., Viljanen, A., Naum, G., Viljanen, T., Oikonen, V., et al. (2006). 18F-FDG assessment of glucose disposal and production rates during fasting and insulin stimulation: a validation study. J Nucl Med *47*, 1016-1022.

Iozzo, P., Hallsten, K., Oikonen, V., Virtanen, K.A., Parkkola, R., Kemppainen, J., Solin, O., Lonnqvist, F., Ferrannini, E., Knuuti, J., et al. (2003). Effects of metformin and rosiglitazone monotherapy on insulin-mediated hepatic glucose uptake and their relation to visceral fat in type 2 diabetes. Diabetes care *26*, 2069-2074.

Irwin, N., and Flatt, P.R. (2013). Enteroendocrine hormone mimetics for the treatment of obesity and diabetes. Current opinion in pharmacology *13*, 989-995.

Ishizu, K., Nishizawa, S., Yonekura, Y., Sadato, N., Magata, Y., Tamaki, N., Tsuchida, T., Okazawa, H., Miyatake, S., Ishikawa, M., et al. (1994). Effects of hyperglycemia on FDG uptake in human brain and glioma. J Nucl Med *35*, 1104-1109.

Jones, D.S., Podolsky, S.H., and Greene, J.A. (2012). The burden of disease and the changing task of medicine. The New England journal of medicine *366*, 2333-2338.

Jorgensen, N.B., Jacobsen, S.H., Dirksen, C., Bojsen-Moller, K.N., Naver, L., Hvolris, L., Clausen, T.R., Wulff, B.S., Worm, D., Lindqvist Hansen, D., et al. (2012). Acute and long-term effects of Roux-en-Y gastric bypass on glucose metabolism in subjects with Type 2 diabetes and normal glucose tolerance. American journal of physiology. Endocrinology and metabolism *303*, E122-131.

Juurlink, D.N., Gomes, T., Lipscombe, L.L., Austin, P.C., Hux, J.E., and Mamdani, M.M. (2009). Adverse cardiovascular events during treatment with pioglitazone and rosiglitazone: population based cohort study. BMJ *339*, b2942.

Kahn, S.E., Cooper, M.E., and Del Prato, S. (2014). Pathophysiology and treatment of type 2 diabetes: perspectives on the past, present, and future. Lancet *383*, 1068-1083.

Kahn, S.E., Hull, R.L., and Utzschneider, K.M. (2006). Mechanisms linking obesity to insulin resistance and type 2 diabetes. Nature *444*, 840-846.

Kellett, G.L., and Helliwell, P.A. (2000). The diffusive component of intestinal glucose absorption is mediated by the glucose-induced recruitment of GLUT2 to the brush-border membrane. The Biochemical journal *350 Pt 1*, 155-162.

Kelly, T., Yang, W., Chen, C.S., Reynolds, K., and He, J. (2008). Global burden of obesity in 2005 and projections to 2030. Int J Obes (Lond) *32*, 1431-1437.

Kety, S.S., and Schmidt, C.F. (1946). Measurement of cerebral blood flow and cerebral oxygen consumption in man. Federation proceedings *5*, 264.

Kiss, J., Naum, A., Kudomi, N., Knuuti, J., Iozzo, P., Savunen, T., and Nuutila, P. (2009). Non-invasive diagnosis of acute mesenteric ischaemia using PET. European journal of nuclear medicine and molecular imaging *36*, 1338-1345.

Koffert, J., Honka, H., Teuho, J., Kauhanen, S., Hurme, S., Parkkola, R., Oikonen, V., Mari, A., Lindqvist, A., Wierup, N., et al. (2017). Effects of meal and incretins in the regulation of splanchnic blood flow. Endocr Connect *6*, 179-187.

Kogire, M., Inoue, K., Sumi, S., Doi, R., Takaori, K., Yun, M., Fujii, N., Yajima, H., and Tobe, T. (1988). Effects of synthetic human gastric inhibitory polypeptide on splanchnic circulation in dogs. Gastroenterology *95*, 1636-1640.

Korthuis, R.J., Benoit, J.N., Kvietys, P.R., Laughlin, M.H., Taylor, A.E., and Granger, D.N. (1987). Intestinal hyperemia in experimental diabetes mellitus. The American journal of physiology *253*, G26-32.

Krarup, T., Saurbrey, N., Moody, A.J., Kuhl, C., and Madsbad, S. (1987). Effect of porcine gastric inhibitory polypeptide on beta-cell function in type I and type II diabetes mellitus. Metabolism: clinical and experimental *36*, 677-682.

Krebs, H.A. (1972). Some aspects of the regulation of fuel supply in omnivorous animals. Advances in enzyme regulation *10*, 397-420.

Kremen, A.J., Linner, J.H., and Nelson, C.H. (1954). An experimental evaluation of the nutritional importance of proximal and distal small intestine. Ann Surg *140*, 439-448.

Kvietys, P.R., Gallavan, R.H., and Chou, C.C. (1980). Contribution of bile to postprandial intestinal hyperemia. The American journal of physiology *238*, G284-288.

Kvietys, P.R., and Granger, D.N. (1981). Effect of volatile fatty acids on blood flow and oxygen uptake by the dog colon. Gastroenterology *80*, 962-969.

Labbe, S.M., Croteau, E., Grenier-Larouche, T., Frisch, F., Ouellet, R., Langlois, R., Guerin, B., Turcotte, E.E., and Carpentier, A.C. (2011a). Normal postprandial nonesterified fatty acid uptake in muscles despite increased circulating fatty acids in type 2 diabetes. Diabetes *60*, 408-415.

Labbe, S.M., Grenier-Larouche, T., Croteau, E., Normand-Lauziere, F., Frisch, F., Ouellet, R., Guerin, B., Turcotte, E.E., and Carpentier, A.C.

(2011b). Organ-specific dietary fatty acid uptake in humans using positron emission tomography coupled to computed tomography. American journal of physiology. Endocrinology and metabolism *300*, E445-453.

Laferrere, B., Heshka, S., Wang, K., Khan, Y., McGinty, J., Teixeira, J., Hart, A.B., and Olivan, B. (2007). Incretin levels and effect are markedly enhanced 1 month after Roux-en-Y gastric bypass surgery in obese patients with type 2 diabetes. Diabetes care *30*, 1709-1716.

Laferrere, B., Teixeira, J., McGinty, J., Tran, H., Egger, J.R., Colarusso, A., Kovack, B., Bawa, B., Koshy, N., Lee, H., et al. (2008). Effect of weight loss by gastric bypass surgery versus hypocaloric diet on glucose and incretin levels in patients with type 2 diabetes. J Clin Endocrinol Metab *93*, 2479-2485.

Larson-Meyer, D.E., Newcomer, B.R., Ravussin, E., Volaufova, J., Bennett, B., Chalew, S., Cefalu, W.T., and Sothern, M. (2011). Intrahepatic and intramyocellular lipids are determinants of insulin resistance in prepubertal children. Diabetologia *54*, 869-875.

Laspa, E., Christen, A., Efstathiadou, Z., Johnston, D.G., and Godsland, I.F. (2007). Long-term changes and variability in diabetes risk factors prior to the development of impaired glucose homeostasis. Diabetic medicine : a journal of the British Diabetic Association *24*, 1269-1278.

le Roux, C.W., Borg, C., Wallis, K., Vincent, R.P., Bueter, M., Goodlad, R., Ghatei, M.A., Patel, A., Bloom, S.R., and Aylwin, S.J. (2010). Gut hypertrophy after gastric bypass is associated with increased glucagon-like peptide 2 and intestinal crypt cell proliferation. Ann Surg *252*, 50-56.

LeBlanc, A.D., Riley, R.C., and Robinson, R.G. (1974). Simultaneous measurement of total and nutritional coronary blood flow in dogs. Circulation *49*, 338-347.

Lenzen, S., Lortz, S., and Tiedge, M. (1996). Effect of metformin on SGLT1, GLUT2, and GLUT5 hexose transporter gene expression in small intestine from rats. Biochemical pharmacology *51*, 893-896.

Lewis, J.D., Ferrara, A., Peng, T., Hedderson, M., Bilker, W.B., Quesenberry, C.P., Jr., Vaughn, D.J., Nessel, L., Selby, J., and Strom, B.L. (2011). Risk of bladder cancer among diabetic patients treated with pioglitazone: interim report of a longitudinal cohort study. Diabetes care *34*, 916-922.

Lieverse, R.J., Jansen, J.B., Masclee, A.A., and Lamers, C.B. (1995). Satiety effects of a physiological dose of cholecystokinin in humans. Gut *36*, 176-179.

Locke, A.E., Kahali, B., Berndt, S.I., Justice, A.E., Pers, T.H., Day, F.R., Powell, C., Vedantam, S., Buchkovich, M.L., Yang, J., et al. (2015). Genetic studies of body mass index yield new insights for obesity biology. Nature *518*, 197-206.

Lorch, E. (1971). Inhibition of intestinal absorption and improvement of oral glucose tolerance by biguanides in the normal and in the streptozotocin-diabetic rat. Diabetologia *7*, 195-203.

Lucas, P.D., and Foy, J.M. (1977). Effects of experimental diabetes and genetic obesity on regional blood flow in the rat. Diabetes *26*, 786-792.

Lund, M.T., Taudorf, L., Hartmann, B., Helge, J.W., Holst, J.J., and Dela, F. (2013). Meal induced gut hormone secretion is altered in aerobically trained compared to sedentary young healthy males. Eur J Appl Physiol *113*, 2737-2747.

Lyons, K., Seghers, V., Williams, J.L., Sorensen, J.I., Paldino, M.J., Krishnamurthy, R., and Rohren, E.M. (2015). Qualitative FDG PET Image Assessment Using Automated Three-Segment MR Attenuation Correction Versus CT Attenuation Correction in a Tertiary Pediatric Hospital: A Prospective Study. AJR. American journal of roentgenology *205*, 652-658.

Ma, J., Pilichiewicz, A.N., Feinle-Bisset, C., Wishart, J.M., Jones, K.L., Horowitz, M., and Rayner, C.K. (2012). Effects of variations in duodenal glucose load on glycaemic, insulin, and incretin responses in type 2 diabetes. Diabetic medicine : a journal of the British Diabetic Association *29*, 604-608.

Maeda, N., Shimomura, I., Kishida, K., Nishizawa, H., Matsuda, M., Nagaretani, H., Furuyama, N., Kondo, H., Takahashi, M., Arita, Y., et al. (2002). Diet-induced insulin resistance in mice lacking adiponectin/ACRP30. Nat Med *8*, 731-737.

Mahawar, K.K., and Sharples, A.J. (2017). Contribution of Malabsorption to Weight Loss After Roux-en-Y Gastric Bypass: a Systematic Review. Obesity surgery *27*, 2194-2206.

Makinen, J., Hannukainen, J.C., Karmi, A., Immonen, H.M., Soinio, M., Nelimarkka, L., Savisto, N., Helmio, M., Ovaska, J., Salminen, P., et al. (2015). Obesity-associated intestinal insulin resistance is ameliorated after bariatric surgery. Diabetologia *58*, 1055-1062.

Marathe, C.S., Rayner, C.K., Jones, K.L., and Horowitz, M. (2013). Relationships between gastric emptying, postprandial glycemia, and incretin hormones. Diabetes care *36*, 1396-1405.

Marso, S.P., Daniels, G.H., Brown-Frandsen, K., Kristensen, P., Mann, J.F., Nauck, M.A., Nissen, S.E., Pocock, S., Poulter, N.R., Ravn, L.S., et al. (2016). Liraglutide and Cardiovascular Outcomes in Type 2 Diabetes. The New England journal of medicine *375*, 311-322.

Martinez Moreno, J.M., Reyes-Ortiz, A., Lage Sanchez, J.M., Sanchez-Gallegos, P., and Garcia-Caballero, M. (2017). Timeline of Intestinal Adaptation After Malabsortive Surgery: Effect of

Luminal Nutrients, Biliopancreatic Secretion, and Glutamine Supplementation. Obesity surgery *27*, 3133-3141.

Mason, E.E., and Ito, C. (1967). Gastric bypass in obesity. Surg Clin North Am *47*, 1345-1351.

Massollo, M., Marini, C., Brignone, M., Emionite, L., Salani, B., Riondato, M., Capitanio, S., Fiz, F., Democrito, A., Amaro, A., et al. (2013). Metformin temporal and localized effects on gut glucose metabolism assessed using 18F-FDG PET in mice. J Nucl Med *54*, 259-266.

Matsuda, M., Shimomura, I., Sata, M., Arita, Y., Nishida, M., Maeda, N., Kumada, M., Okamoto, Y., Nagaretani, H., Nishizawa, H., et al. (2002). Role of adiponectin in preventing vascular stenosis. The missing link of adipo-vascular axis. J Biol Chem *277*, 37487-37491.

Matthews, D.R., Hosker, J.P., Rudenski, A.S., Naylor, B.A., Treacher, D.F., and Turner, R.C. (1985). Homeostasis model assessment: insulin resistance and beta-cell function from fasting plasma glucose and insulin concentrations in man. Diabetologia *28*, 412-419.

McNeil, N.I., Cummings, J.H., and James, W.P. (1978). Short chain fatty acid absorption by the human large intestine. Gut *19*, 819-822.

Meeran, K., O'Shea, D., Edwards, C.M., Turton, M.D., Heath, M.M., Gunn, I., Abusnana, S., Rossi, M., Small, C.J., Goldstone, A.P., et al. (1999). Repeated intracerebroventricular administration of glucagon-like peptide-1-(7-36) amide or exendin-(9-39) alters body weight in the rat. Endocrinology *140*, 244-250.

Mehranian, A., Arabi, H., and Zaidi, H. (2016). Quantitative analysis of MRI-guided attenuation correction techniques in time-of-flight brain PET/MRI. Neuroimage *130*, 123-133.

Mehta, A., Marso, S.P., and Neeland, I.J. (2017). Liraglutide for weight management: a critical review of the evidence. Obes Sci Pract *3*, 3-14.

Melissas, J., Leventi, A., Klinaki, I., Perisinakis, K., Koukouraki, S., de Bree, E., and Karkavitsas, N. (2013). Alterations of global gastrointestinal motility after sleeve gastrectomy: a prospective study. Ann Surg *258*, 976-982.

Meng, Y., Bai, H., Wang, S., Li, Z., Wang, Q., and Chen, L. (2017). Efficacy of low carbohydrate diet for type 2 diabetes mellitus management: A systematic review and meta-analysis of randomized controlled trials. Diabetes Res Clin Pract *131*, 124-131.

Miller, R.E. (1981). Pancreatic neuroendocrinology: peripheral neural mechanisms in the regulation of the Islets of Langerhans. Endocr Rev *2*, 471-494.

Minassian, C., Tarpin, S., and Mithieux, G. (1998). Role of glucose-6 phosphatase, glucokinase, and glucose-6 phosphate in liver insulin resistance and its correction by metformin. Biochemical pharmacology *55*, 1213-1219.

Mithieux, G. (2001). New data and concepts on glutamine and glucose metabolism in the gut. Current opinion in clinical nutrition and metabolic care *4*, 267-271.

Mithieux, G., Rajas, F., and Zitoun, C. (2006). Glucose utilization is suppressed in the gut of insulin-resistant high fat-fed rats and is restored by metformin. Biochemical pharmacology *72*, 1757-1762.

Miyazaki, Y., Glass, L., Triplitt, C., Matsuda, M., Cusi, K., Mahankali, A., Mahankali, S., Mandarino, L.J., and DeFronzo, R.A. (2001). Effect of rosiglitazone on glucose and non-esterified fatty acid metabolism in Type II diabetic patients. Diabetologia *44*, 2210-2219.

Morinigo, R., Lacy, A.M., Casamitjana, R., Delgado, S., Gomis, R., and Vidal, J. (2006a). GLP-1 and changes in glucose tolerance following gastric bypass surgery in morbidly obese subjects. Obesity surgery *16*, 1594-1601.

Morinigo, R., Moize, V., Musri, M., Lacy, A.M., Navarro, S., Marin, J.L., Delgado, S., Casamitjana, R., and Vidal, J. (2006b). Glucagon-like peptide-1, peptide YY, hunger, and satiety after gastric bypass surgery in morbidly obese subjects. J Clin Endocrinol Metab *91*, 1735-1740.

Morinigo, R., Vidal, J., Lacy, A.M., Delgado, S., Casamitjana, R., and Gomis, R. (2008). Circulating peptide YY, weight loss, and glucose homeostasis after gastric bypass surgery in morbidly obese subjects. Ann Surg *247*, 270-275.

Morris, A.P., Voight, B.F., Teslovich, T.M., Ferreira, T., Segre, A.V., Steinthorsdottir, V., Strawbridge, R.J., Khan, H., Grallert, H., Mahajan, A., et al. (2012). Large-scale association analysis provides insights into the genetic architecture and pathophysiology of type 2 diabetes. Nat Genet *44*, 981-990.

Mortensen, K., Petersen, L.L., and Orskov, C. (2000). Colocalization of GLP-1 and GIP in human and porcine intestine. Annals of the New York Academy of Sciences *921*, 469-472.

Moulson, C.L., Lin, M.H., White, J.M., Newberry, E.P., Davidson, N.O., and Miner, J.H. (2007). Keratinocyte-specific expression of fatty acid transport protein 4 rescues the wrinkle-free phenotype in Slc27a4/Fatp4 mutant mice. J Biol Chem *282*, 15912-15920.

Mumphrey, M.B., Hao, Z., Townsend, R.L., Patterson, L.M., and Berthoud, H.R. (2015). Sleeve Gastrectomy Does Not Cause Hypertrophy and Reprogramming of Intestinal Glucose Metabolism in Rats. Obesity surgery *25*, 1468-1473.

Muscelli, E., Mari, A., Casolaro, A., Camastra, S., Seghieri, G., Gastaldelli, A., Holst, J.J., and

Ferrannini, E. (2008). Separate impact of obesity and glucose tolerance on the incretin effect in normal subjects and type 2 diabetic patients. Diabetes *57*, 1340-1348.

Nassir, F., Wilson, B., Han, X., Gross, R.W., and Abumrad, N.A. (2007). CD36 is important for fatty acid and cholesterol uptake by the proximal but not distal intestine. J Biol Chem *282*, 19493-19501.

Natalie Nelissen, J.a.P.D. (2012). Kinetic Modelling in Human Brain Imaging, Positron Emission Tomography - Current Clinical and Research Aspects,.

Nauck, M., Stockmann, F., Ebert, R., and Creutzfeldt, W. (1986a). Reduced incretin effect in type 2 (non-insulin-dependent) diabetes. Diabetologia *29*, 46-52.

Nauck, M.A. (2009). Unraveling the science of incretin biology. Eur J Intern Med *20 Suppl 2*, S303-308.

Nauck, M.A., Heimesaat, M.M., Orskov, C., Holst, J.J., Ebert, R., and Creutzfeldt, W. (1993). Preserved incretin activity of glucagon-like peptide 1 [7-36 amide] but not of synthetic human gastric inhibitory polypeptide in patients with type-2 diabetes mellitus. The Journal of clinical investigation *91*, 301-307.

Nauck, M.A., Homberger, E., Siegel, E.G., Allen, R.C., Eaton, R.P., Ebert, R., and Creutzfeldt, W. (1986b). Incretin effects of increasing glucose loads in man calculated from venous insulin and C-peptide responses. J Clin Endocrinol Metab *63*, 492-498.

Nauck, M.A., Niedereichholz, U., Ettler, R., Holst, J.J., Orskov, C., Ritzel, R., and Schmiegel, W.H. (1997). Glucagon-like peptide 1 inhibition of gastric emptying outweighs its insulinotropic effects in healthy humans. The American journal of physiology *273*, E981-988.

Neal, B., Perkovic, V., and Matthews, D.R. (2017). Canagliflozin and Cardiovascular and Renal Events in Type 2 Diabetes. The New England journal of medicine *377*, 2099.

Neumiller, J.J., White, J.R., Jr., and Campbell, R.K. (2010). Sodium-glucose co-transport inhibitors: progress and therapeutic potential in type 2 diabetes mellitus. Drugs *70*, 377-385.

Nguyen, N.Q., Debreceni, T.L., Bambrick, J.E., Bellon, M., Wishart, J., Standfield, S., Rayner, C.K., and Horowitz, M. (2014). Rapid gastric and intestinal transit is a major determinant of changes in blood glucose, intestinal hormones, glucose absorption and postprandial symptoms after gastric bypass. Obesity (Silver Spring) *22*, 2003-2009.

Nicholson, J.K., Holmes, E., Kinross, J., Burcelin, R., Gibson, G., Jia, W., and Pettersson, S. (2012). Host-gut microbiota metabolic interactions. Science *336*, 1262-1267.

Niot, I., Poirier, H., Tran, T.T., and Besnard, P. (2009). Intestinal absorption of long-chain fatty acids: evidence and uncertainties. Prog Lipid Res *48*, 101-115.

Nissen, S.E., Nicholls, S.J., Wolski, K., Howey, D.C., McErlean, E., Wang, M.D., Gomez, E.V., and Russo, J.M. (2007). Effects of a potent and selective PPAR-alpha agonist in patients with atherogenic dyslipidemia or hypercholesterolemia: two randomized controlled trials. JAMA *297*, 1362-1373.

Nolan, J.J., Ludvik, B., Beerdsen, P., Joyce, M., and Olefsky, J. (1994). Improvement in glucose tolerance and insulin resistance in obese subjects treated with troglitazone. The New England journal of medicine *331*, 1188-1193.

Nuutila, P., Koivisto, V.A., Knuuti, J., Ruotsalainen, U., Teras, M., Haaparanta, M., Bergman, J., Solin, O., Voipio-Pulkki, L.M., Wegelius, U., et al. (1992). Glucose-free fatty acid cycle operates in human heart and skeletal muscle in vivo. The Journal of clinical investigation *89*, 1767-1774.

Nyhof, R.A., and Chou, C.C. (1983). Evidence against local neural mechanism for intestinal postprandial hyperemia. The American journal of physiology *245*, H437-446.

Okuyama, M., Hatori, Y., and Shigematsu, A. (1994). Autoradioluminography, a novel quantitative method of TLC-autoradiography. Biol Pharm Bull *17*, 559-563.

Olshansky, S.J., Passaro, D.J., Hershow, R.C., Layden, J., Carnes, B.A., Brody, J., Hayflick, L., Butler, R.N., Allison, D.B., and Ludwig, D.S. (2005). A potential decline in life expectancy in the United States in the 21st century. The New England journal of medicine *352*, 1138-1145.

Ornellas, T., and Chavez, B. (2011). Naltrexone SR/Bupropion SR (Contrave): A New Approach to Weight Loss in Obese Adults. P T *36*, 255-262.

Otsuki, M. (2000). Pathophysiological role of cholecystokinin in humans. J Gastroenterol Hepatol *15 Suppl*, D71-83.

Parikh, M., Chung, M., Sheth, S., McMacken, M., Zahra, T., Saunders, J.K., Ude-Welcome, A., Dunn, V., Ogedegbe, G., Schmidt, A.M., et al. (2014). Randomized pilot trial of bariatric surgery versus intensive medical weight management on diabetes remission in type 2 diabetic patients who do NOT meet NIH criteria for surgery and the role of soluble RAGE as a novel biomarker of success. Ann Surg *260*, 617-622; discussion 622-614.

Pathak, V., Flatt, P.R., and Irwin, N. (2018). Cholecystokinin (CCK) and related adjunct peptide therapies for the treatment of obesity and type 2 diabetes. Peptides *100*, 229-235.

Patlak, C.S., and Blasberg, R.G. (1985). Graphical evaluation of blood-to-brain transfer constants from multiple-time uptake data. Generalizations. J Cereb Blood Flow Metab *5*, 584-590.

Patriti, A., Aisa, M.C., Annetti, C., Sidoni, A., Galli, F., Ferri, I., Gulla, N., and Donini, A. (2007). How the hindgut can cure type 2 diabetes. Ileal transposition improves glucose metabolism and beta-cell function in Goto-kakizaki rats through an enhanced Proglucagon gene expression and L-cell number. Surgery *142*, 74-85.

Patriti, A., Facchiano, E., Annetti, C., Aisa, M.C., Galli, F., Fanelli, C., and Donini, A. (2005). Early improvement of glucose tolerance after ileal transposition in a non-obese type 2 diabetes rat model. Obesity surgery *15*, 1258-1264.

Peeters, A., Barendregt, J.J., Willekens, F., Mackenbach, J.P., Al Mamun, A., Bonneux, L., Nedcom, t.N.E., and Demography Compression of Morbidity Research, G. (2003). Obesity in adulthood and its consequences for life expectancy: a life-table analysis. Ann Intern Med *138*, 24-32.

Perley, M.J., and Kipnis, D.M. (1967). Plasma insulin responses to oral and intravenous glucose: studies in normal and diabetic sujbjects. The Journal of clinical investigation *46*, 1954-1962.

Phelps, M.E., Huang, S.C., Hoffman, E.J., Selin, C., Sokoloff, L., and Kuhl, D.E. (1979). Tomographic measurement of local cerebral glucose metabolic rate in humans with (F-18)2-fluoro-2-deoxy-D-glucose: validation of method. Ann Neurol *6*, 371-388.

Pilichiewicz, A.N., Chaikomin, R., Brennan, I.M., Wishart, J.M., Rayner, C.K., Jones, K.L., Smout, A.J., Horowitz, M., and Feinle-Bisset, C. (2007a). Load-dependent effects of duodenal glucose on glycemia, gastrointestinal hormones, antropyloroduodenal motility, and energy intake in healthy men. American journal of physiology. Endocrinology and metabolism *293*, E743-753.

Pilichiewicz, A.N., Papadopoulos, P., Brennan, I.M., Little, T.J., Meyer, J.H., Wishart, J.M., Horowitz, M., and Feinle-Bisset, C. (2007b). Load-dependent effects of duodenal lipid on antropyloroduodenal motility, plasma CCK and PYY, and energy intake in healthy men. American journal of physiology. Regulatory, integrative and comparative physiology *293*, R2170-2178.

Plamboeck, A., Holst, J.J., Carr, R.D., and Deacon, C.F. (2005). Neutral endopeptidase 24.11 and dipeptidyl peptidase IV are both mediators of the degradation of glucagon-like peptide 1 in the anaesthetised pig. Diabetologia *48*, 1882-1890.

Plum, L., Ahmed, L., Febres, G., Bessler, M., Inabnet, W., Kunreuther, E., McMahon, D.J., and Korner, J. (2011). Comparison of glucostatic parameters after hypocaloric diet or bariatric surgery and equivalent weight loss. Obesity (Silver Spring) *19*, 2149-2157.

Polidori, D., Sha, S., Mudaliar, S., Ciaraldi, T.P., Ghosh, A., Vaccaro, N., Farrell, K., Rothenberg, P., and Henry, R.R. (2013). Canagliflozin lowers postprandial glucose and insulin by delaying intestinal glucose absorption in addition to increasing urinary glucose excretion: results of a randomized, placebo-controlled study. Diabetes care *36*, 2154-2161.

Polinski, J.M., Smith, B.F., Curtis, B.H., Seeger, J.D., Choudhry, N.K., Connolly, J.G., and Shrank, W.H. (2013). Barriers to insulin progression among patients with type 2 diabetes: a systematic review. Diabetes Educ *39*, 53-65.

Popkin, B.M., and Hawkes, C. (2016). Sweetening of the global diet, particularly beverages: patterns, trends, and policy responses. Lancet Diabetes Endocrinol *4*, 174-186.

Prattala, R., Sippola, R., Lahti-Koski, M., Laaksonen, M.T., Makinen, T., and Roos, E. (2012). Twenty-five year trends in body mass index by education and income in Finland. BMC Public Health *12*, 936.

Premen, A.J., Kvietys, P.R., and Granger, D.N. (1985). Postprandial regulation of intestinal blood flow: role of gastrointestinal hormones. The American journal of physiology *249*, G250-255.

Prinzen, F.W., and Bassingthwaighte, J.B. (2000). Blood flow distributions by microsphere deposition methods. Cardiovasc Res *45*, 13-21.

Psichas, A., Reimann, F., and Gribble, F.M. (2015). Gut chemosensing mechanisms. The Journal of clinical investigation *125*, 908-917.

Pugmire, B.S., Guimaraes, A.R., Lim, R., Friedmann, A.M., Huang, M., Ebb, D., Weinstein, H., Catalano, O.A., Mahmood, U., Catana, C., et al. (2016). Simultaneous whole body (18)F-fluorodeoxyglucose positron emission tomography magnetic resonance imaging for evaluation of pediatric cancer: Preliminary experience and comparison with (18)F-fluorodeoxyglucose positron emission tomography computed tomography. World J Radiol *8*, 322-330.

Qamar, M.I., Read, A.E., Skidmore, R., Evans, J.M., and Wells, P.N. (1986). Transcutaneous Doppler ultrasound measurement of superior mesenteric artery blood flow in man. Gut *27*, 100-105.

Quercia, I., Dutia, R., Kotler, D.P., Belsley, S., and Laferrere, B. (2014). Gastrointestinal changes after bariatric surgery. Diabetes Metab *40*, 87-94.

Radziuk, J., and Pye, S. (2002). Quantitation of basal endogenous glucose production in Type II diabetes: importance of the volume of distribution. Diabetologia *45*, 1053-1084.

Rahman, M., and Berenson, A.B. (2010). Accuracy of current body mass index obesity classification for

white, black, and Hispanic reproductive-age women. Obstet Gynecol *115*, 982-988.

Rajas, F., Bruni, N., Montano, S., Zitoun, C., and Mithieux, G. (1999). The glucose-6 phosphatase gene is expressed in human and rat small intestine: regulation of expression in fasted and diabetic rats. Gastroenterology *117*, 132-139.

Rajas, F., Croset, M., Zitoun, C., Montano, S., and Mithieux, G. (2000). Induction of PEPCK gene expression in insulinopenia in rat small intestine. Diabetes *49*, 1165-1168.

Ramnanan, C.J., Edgerton, D.S., and Cherrington, A.D. (2012). Evidence against a physiologic role for acute changes in CNS insulin action in the rapid regulation of hepatic glucose production. Cell metabolism *15*, 656-664.

Raybould, H.E., Cooke, H.J., and Christofi, F.L. (2004). Sensory mechanisms: transmitters, modulators and reflexes. Neurogastroenterology and motility : the official journal of the European Gastrointestinal Motility Society *16 Suppl 1*, 60-63.

Rayner, C.K., Samsom, M., Jones, K.L., and Horowitz, M. (2001). Relationships of upper gastrointestinal motor and sensory function with glycemic control. Diabetes care *24*, 371-381.

Ronnestad, I., Akiba, Y., Kaji, I., and Kaunitz, J.D. (2014). Duodenal luminal nutrient sensing. Current opinion in pharmacology *19*, 67-75.

Rothman, K.J. (2008). BMI-related errors in the measurement of obesity. Int J Obes (Lond) *32 Suppl 3*, S56-59.

Rothschild, A.M., Gomes, E.L., and Fortunato, I.C. (1998). Bradykinin release from high molecular weight kininogen and increase in plasma kallikrein-like activity following sensory stimulation by food in the rat. Naunyn-Schmiedeberg's archives of pharmacology *358*, 483-488.

Rozsa, Z., and Jacobson, E.D. (1989). Capsaicin-sensitive nerves are involved in bile-oleate-induced intestinal hyperemia. The American journal of physiology *256*, G476-481.

Rubino, F., Forgione, A., Cummings, D.E., Vix, M., Gnuli, D., Mingrone, G., Castagneto, M., and Marescaux, J. (2006). The mechanism of diabetes control after gastrointestinal bypass surgery reveals a role of the proximal small intestine in the pathophysiology of type 2 diabetes. Ann Surg *244*, 741-749.

Rubino, F., Gagner, M., Gentileschi, P., Kini, S., Fukuyama, S., Feng, J., and Diamond, E. (2004). The early effect of the Roux-en-Y gastric bypass on hormones involved in body weight regulation and glucose metabolism. Ann Surg *240*, 236-242.

Rubino, F., and Marescaux, J. (2004). Effect of duodenal-jejunal exclusion in a non-obese animal model of type 2 diabetes: a new perspective for an old disease. Ann Surg *239*, 1-11.

Rubino, F., Nathan, D.M., Eckel, R.H., Schauer, P.R., Alberti, K.G., Zimmet, P.Z., Del Prato, S., Ji, L., Sadikot, S.M., Herman, W.H., et al. (2016). Metabolic Surgery in the Treatment Algorithm for Type 2 Diabetes: A Joint Statement by International Diabetes Organizations. Surg Obes Relat Dis *12*, 1144-1162.

Rudolph, A.M., and Heymann, M.A. (1967). The circulation of the fetus in utero. Methods for studying distribution of blood flow, cardiac output and organ blood flow. Circ Res *21*, 163-184.

Rudolph, A.M., and Heymann, M.A. (1976). Cardiac output in the fetal lamb: the effects of spontaneous and induced changes of heart rate on right and left ventricular output. Am J Obstet Gynecol *124*, 183-192.

Ryskjaer, J., Deacon, C.F., Carr, R.D., Krarup, T., Madsbad, S., Holst, J., and Vilsboll, T. (2006). Plasma dipeptidyl peptidase-IV activity in patients with type-2 diabetes mellitus correlates positively with HbAlc levels, but is not acutely affected by food intake. European journal of endocrinology / European Federation of Endocrine Societies *155*, 485-493.

Saeidi, N., Meoli, L., Nestoridi, E., Gupta, N.K., Kvas, S., Kucharczyk, J., Bonab, A.A., Fischman, A.J., Yarmush, M.L., and Stylopoulos, N. (2013). Reprogramming of intestinal glucose metabolism and glycemic control in rats after gastric bypass. Science *341*, 406-410.

Salyers, A.A.L., J.A.Z. (1983). Carboydrate metabolism in the human colon. In Human intestinal microflora in health and disease. H. DJ, ed. (New York: Academic Press), pp. 129-146.

Saris, W.H., Blair, S.N., van Baak, M.A., Eaton, S.B., Davies, P.S., Di Pietro, L., Fogelholm, M., Rissanen, A., Schoeller, D., Swinburn, B., et al. (2003). How much physical activity is enough to prevent unhealthy weight gain? Outcome of the IASO 1st Stock Conference and consensus statement. Obes Rev *4*, 101-114.

Sattar, N., McConnachie, A., Ford, I., Gaw, A., Cleland, S.J., Forouhi, N.G., McFarlane, P., Shepherd, J., Cobbe, S., and Packard, C. (2007). Serial metabolic measurements and conversion to type 2 diabetes in the west of Scotland coronary prevention study: specific elevations in alanine aminotransferase and triglycerides suggest hepatic fat accumulation as a potential contributing factor. Diabetes *56*, 984-991.

Schirra, J., Katschinski, M., Weidmann, C., Schafer, T., Wank, U., Arnold, R., and Goke, B. (1996). Gastric emptying and release of incretin hormones after glucose ingestion in humans. The Journal of clinical investigation *97*, 92-103.

Schopman, J.E., Simon, A.C., Hoefnagel, S.J., Hoekstra, J.B., Scholten, R.J., and Holleman, F.

(2014). The incidence of mild and severe hypoglycaemia in patients with type 2 diabetes mellitus treated with sulfonylureas: a systematic review and meta-analysis. Diabetes Metab Res Rev *30*, 11-22.

Schwartz, G.J. (2000). The role of gastrointestinal vagal afferents in the control of food intake: current prospects. Nutrition *16*, 866-873.

Scott, R.A., Lagou, V., Welch, R.P., Wheeler, E., Montasser, M.E., Luan, J., Magi, R., Strawbridge, R.J., Rehnberg, E., Gustafsson, S., et al. (2012). Large-scale association analyses identify new loci influencing glycemic traits and provide insight into the underlying biological pathways. Nat Genet *44*, 991-1005.

Seuring, T., Archangelidi, O., and Suhrcke, M. (2015). The Economic Costs of Type 2 Diabetes: A Global Systematic Review. Pharmacoeconomics *33*, 811-831.

Shaw, D., Gohil, K., and Basson, M.D. (2012). Intestinal mucosal atrophy and adaptation. World journal of gastroenterology : WJG *18*, 6357-6375.

Shin, N.R., Lee, J.C., Lee, H.Y., Kim, M.S., Whon, T.W., Lee, M.S., and Bae, J.W. (2013). An increase in the Akkermansia spp. population induced by metformin treatment improves glucose homeostasis in diet-induced obese mice. Gut.

Shyangdan, D.S., Royle, P., Clar, C., Sharma, P., Waugh, N., and Snaith, A. (2011). Glucagon-like peptide analogues for type 2 diabetes mellitus. Cochrane Database Syst Rev, CD006423.

Sidossis, L.S., Stuart, C.A., Shulman, G.I., Lopaschuk, G.D., and Wolfe, R.R. (1996). Glucose plus insulin regulate fat oxidation by controlling the rate of fatty acid entry into the mitochondria. The Journal of clinical investigation *98*, 2244-2250.

Silverstein, R.L., and Febbraio, M. (2009). CD36, a scavenger receptor involved in immunity, metabolism, angiogenesis, and behavior. Sci Signal *2*, re3.

Sjolund, K., Sanden, G., Hakanson, R., and Sundler, F. (1983). Endocrine cells in human intestine: an immunocytochemical study. Gastroenterology *85*, 1120-1130.

Sjostrom, L. (2013). Review of the key results from the Swedish Obese Subjects (SOS) trial - a prospective controlled intervention study of bariatric surgery. J Intern Med *273*, 219-234.

Sjostrom, L., Gummesson, A., Sjostrom, C.D., Narbro, K., Peltonen, M., Wedel, H., Bengtsson, C., Bouchard, C., Carlsson, B., Dahlgren, S., et al. (2009). Effects of bariatric surgery on cancer incidence in obese patients in Sweden (Swedish Obese Subjects Study): a prospective, controlled intervention trial. The lancet oncology *10*, 653-662.

Sjostrom, L., Narbro, K., Sjostrom, C.D., Karason, K., Larsson, B., Wedel, H., Lystig, T., Sullivan, M., Bouchard, C., Carlsson, B., et al. (2007). Effects of bariatric surgery on mortality in Swedish obese subjects. The New England journal of medicine *357*, 741-752.

Sjostrom, L., Peltonen, M., Jacobson, P., Sjostrom, C.D., Karason, K., Wedel, H., Ahlin, S., Anveden, A., Bengtsson, C., Bergmark, G., et al. (2012). Bariatric surgery and long-term cardiovascular events. JAMA *307*, 56-65.

Sjostrom, L., Rissanen, A., Andersen, T., Boldrin, M., Golay, A., Koppeschaar, H.P., and Krempf, M. (1998). Randomised placebo-controlled trial of orlistat for weight loss and prevention of weight regain in obese patients. European Multicentre Orlistat Study Group. Lancet *352*, 167-172.

Sleisenger, M.H., Feldman, M., Friedman, L.S., and Brandt, L.J. (2010). Sleisenger and Fordtran's gastrointestinal and liver disease : pathophysiology, diagnosis, management. (Philadelphia , PA: Saunders/Elsevier).

Sliwkowski, M.B., and Windmueller, H.G. (1984). Rat liver and small intestine produce proapolipoprotein A-I which is slowly processed to apolipoprotein A-I in the circulation. J Biol Chem *259*, 6459-6465.

Snyder WS, C.M., Nasset ES, Karhausen LR, Howells GP, Tipton IH (1975). Report of the Task Group on Reference Man. Pergamon Press: Oxford.

Snyder WS CM, N.E., Karhausen LR, Howells GP, Tipton IH (1975). Report of the Task Group on Reference Man. (Oxford, United Kingdom: Pregamon Press).

Sokoloff, L., Reivich, M., Kennedy, C., Des Rosiers, M.H., Patlak, C.S., Pettigrew, K.D., Sakurada, O., and Shinohara, M. (1977). The [14C]deoxyglucose method for the measurement of local cerebral glucose utilization: theory, procedure, and normal values in the conscious and anesthetized albino rat. J Neurochem *28*, 897-916.

Someya, N., Endo, M.Y., Fukuba, Y., and Hayashi, N. (2008). Blood flow responses in celiac and superior mesenteric arteries in the initial phase of digestion. American journal of physiology. Regulatory, integrative and comparative physiology *294*, R1790-1796.

Spanoudaki, V.C., and Ziegler, S.I. (2008). PET & SPECT instrumentation. Handb Exp Pharmacol, 53-74.

Sparks, H.V., Jr. (1980). Effect of local metabolic factors on vascular smooth muscle. In Handbook of Physiology. Sect. 2. M. Bethesda, ed. (Am. Physiol. Soc.).

Stabin, M.G., and Brill, A.B. (2008). Radiation dosimetry and exposure in nuclear medicine. Seminars in nuclear medicine *38*, 306-307.

Starlinger, M., Schiessel, R., Hung, C.R., and Silen, W. (1981). H+ back diffusion stimulating gastric mucosal blood flow in the rabbit fundus. Surgery *89*, 232-236.

Stearns, A.T., Balakrishnan, A., and Tavakkolizadeh, A. (2009). Impact of Roux-en-Y gastric bypass surgery on rat intestinal glucose transport. Am J Physiol Gastrointest Liver Physiol *297*, G950-957.

Stevens, J., Cai, J., Pamuk, E.R., Williamson, D.F., Thun, M.J., and Wood, J.L. (1998). The effect of age on the association between body-mass index and mortality. The New England journal of medicine *338*, 1-7.

Storch, J., Zhou, Y.X., and Lagakos, W.S. (2008). Metabolism of apical versus basolateral sn-2-monoacylglycerol and fatty acids in rodent small intestine. J Lipid Res *49*, 1762-1769.

Su, X., and Abumrad, N.A. (2009). Cellular fatty acid uptake: a pathway under construction. Trends Endocrinol Metab *20*, 72-77.

Svensson, A.M., Ostenson, C.G., Efendic, S., and Jansson, L. (2007). Effects of glucagon-like peptide-1-(7-36)-amide on pancreatic islet and intestinal blood perfusion in Wistar rats and diabetic GK rats. Clin Sci (Lond) *112*, 345-351.

Tabak, A.G., Jokela, M., Akbaraly, T.N., Brunner, E.J., Kivimaki, M., and Witte, D.R. (2009). Trajectories of glycaemia, insulin sensitivity, and insulin secretion before diagnosis of type 2 diabetes: an analysis from the Whitehall II study. Lancet *373*, 2215-2221.

Taqi, E., Wallace, L.E., de Heuvel, E., Chelikani, P.K., Zheng, H., Berthoud, H.R., Holst, J.J., and Sigalet, D.L. (2010). The influence of nutrients, biliary-pancreatic secretions, and systemic trophic hormones on intestinal adaptation in a Roux-en-Y bypass model. J Pediatr Surg *45*, 987-995.

Taylor, R. (2008). Pathogenesis of type 2 diabetes: tracing the reverse route from cure to cause. Diabetologia *51*, 1781-1789.

Tchkonia, T., Thomou, T., Zhu, Y., Karagiannides, I., Pothoulakis, C., Jensen, M.D., and Kirkland, J.L. (2013). Mechanisms and metabolic implications of regional differences among fat depots. Cell metabolism *17*, 644-656.

Thayer, K.A., Heindel, J.J., Bucher, J.R., and Gallo, M.A. (2012). Role of environmental chemicals in diabetes and obesity: a National Toxicology Program workshop review. Environ Health Perspect *120*, 779-789.

Titchenell, P.M., Chu, Q., Monks, B.R., and Birnbaum, M.J. (2015). Hepatic insulin signalling is dispensable for suppression of glucose output by insulin in vivo. Nat Commun *6*, 7078.

Tobin, V., Le Gall, M., Fioramonti, X., Stolarczyk, E., Blazquez, A.G., Klein, C., Prigent, M., Serradas, P., Cuif, M.H., Magnan, C., et al. (2008). Insulin internalizes GLUT2 in the enterocytes of healthy but not insulin-resistant mice. Diabetes *57*, 555-562.

Toft-Nielsen, M.B., Damholt, M.B., Madsbad, S., Hilsted, L.M., Hughes, T.E., Michelsen, B.K., and Holst, J.J. (2001). Determinants of the impaired secretion of glucagon-like peptide-1 in type 2 diabetic patients. J Clin Endocrinol Metab *86*, 3717-3723.

Tougas, G., Eaker, E.Y., Abell, T.L., Abrahamsson, H., Boivin, M., Chen, J., Hocking, M.P., Quigley, E.M., Koch, K.L., Tokayer, A.Z., et al. (2000). Assessment of gastric emptying using a low fat meal: establishment of international control values. Am J Gastroenterol *95*, 1456-1462.

Trahair, L.G., Horowitz, M., Hausken, T., Feinle-Bisset, C., Rayner, C.K., and Jones, K.L. (2014). Effects of exogenous glucagon-like peptide-1 on the blood pressure, heart rate, mesenteric blood flow, and glycemic responses to intraduodenal glucose in healthy older subjects. J Clin Endocrinol Metab *99*, E2628-2634.

Trahair, L.G., Vanis, L., Gentilcore, D., Lange, K., Rayner, C.K., Horowitz, M., and Jones, K.L. (2012). Effects of variations in duodenal glucose load on blood pressure, heart rate, superior mesenteric artery blood flow and plasma noradrenaline in healthy young and older subjects. Clin Sci (Lond) *122*, 271-279.

Trotter, P.J., and Storch, J. (1991). Fatty acid uptake and metabolism in a human intestinal cell line (Caco-2): comparison of apical and basolateral incubation. J Lipid Res *32*, 293-304.

Turkington, T.G. (2001). Introduction to PET instrumentation. J Nucl Med Technol *29*, 4-11.

Turner, R.C., and Holman, R.R. (1995). Lessons from UK prospective diabetes study. Diabetes Res Clin Pract *28 Suppl*, S151-157.

Vahl, T.P., Tauchi, M., Durler, T.S., Elfers, E.E., Fernandes, T.M., Bitner, R.D., Ellis, K.S., Woods, S.C., Seeley, R.J., Herman, J.P., et al. (2007). Glucagon-like peptide-1 (GLP-1) receptors expressed on nerve terminals in the portal vein mediate the effects of endogenous GLP-1 on glucose tolerance in rats. Endocrinology *148*, 4965-4973.

Vatner, S.F., Franklin, D., and Van Citters, R.L. (1970). Coronary and visceral vasoactivity associated with eating and digestion in the conscious dog. The American journal of physiology *219*, 1380-1385.

Vilsboll, T., Krarup, T., Madsbad, S., and Holst, J.J. (2003a). Both GLP-1 and GIP are insulinotropic at basal and postprandial glucose levels and contribute nearly equally to the incretin effect of a meal in healthy subjects. Regulatory peptides *114*, 115-121.

Vilsboll, T., Krarup, T., Sonne, J., Madsbad, S., Volund, A., Juul, A.G., and Holst, J.J. (2003b). Incretin secretion in relation to meal size and body weight in healthy subjects and people with type 1 and type 2 diabetes mellitus. J Clin Endocrinol Metab *88*, 2706-2713.

Vollmer, K., Holst, J.J., Baller, B., Ellrichmann, M., Nauck, M.A., Schmidt, W.E., and Meier, J.J. (2008). Predictors of incretin concentrations in subjects with normal, impaired, and diabetic glucose tolerance. Diabetes *57*, 678-687.

Wadden, T.A., Foreyt, J.P., Foster, G.D., Hill, J.O., Klein, S., O'Neil, P.M., Perri, M.G., Pi-Sunyer, F.X., Rock, C.L., Erickson, J.S., et al. (2011). Weight loss with naltrexone SR/bupropion SR combination therapy as an adjunct to behavior modification: the COR-BMOD trial. Obesity (Silver Spring) *19*, 110-120.

Walker, J., Jijon, H.B., Diaz, H., Salehi, P., Churchill, T., and Madsen, K.L. (2005). 5-aminoimidazole-4-carboxamide riboside (AICAR) enhances GLUT2-dependent jejunal glucose transport: a possible role for AMPK. The Biochemical journal *385*, 485-491.

Wang, T.T., Hu, S.Y., Gao, H.D., Zhang, G.Y., Liu, C.Z., Feng, J.B., and Frezza, E.E. (2008). Ileal transposition controls diabetes as well as modified duodenal jejunal bypass with better lipid lowering in a nonobese rat model of type II diabetes by increasing GLP-1. Ann Surg *247*, 968-975.

Whalen, K., Miller, S., and Onge, E.S. (2015). The Role of Sodium-Glucose Co-Transporter 2 Inhibitors in the Treatment of Type 2 Diabetes. Clin Ther *37*, 1150-1166.

White, J.R., Jr. (2014). A Brief History of the Development of Diabetes Medications. Diabetes Spectr *27*, 82-86.

Wilcock, C., and Bailey, C.J. (1990). Sites of metformin-stimulated glucose metabolism. Biochemical pharmacology *39*, 1831-1834.

Wilcock, C., and Bailey, C.J. (1994). Accumulation of metformin by tissues of the normal and diabetic mouse. Xenobiotica; the fate of foreign compounds in biological systems *24*, 49-57.

Willems, M., Quartero, A.O., and Numans, M.E. (2001). How useful is paracetamol absorption as a marker of gastric emptying? A systematic literature study. Dig Dis Sci *46*, 2256-2262.

Willson, T.M., Lambert, M.H., and Kliewer, S.A. (2001). Peroxisome proliferator-activated receptor gamma and metabolic disease. Annu Rev Biochem *70*, 341-367.

Windmueller, H.G., and Spaeth, A.E. (1978). Identification of ketone bodies and glutamine as the major respiratory fuels in vivo for postabsorptive rat small intestine. J Biol Chem *253*, 69-76.

Wittgrove, A.C., Clark, G.W., and Tremblay, L.J. (1994). Laparoscopic Gastric Bypass, Roux-en-Y: Preliminary Report of Five Cases. Obesity surgery *4*, 353-357.

Wood, J.D. (2008). Enteric nervous system: reflexes, pattern generators and motility. Curr Opin Gastroenterol *24*, 149-158.

Wren, A.M., Seal, L.J., Cohen, M.A., Brynes, A.E., Frost, G.S., Murphy, K.G., Dhillo, W.S., Ghatei, M.A., and Bloom, S.R. (2001). Ghrelin enhances appetite and increases food intake in humans. J Clin Endocrinol Metab *86*, 5992.

Wright, E.M., Hirayama, B.A., and Loo, D.F. (2007). Active sugar transport in health and disease. J Intern Med *261*, 32-43.

Wu, L., Olverling, A., Huang, Z., Jansson, L., Chao, H., Gao, X., and Sjoholm, A. (2012). GLP-1, exendin-4 and C-peptide regulate pancreatic islet microcirculation, insulin secretion and glucose tolerance in rats. Clin Sci (Lond) *122*, 375-384.

Xu, G., Stoffers, D.A., Habener, J.F., and Bonner-Weir, S. (1999). Exendin-4 stimulates both beta-cell replication and neogenesis, resulting in increased beta-cell mass and improved glucose tolerance in diabetic rats. Diabetes *48*, 2270-2276.

Yen, M., and Ewald, M.B. (2012). Toxicity of weight loss agents. J Med Toxicol *8*, 145-152.

Yip, R.G., and Wolfe, M.M. (2000). GIP biology and fat metabolism. Life Sci *66*, 91-103.

Zaidi, H., Ojha, N., Morich, M., Griesmer, J., Hu, Z., Maniawski, P., Ratib, O., Izquierdo-Garcia, D., Fayad, Z.A., and Shao, L. (2011). Design and performance evaluation of a whole-body Ingenuity TF PET-MRI system. Phys Med Biol *56*, 3091-3106.

Zanotti-Fregonara, P., Liow, J.S., Fujita, M., Dusch, E., Zoghbi, S.S., Luong, E., Boellaard, R., Pike, V.W., Comtat, C., and Innis, R.B. (2011). Image-derived input function for human brain using high resolution PET imaging with [C](R)-rolipram and [C]PBR28. PLoS One *6*, e17056.

Zanzonico, P. (2012). Principles of nuclear medicine imaging: planar, SPECT, PET, multi-modality, and autoradiography systems. Radiation research *177*, 349-364.

Zhou, G., Myers, R., Li, Y., Chen, Y., Shen, X., Fenyk-Melody, J., Wu, M., Ventre, J., Doebber, T., Fujii, N., et al. (2001). Role of AMP-activated protein kinase in mechanism of metformin action. The Journal of clinical investigation *108*, 1167-1174.

Zinman, B., Wanner, C., Lachin, J.M., Fitchett, D., Bluhmki, E., Hantel, S., Mattheus, M., Devins, T., Johansen, O.E., Woerle, H.J., et al. (2015). Empagliflozin, Cardiovascular Outcomes, and Mortality in Type 2 Diabetes. The New England journal of medicine *373*, 2117-2128.

Annales Universitatis Turkuensis

Turun yliopisto
University of Turku

Painosalama Oy, Turku, Finland 2018

ISBN 978-951-29-7247-0 (PRINT)
ISBN 978-951-29-7248-7 (PDF)
ISSN 0355-9483 (Print) | ISSN 2343-3213 (Online)